ANALYSIS OF PHOTORELEASE OF NITRIC OXIDE FROM RUTHENIUM COMPLEXES

A DISSERTATION

Submitted in partial fulfillment of the requirements for the award of the degree

of

MASTER OF TECHNOLOGY

in

ADVANCED CHEMICAL ANALYSIS

By

AAKASH MITTAL

DEPARTMENT OF CHEMISTRY
INDIAN INSTITUTE OF TECHNOLOGY ROORKEE
ROORKEE - 247 667 (INDIA)

JUNE, 2008

Declaration

I, Aakash Mittal, hereby declare that the work presented in this dissertation thesis entitled **"ANALYSIS OF PHOTORELEASE OF NITRIC OXIDE FROM RUTHENIUM COMPLEXES"**, being submitted in the partial fulfillment of the requirements for the award of the degree of **MASTER OF TECHNOLOGY** with specialization in **ADVANCED CHEMICAL ANALYSIS**, in the Department of Chemistry, Indian Institute of Technology Roorkee, is an authentic record of my own work carried out from July 2007 to May 2008, under the guidance and supervision of Dr.Kaushik Ghosh, Assistant Professor, Department of Chemistry, Indian Institute of Technology Roorkee.

The results embodied in this dissertation have not been submitted for the award of any other degree or diploma.

Aakash Mittal

Date: 27 MAY 2008

AAKASH MITTAL

INDIAN INSTITUTE OF TECHNOLOGY, ROORKEE
DEPARTMENT OF CHEMISTRY
ROORKEE - 247 667, UTTARANCHAL, INDIA
Tel : +91-1332-285547 (off) 285365 (res)
Fax : +91-1332-273560
E-mail : ghoshfcy@iitr.ernet.in, ghoshpdf@yahoo.com

Dr. Kaushik Ghosh
Assistant Professor

CERTIFICATE

This is to certify that the thesis entitled "ANALYSIS OF PHOTORELEASE OF NITRIC OXIDE FROM RUTHENIUM COMPLEXES" submitted by Aakash Mittal who got his name registered on 25 July 2006 for the award of Master of Technology degree in Advanced Chemical Analysis of Indian Institute of Technology Roorkee, is absolutely based upon his work under my supervision and that neither this thesis nor any part of it has been submitted for any degree/diploma or any other academic award anywhere before.

Date: 27/5/08

Dr. Kaushik Ghosh
Assistant Professor
Indian Institute of Technology, Roorkee
Department of Chemistry
Roorkee-247 667 Uttaranchal (INDIA)

Contents

Acknowledgements

It gives me immense pleasure to thank my supervisor Dr.Kaushik Ghosh, Assistant Professor, Department of Chemistry, IIT Roorkee who introduced me to this interesting field of chemistry. I gratefully acknowledge his academic guidance, stimulating discussions and unfailing support.

I take this opportunity to express my heartfelt thanks to Dr.R.K. Dutta, Co-ordinator of M.Tech. Programme who believed in us and was always there to help us out.

It is my great pleasure to thank Ms.Nidhi Tyagi and Mr.Pramod Kumar, who taught me everything, of whatever little I know of practical chemistry. I extend my deepest regards and thank Ms.Payal Tyagi, Ms.Prachi Singh, Mr.Sushil Kumar and Ms.Neha Kapoor who shared their hands on experience and spared their invaluable time just to help me. I am grateful to Mr.Sushil Sharma, Mr.Varun Mohan and Mr.Dhirendra Kumar who helped me in little bit of everything.

My special thanks to Mr.Deepak Singh, Technical Assistant, NMR Lab, Institute Instrumentation Center for his kind cooperation.

I also thank all the staff members of the Department of Chemistry for their cooperation and assistance in the completion of my dissertation work.

I deeply acknowledge the financial assistance by MHRD, India in the form of assistantship.

One of the greatest joys of being here was the opportunity to make some truly wonderful friends.

Date: 27 MAY 2008

Aakash Mittal

Aakash Mittal

ABSTRACT

Three ligands L^1, L^2, L^3 and their corresponding organometallic ruthenium complexes $Ru(PPh_3)_2L^nCl$ $(n = 1 - 3)$ have been synthesized and characterized by IR spectroscopy, GC-MS, UV-Vis spectrophotometry, NMR spectroscopy. Reactivity of nitric oxide was investigated with these three complexes. The resultant ruthenium nitrosyl complexes $Ru(PPh_3)_2L^n(NO)$ were characterized by IR spectroscopy, UV-Vis spectrophotometry, ^1H, ^{13}C and ^{31}P NMR spectroscopy. Interaction of visible light was investigated with these ruthenium nitrosyl complexes and ligated NO was speculated to be photolabile. The photoreleased NO has been trapped by reduced myoglobin.

Chapter 1

Introduction and Review of Literature

Nitric oxide is a signaling molecule with exceptional abilities in the cell's repertoire. It is utilized by the cell in numerous physiological processes. This new role for NO led *Science* magazine to designate NO as *Molecule of the Year* in 1992 [1]. The plural roles of NO earned Furchgott, Ignarro and Murad the Nobel Prize in Physiology or Medicine in 1998 [2-4].

1.1 Role of NO in Biology

NO radical has a small lifetime as its diffusion is limited by multiple scavenging reactions, so the mode of signaling is primarily autocrine and paracrine in nature. Endocrine NO signaling has been discussed by Lundberg and *et.al.* [5]. NO has been identified as the elusive *Endothelium-derived Relaxation Factor* (EDRF) [6]. NO, a potent vasodilator, regulates the cardiovascular system [6,7], reduces platelet aggregation and adhesion [8], mediates neurotransmission [9], modulates renal functioning [10] by activating guanylate cyclase. NO is also involved in anti-tumor and anti-pathogen host response [11,12] of the immune system. Reversible coordination to iron (heme and non-heme) centers [13,14] and interaction with thiol groups [15] allows NO to control the activity of various enzymes [16]. NO has been implicated in a number of pathophysiological conditions such as arthritis, atherosclerosis, cancer, diabetes, neuronal diseases, stroke, myocardial infarction. On one hand NO has the ability to promote cell growth and on the other, the potential to inhibit enzyme function, induce DNA damage, lipid peroxidation and apoptosis or programmed cell death [17,18].

1.2 NO Donors

The exceptional roles that NO plays have raised interest in exogenous NO donors that can deliver NO to specific targets under controlled conditions. Donors that provide NO upon exposure to light have drawn special attention because of their utility in *photodynamic therapy* [19,20] for treating selected types of cancers and use as antiviral drugs [21]. Wang and co-workers [22] have reviewed the current major classes of nitric oxide donors (*Figures 1.1,1.2*), their chemical activities and biological applications.

1.2.1 Organic Nitrates

Organic nitrates ($RONO_2$) are nitric acid esters of mono- and poly-hydric alcohols and represent the oldest class of NO donors with clinical applications. Glyceryl trinitrate (GTN), pentaerythrityl tetranitrate (PETN), isosorbide dinitrate (ISDN), isosorbide 5-mononitrate (ISMO), and nicorandil are representative organic nitrates. They are used to relieve angina pectoris, treat acute myocardial infarction, congestive heart failure, and control blood pressure.

1.2.2 Organic Nitrites

Organic nitrites are esters between alcohols and nitrous acid. Some of them, such as butyl nitrite (BN), isobutyl nitrite (ISBN), tert-butyl nitrite (TBN), amyl nitrite (AMN), and isoamyl nitrite (IAMN), have been clinically used as vasodilators for a long time.

1.2.3 Metal-NO Complexes

NO is a powerful coordinating ligand to metal ions and thus metal nitrosyl complexes may be used as NO donors. The most widely studied metal nitrosyl is sodium nitroprusside ($Na_2[Fe(CN)_5NO]$, SNP). It is powerful vasodilator and is effective at doses that do not produce toxic amounts of cyanide. It is used for treating advanced heart failure, hypertension and inhibits platelet aggregation.

Dinitrosyl iron thiol complexes (DNICs) are mononuclear iron nitrosyls known to store and transport NO *in vivo* and as intermediates of iron-catalyzed degradation and formation of *S*-nitrosothiols. They have been shown to inhibit platelet aggregation, relax vascular vessels, reduce blood pressure, enhance cardiac resistance to ischemia, and reperfusion. Iron-sulfur cluster nitrosyls are integral part of several enzymes.

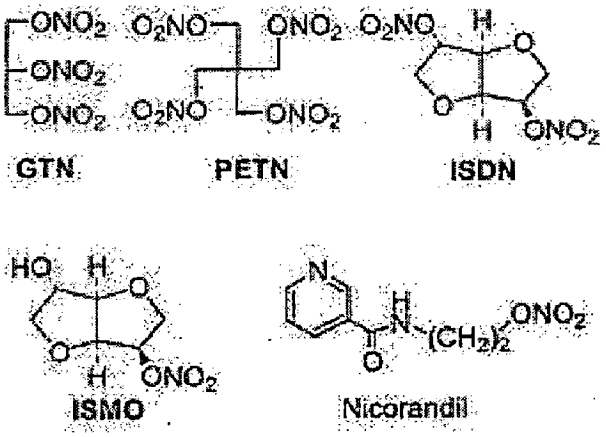

(a) Organic Nitrates

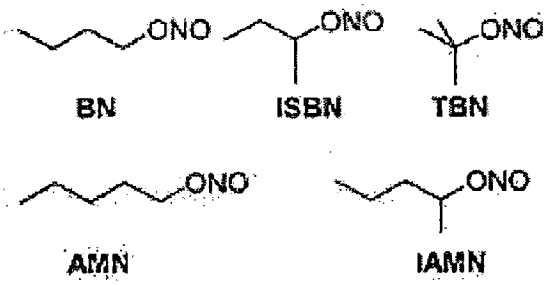

(b) Organic Nitrites

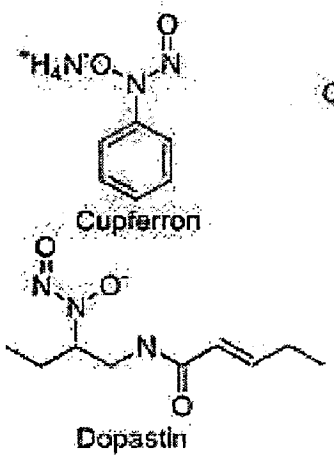

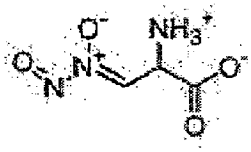

(c) Nitrosamines

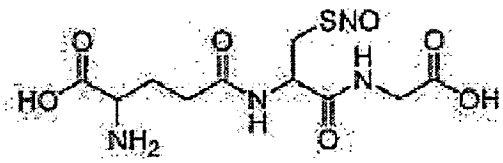

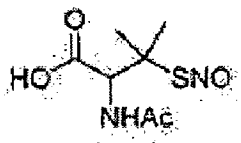

(d) Nitrosothiols

Figure 1.1: Various NO Donors

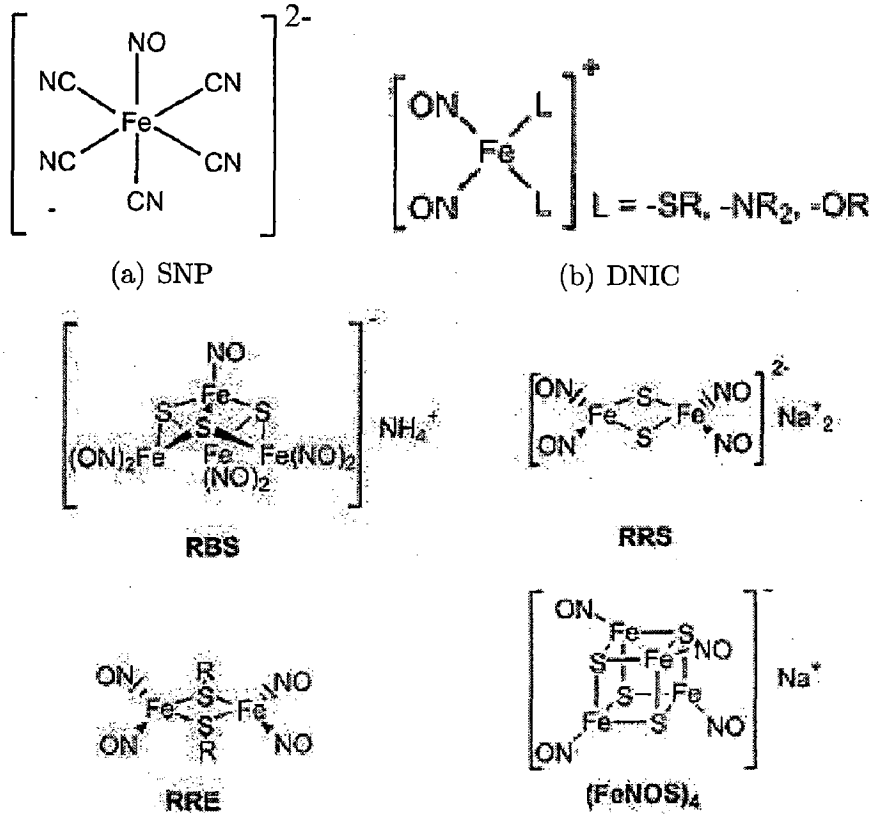

(a) SNP (b) DNIC

(c) Iron-Sulphur Cluster Nitrosyls

Figure 1.2: Various Metal-NO Donors

Synthetic iron-sulfur cluster nitrosyls include Roussins black salt, Roussins red salt (RBS, $[Fe_4S_3(NO)_7]^-$. RRS, $[Fe_2S_2(NO)_4]^{2-}$), Roussins red esters (RRE, R = aliphatic group, $Fe_2(SR)_2(NO)_4$), and tetranitrosyl-tetra-μ3-sulfidotetrahedro-tetrairon ($(FeNOS)_4$). RBS has been tested as an NO-releasing drug for thermo-/photochemical delivery of NO to vascular and brain tissues. RBS inhibits the ADP-induced platelet aggregation by extracellular release of NO. RBS, RRE, and $(FeNOS)_4$ have bacteriostatic effects.

Metal nitrosyl compounds (M-NO, M = Fe, Mn, Ru, Cr, Mo, etc.) and iron-porphyrin nitrosyls have recently come to light as photosensitive precursors of NO. To tune the release of NO the ligand frame around the metal centre has been varied.

1.2.4 *N*-Nitrosamines, *N*-Hydroxy-*N*-nitrosamines and *N*-Nitrosimines

N-Nitrosamines have been shown to be inhibitors of cysteine-containing enzymes. They exhibit vasodilation and mutagenicity as a result of NO release and have diabetogenic, carcinogenic, antimicrobial and antitumor activity.

Cupferron, alanosine, and dopastin belong to the *N*-Hydroxy-*N*-nitrosamines class. They are potent antihypertensive agents and inhibitors of platelet aggregation.

N-Nitrosimines inhibit platelet aggregation *in vitro*. Some of them also exhibit antithrombotic and blood pressure lowering abilities *in vivo*.

1.2.5 Nitrosothiols

Nitrosothiols (RSNOs) are unstable compounds and are proposed to be potential NO storage, transfer, and delivery vehicles. Many NO related biological functions have been directly associated with RSNOs. They have been shown to be intermediates of the function of some nitrovasodilators such as nitroglycerin. They themselves can be used as potent antiplatelet agents and vasodilators. RSNOs protect against cellular toxicity associated with oxidative stress. GSNO has been shown to protect the lung epithelium from oxidant-induced increases in monolayer permeability as well as the protection of endothelial cells from the toxic effects of oxidized low density lipoprotein. They can also inactivate aconitase and inhibit the uptake of norepinephrine in sympathetic neurons.

1.2.6 Other Classes of NO Donors

C – **Nitrosocompounds** contain a nitroso group attached to a carbon atom such as 2-methyl-2-nitrosopropane (MNP). MNP can be used for delivering NO in a photochemically controlled manner. Substituted MNPs have been shown to inhibit platelet aggregation and have considerable *in vitro* anti-platelet activity.

Diazetinedioxides(DD) are four-membered heterocycles known to exert strong vasorelaxation and anti-aggregation effects.

Furoxans have been shown to exert a variety of NO-related bioactivities, including cytotoxicity, mutagenicity, immunosuppression, central muscle relaxant properties, anticonvulsive effects, monoamino oxidase inhibition, and direct vasodilator and blood pressure lowering activities.

Benzofuroxans can be used as *in vitro* inhibitors of RNA synthesis in sheep lymphocytes, being potent antileukemic and immunosuppressive drugs. Derivatives of benzofuroxan have been found to be potent *in vivo* and *in vitro* vasodilators.

Oxatriazole – 5 – imines are potent blood pressure depressant, antiplatelet, fibrinolytic, thrombolytic, broncholytic agents and cause concentration dependent induction of apoptosis.

Sydnonimines have been used as antihypertensive agents. Molsidomine has been used in several European countries as an antianginal drug which brings about the reduction of the venous return, cardiac output, ventricular work, and myocardial oxygen consumption.

Oximes are potent vasodilators, have anti-platelet effects and have protective effects on ischemic acute renal failure in rats.

Hydroxylamines cause dose-dependent vasodilation in the blood vessels of rat kidneys, relax endothelium denuded rat aortic rings and rabbit aortic strips in a dose-dependent manner, inhibit insulin release and activate K^+ channels.

$N-$**Hydroxyguanidines**, combine the imino group of guanidine with hydroxylamino group of hydroxyurea. They have been shown to exhibit cytotoxicity in human leukemic cells, antitumor activity *in vivo* and antihypertensive activty.

Hydroxyurea, a derivative of hydroxylamine has been implicated as an antitumor agent. It is a standard therapy for chronic myelogenous leukemia, polycythemia vera, and myeloproliferative disorders, and is considered as an effective systemic agent for treatment of severe psoriasis, a persistent skin disease caused by an abnormality in the functioning of key white cells in the blood stream triggering skin inflammation. As an antiretroviral agent, hydroxyurea was found to block ribonucleotide reductase and result in inhibition of proviral DNA synthesis. This provides the basis to study the inhibition of human immunodeficiency virus (HIV) replication by hydroxyurea, making it a possible candidate for AIDS therapy.

1.3 Photolabile Metal Nitrosyl Complexes

Various research groups around the world are involved in synthesizing metal nitrosyl complexes for photorelease of NO. Mascharak and co-workers have synthesized numerous such complexes. $[Fe(PaPy_3)(NO)](ClO_4)_2$ ($PaPy_3H$ is N,N-bis(2-pyridylmethyl)amine-N-ethyl-2-pyridine-2-carboxamide), $[(PcPy_3)Fe(NO)](ClO_4)_2$ and $[(MePcPy_3)Fe(NO)](ClO_4)_2$ ($PcPy_3H$ is N-(2-pyridylmethyl)-2-(bis(2-pyridyl methyl)-amine)-ethanamide and $MePcPy_3H$ is N-(1-(2-pyridylethyl)-2-(bis(2-pyridyl methyl)-amine)-ethanamide) [23,24], belong to $\{Fe-NO\}^6$ family and rapidly release NO when exposed to light.

The $\{Mn-NO\}^6$ nitrosyl $[Mn(PaPy_3)(NO)]ClO_4$ too exhibits photolability of the bound NO [25]. The Ru(III) complex of the same ligand, $[Ru(PaPy_3)(NO)](BF_4)_2$, releases NO upon exposure to low intensity UV light [26]. To enhance photolability of $Ru-NO$ unit, this group utilized the greater light-harvesting properties of the quinoline moiety to synthesize $[Ru(PaPy_2Q)(NO)](BF_4)_2$ ($PaPy_2QH$ is N,N-bis

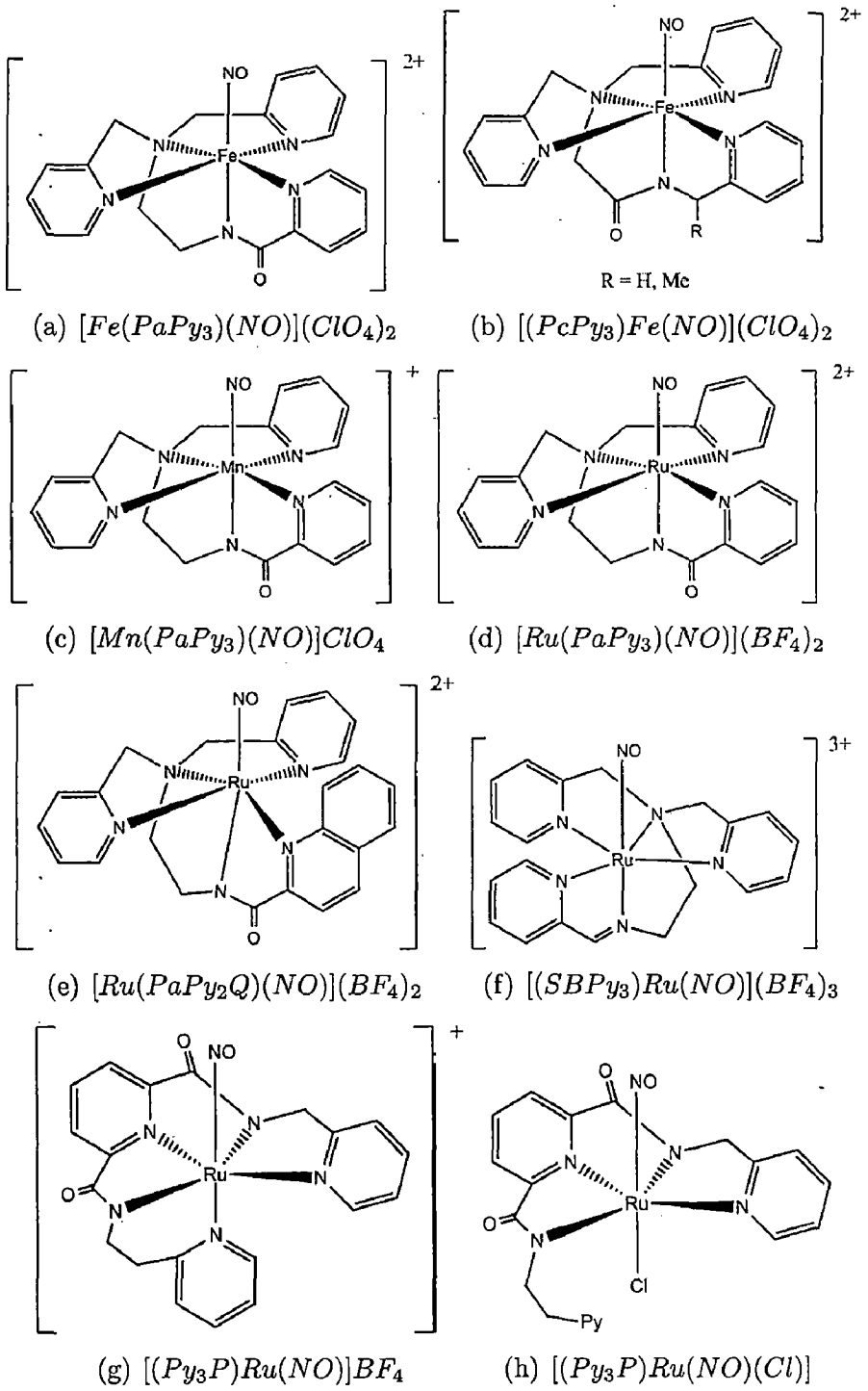

(a) $[Fe(PaPy_3)(NO)](ClO_4)_2$ (b) $[(PcPy_3)Fe(NO)](ClO_4)_2$

(c) $[Mn(PaPy_3)(NO)]ClO_4$ (d) $[Ru(PaPy_3)(NO)](BF_4)_2$

(e) $[Ru(PaPy_2Q)(NO)](BF_4)_2$ (f) $[(SBPy_3)Ru(NO)](BF_4)_3$

(g) $[(Py_3P)Ru(NO)]BF_4$ (h) $[(Py_3P)Ru(NO)(Cl)]$

Figure 1.3: Photolabile Metal Nitrosyls

(2-pyridylmethyl)amine-*N*-ethyl-2-quinaldine-2-carboxamide) [27,28].

$[(SBPy_3)Ru(NO)](BF_4)_3$ releases NO under low-intensity UV illumination while ($[(Py_3P)Ru(NO)]BF_4$ and $[(Py_3P)Ru(NO)(Cl)]$ (SBPy$_3$ is *N,N*-bis(2-pyridylmethyl) -amine-*N*-ethyl-2-pyridine-2-aldimine, Py$_3$PH$_2$ is *N,N*-bis(2-(2-pyridyl)ethyl)pyridine-2,6-dicarboxamide) exhibit considerable photoactivity under visible light [28,29]. This group investigated the effect of in-plane and axial ligands with carboxamide group in

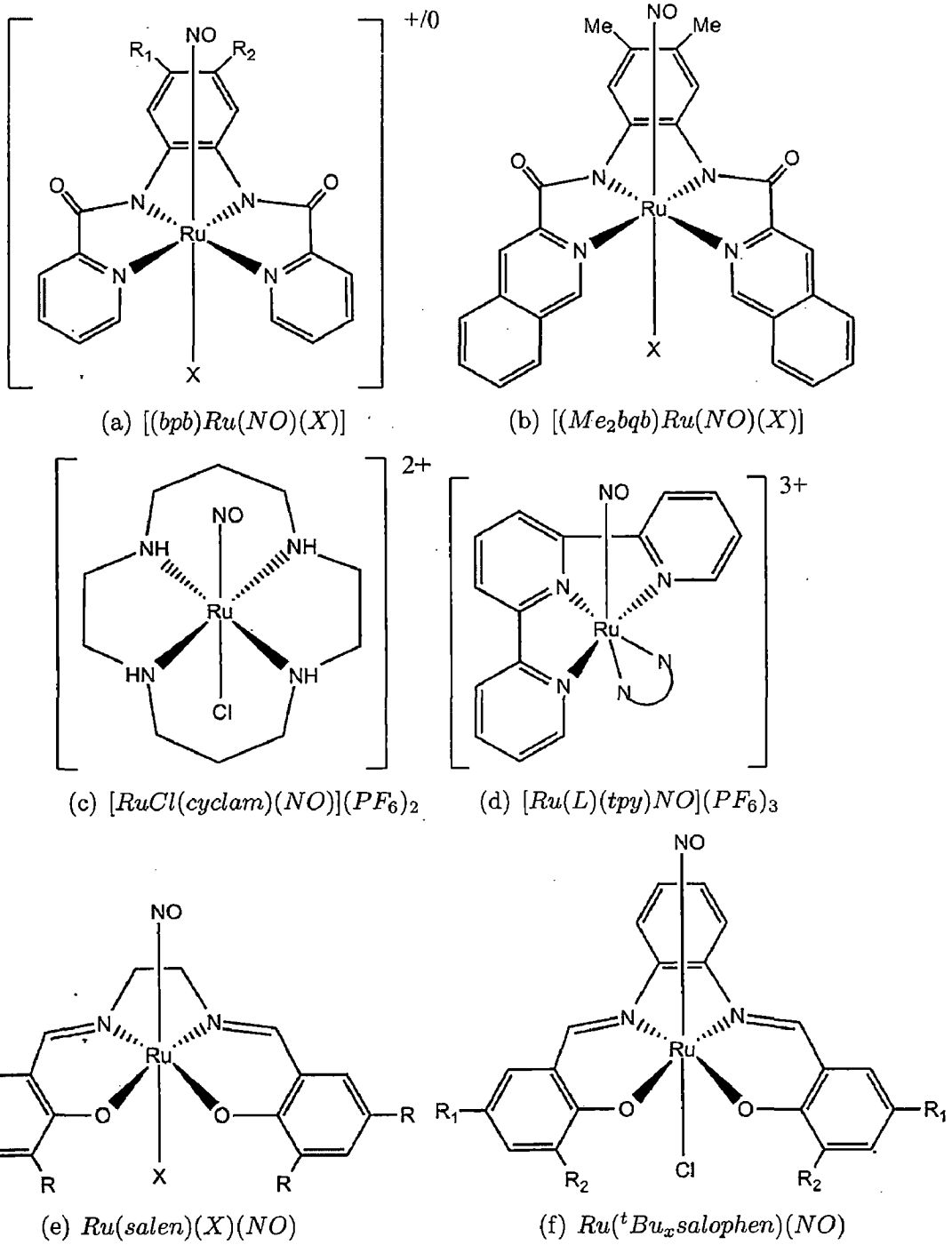

Figure 1.4: Photolabile Metal Nitrosyls

ruthenium nitrosyls by studying $[(bpb)Ru(NO)(Cl)]$, $[(Me_2bpb)Ru(NO)(Cl)]$, $[(Me_2bpb)Ru(NO)(py)](BF_4)$ and $[(Me_2bqb)Ru(NO)(Cl)]$ (py is pyridine, H_2bpb is 1,2-bis(pyridine-2-carboxamido) benzene, H_2Me_2bpb is 1,2-bis(pyridine-2-carboxamido)-4,5-dimethylbenzene, H_2Me_2bqb is 1,2-bis(quinaldine-2-carboxamido)-4,5-dimethylbenzene) [29,30].

To increase the photosensitivity of ruthenium nitrosyls to visible light, this group

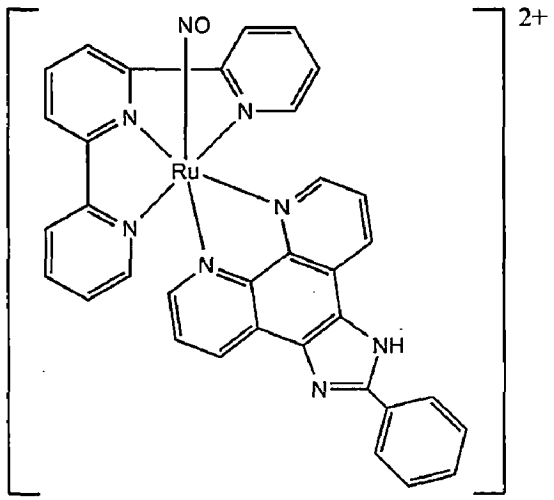

(a) $[Ru^{II}(trpy)(L)(NO^{\cdot})]^{2+}$

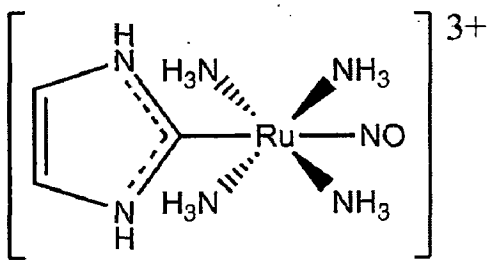

(b) *trans*-$[Ru(NH_3)_4(Im)(NO)]Cl_3$

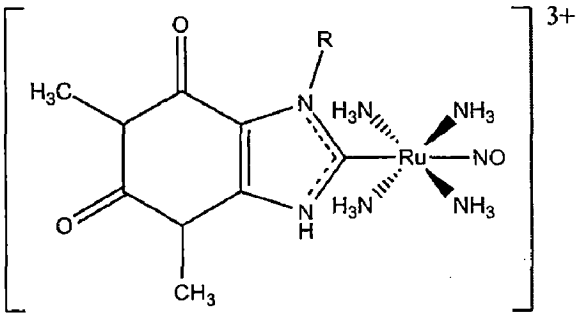

(c) *trans*-$[Ru(NH_3)_4L(NO)]Cl_3$

Figure 1.5: Photolabile Metal Nitrosyls

has synthesized $[(Me_2bpb)Ru(NO)(Resf)]$ and $[(Me_2bqb)Ru(NO)(Resf)]$ [31] using Resorufin dye molecule as ligand.

trans-$[RuCl(cyclam)(NO)](PF_6)_2$ (cyclam is 1,4,8,11-tetraazacyclotetradecane) has been reported by da Silva and co-workers to release NO on exposure to near UV radiation [32]. To determine the controlling factors of nitric oxide release, they studied the photoreactivity of $[Ru(bpy)(tpy)NO](PF_6)_3$, $[Ru(NH{\cdot}NHq)(tpy)NO](PF_6)_3$ and $[Ru(NH_2NH_2cat)(tpy)NO](PF_6)_3$ complexes (bpy is 2,2′-bipyridine, tpy is 2,2′:6′,2′′-terpyridine, NH·NHq is quinonediimine and NH2·NH2cat is *o*-phenylenediamine (*Figures 1.3,1.4*) [33].

$[Ru^{II}L(NH_3)_4(pz)Ru^{II}(bpy)_2(NO)](PF_6)_5$, a series of dinuclear nitrosyls synthesized by this group (L = NH_3, py, or 4-acpy) (py is pyridine, bpy is bipridine, pz is pyrazine, 4-acpy is 4-acetylpyridine) also exhibit photorelease of NO [34,35].

Franco and co-workers have studied the photoactivity of complexes of the type *trans*-$[Ru(NH_3)_4L(NO)](BF_4)_3$ (L = 4-pic, imN, L-Hist, py, nic, pz, isn, 4-acpy, $P(OEt)_3$ (4-pic is 4-picoline, imN is imidazole, L-Hist is L-histidine, py is pyridine, nic is nicotinamide, pz is pyrazine, isn is isonicotinamide, 4-acpy is 4-acetylpyridine, $P(OEt)_3$ is triethylphosphite) [36,37].

Ford and co-workers have synthesized and studied the photochemistry of various ruthenium nitrosyls of the type $Ru(L)(X)(NO)$ (L = salen, X= Cl^-, ONO^-, H_2O; L = ^{t}Bu$_4$salen, X = Cl^-; L = ^{t}Bu$_2$salophen, X = Cl^-; L = ^{t}Bu$_4$salophen, X = Cl^-) (salen is *N,N´*-ethylenebis(salicylideneiminato) dianion, ^{t}Bu$_4$salen = *N,N´*-ethylenebis(3,5-di-*tert*-butylsalicylideneiminato) dianion, ^{t}Bu$_2$salophen is *N,N´*-1,2-phenylenediaminebis(3-*tert*-butylsalicylideneiminato) dianion, ^{t}Bu$_4$salophen is *N,N´*-1,2-phenylenebis(3,5-di-*tert*-butylsalicylideneiminato) dianion) [38,39].

$[Ru_3O(CH_3CO_2)_6(pic)_2(NO)]PF_6$ (pic is 4-methylpyridine), a triruthenium nitrosyl cluster with the ability to donate NO photochemically, has been synthesized by Tomazela and co-workers [40].

Lahiri and co-workers have demonstrated the facile photorelease of NO from $[Ru^{II}(trpy)(L)(NO^{\cdot})]^{2+}$ (L = 2-phenylimidazo[4,5-f]1,10-phenanthroline, trpy is 2,2´:6´,2´´-terpyridine) and subsequent trapping of thus released NO with reduced myoglobin (*Figure 1.5*) [41].

Lopes and co-workers have synthesized a series of organoruthenium nitrosyl complexes *trans*-$[Ru(NH_3)_4L(NO)]Cl_3$, L = caffeine, theophylline, imidazole and benzoimidazole in position trans to NO and have reported that these complexes release NO under light irradiation at 330-440 nm [42,43].

1.4 Tuning Photorelease of NO

In a thorough study of the above cited ruthenium nitrosyls, Mascharak and Rose [18,29] have concluded that "*rational ligand design*" and "*coupling to coordinating chromophores*" enables us to tune photorelease of NO. Increasing the number of anionic σ-donors such as amines, phenolates, carboxamides or increasing the electron-donating capacity of coordinating ligands to modulate the energy of the $d_\pi(Ru) \rightarrow \pi^*(NO)$ transition to shift maximum absorption to visible region or use light trapping/ sensitizing dye molecules to enhance absorption of visible light resulting in increased release of NO.

Table 1.1: Ligand Frames of Various Photolabile Metal Nitrosyl Complexes.

Complex	***Ligand Frame***	***Reference***
$[Fe(PaPy_3)(NO)](ClO_4)_2$	Axial NO	[23]
$[(PcPy_3)Fe(NO)](ClO_4)_2$	Axial carboxamido N	
$[(MePcPy_3)Fe(NO)](ClO_4)_2$	Equatorial *tert*-amine N	[24]
$[Mn(PaPy_3)(NO)]ClO_4$	Two equatorial pyridine N	[25]
$[Ru(PaPy_3)(NO)](BF_4)_2$		[26]
$[Ru(PaPy_2Q)(NO)](BF_4)_2$	NO carboxamido N Two pyridine N quinoline N	[27,28]
$[(SBPy_3)Ru(NO)](BF_4)_3$	NO imine N Three pyridine N	[28,29]
$[(Py_3P)Ru(NO)]BF_4$	NO Two carboxamido N Three pyridine N	[28,29]

Continued on Next Page...

Table 1.1 – Continued

Complex	***Ligand Frame***	***Reference***
$[(Py_3P)Ru(NO)(Cl)]$	NO Two carboxamido N Two pyridine N Cl^-	[28,29]
$[(bpb)Ru(NO)(Cl)]$ $[(Me_2bpb)Ru(NO)(Cl)]$		[29,30]
$[(Me_2bpb)Ru(NO)(py)](BF_4)$	NO Two carboxamido N Three pyridine N	[29,30]
$[(Me_2bqb)Ru(NO)(Cl)]$	NO Two carboxamido N Two quinoline N Cl^-	[29,30]
$[(Me_2bpb)Ru(NO)(Resf)]$	NO Two carboxamido N Two pyridine N Resorufin O^-	[31]
$[(Me_2bqb)Ru(NO)(Resf)]$	NO Two carboxamido N Two quinoline N Resorufin O^-	[31]

Continued on Next Page...

Table 1.1 – Continued

Complex	***Ligand Frame***	***Reference***
trans-$[RuCl(cyclam)(NO)](PF_6)_2$	NO Four secondary amine N Cl^-	[32]
$[Ru(bpy)(tpy)NO](PF_6)_3$ $[Ru(NH{\cdot}NHq)(tpy)NO](PF_6)_3$ $[Ru(NH_2NH_2cat)(tpy)NO](PF_6)_3$	NO Three terpyridine N Two bipyridine N or two quinonediimine N or two *o*-phenylenediamine N	[33]
$Ru(L)(X)(NO)$ L = ^{t}Bu$_4$salen, X = Cl^- L = ^{t}Bu$_4$salophen, X = Cl^- L = ^{t}Bu$_2$salophen, X = Cl^- L = salen, X= Cl^-, ONO^-, H_2O	NO Two phenolato O^- Two imine N	[38,39]
$[Ru^{II}(trpy)(L)(NO^{\cdot})]^{2+}$	NO Three terpyridine N Two phenanthroline N	[41]
trans-$[Ru(NH_3)_4L(NO)]Cl_3$ L = caffeine (R=H), theophylline (R=Me), imidazole, benzoimidazole.	NO Four ammine N Ligand L carbon	[42,43]

1.5 Comparison of Ligand Frames of Photolabile Metal Nitrosyls

A comparison among the ligand frames of the various photolabile metal nitrosyl complexes (*Table 1.1*) reveals that nitrogen donors such as carboxamido, imine, amine, pyridine, quinoline; phenolato donors and carbanion donors promote photolability of NO from such complexes.

In light of the above drawn conclusion, in the present study complexes were prepared with a tridentate ligand having a phenolato, an imine nitrogen and a carbanion donor sites besides two triphenylphosphine donors.

Chapter 2

Materials and Methods

2.1 Materials

Chemicals and solvents used in the synthesis of ligands, ruthenium complexes and in the experiments involving transfer of NO to myoglobin have been enlisted in *Table 2.1.* Various laboratory glassware and equipments were also used.

2.2 Methods

2.2.1 Synthesis of Ligands

(a). *2-(benzylideneamino)phenol* (L^1) was synthesized by refluxing 0.224 g (2.05 mmol) of 2-aminophenol with 0.214 g (2 mmol) benzaldehyde in 20 mL ethanol for 2h. On addition of distilled water yellow coloured flakes of the ligand were obtained which were separated by filtration and dried (*Figure 2.1*).

(b). *2-(4-chlorobenzylideneamino)phenol* (L^2) was synthesized by refluxing 0.224 g (2.05 mmol) of 2-aminophenol with 0.281 g (2 mmol) *p*-chlorobenzaldehyde in 20 mL ethanol for 2h. On addition of distilled water dull yellow coloured flakes of the ligand were obtained which were separated by filtration and dried.

(c). *2-(3-nitrobenzylideneamino)phenol* (L^3) was synthesized by refluxing 0.224 g (2.05 mmol) of 2-aminophenol with 0.302 g (2 mmol) *m*-nitrobenzaldehyde in 20 mL ethanol for 2h. On addition of distilled water bright yellow coloured flakes of the ligand were obtained which were separated by filtration and dried.

Table 2.1: Chemicals and Solvents Used

S.No.	*Chemical*	*Grade*	*Make*
1.	2-aminophenol	GR	Loba Chemie
2.	Benzaldehyde	AR	SRL
3.	*p*-chlorobenzaldehyde	AR	SRL
4.	*m*-nitrobenzaldehyde	AR	SRL
5.	*p*-chlorobenzaldehyde	AR	SRL
6.	Triphenylphosphine	Pure	SRL
7.	Ruthenium(III)Tricholride Trihydrate	Pure	SRL
8.	Sodium Nitrite	LR	Rankem
9.	Sodium dihydrogen phosphate dihydrate	AR	Chemport
10.	Disodium hydrogen phosphate anhydrous	AR	Rankem
11.	Sodium Dithionite	GR	Loba Chemie
12.	Myoglobin from equine skeletal muscle	95-100%	Sigma
13.	Sulphuric Acid	AR	Rankem
14.	Ethanol absolute	AR	Changshu Yangyuan
15.	Methanol	AR	s.d.fine
16.	Benzene	AR	SRL
17.	Dichloromethane	LR	Rankem

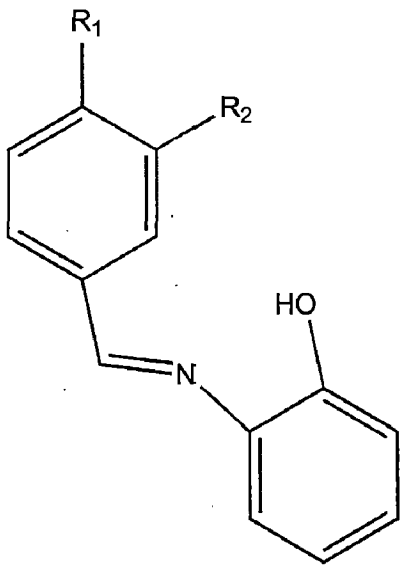

Figure 2.1: Ligand L^n (n=1,R_1=H,R_2=H;n=2,R_1=-Cl,R_2=H;n=3,R_1=H,R_2=-NO_2)

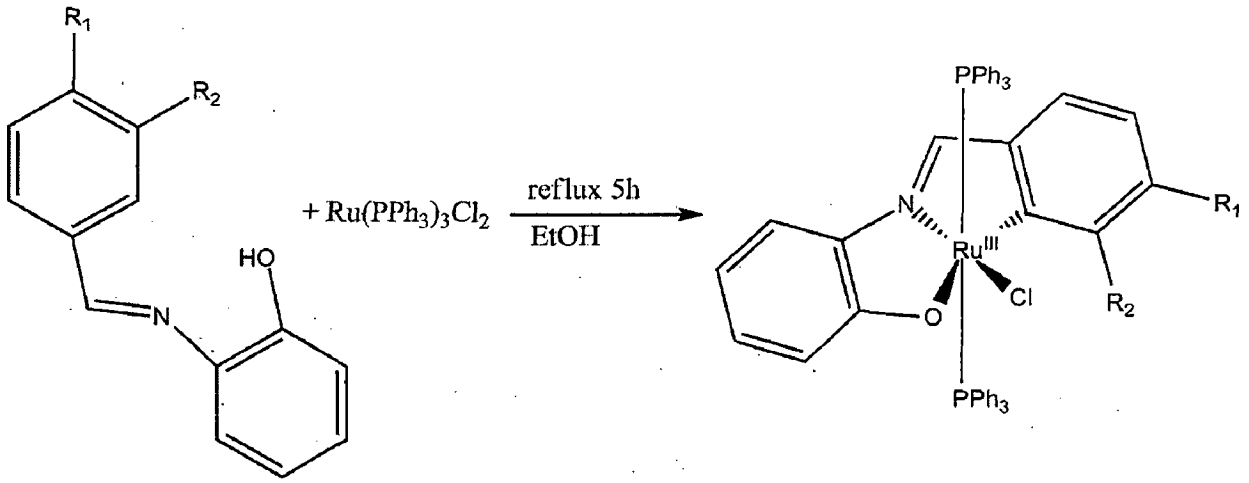

Figure 2.2: Synthesis of $Ru(PPh_3)_2L^nCl$

2.2.2 Synthesis of Ruthenium Complexes

(a). *Dichlorotris(triphenylphosphine)ruthenium(II)* $Ru(PPh_3)_3Cl_2$ was synthesized by the following procedure described by Stephenson and Wilkinson [44]. 1.2 g triphenylphosphine was dissolved in about 30 mL methanol by refluxing. 0.2 g ruthenium(III) chloride trihydrate was dissolved in about 5 mL methanol and added dropwise to the triphenylphosphine solution. Reaction mixture was refluxed for 1.5h, cooled and filtered to give reddish brown crystals of the product.

The complexes $Ru(PPh_3)_2L^1Cl$ and $Ru(PPh_3)_2L^2Cl$ were synthesized by procedure described by Chakravorty and co-workers [45].

(b). *Synthesis of* $Ru(PPh_3)_2L^1Cl$. 0.960 g (0.10 mmol) of $Ru(PPh_3)_3Cl_2$ was suspended in 20 mL ethanol, 0.060 g (0.3 mmol) of ligand L^1 was added and refluxed for 5h. The reaction mixture was filtered after cooling and washed with ethanol to give purple solid (*Figure 2.2*).

(c). *Synthesis of* $Ru(PPh_3)_2L^2Cl$. 0.960 g (0.10 mmol) of $Ru(PPh_3)_3Cl_2$ was suspended in 20 mL ethanol, 0.070 g (0.3 mmol) of ligand L^2 was added and refluxed for 5h. The reaction mixture was filtered after cooling and washed with ethanol to give purple solid.

(d). *Synthesis of* $Ru(PPh_3)_2L^3Cl$ 0.960 g (0.10 mmol) of $Ru(PPh_3)_3Cl_2$ was suspended in 20 mL ethanol, 0.121 g (0.5 mmol) of ligand L^3 was added and refluxed for 5h. The reaction mixture was filtered after cooling and washed with ethanol to give purple solid.

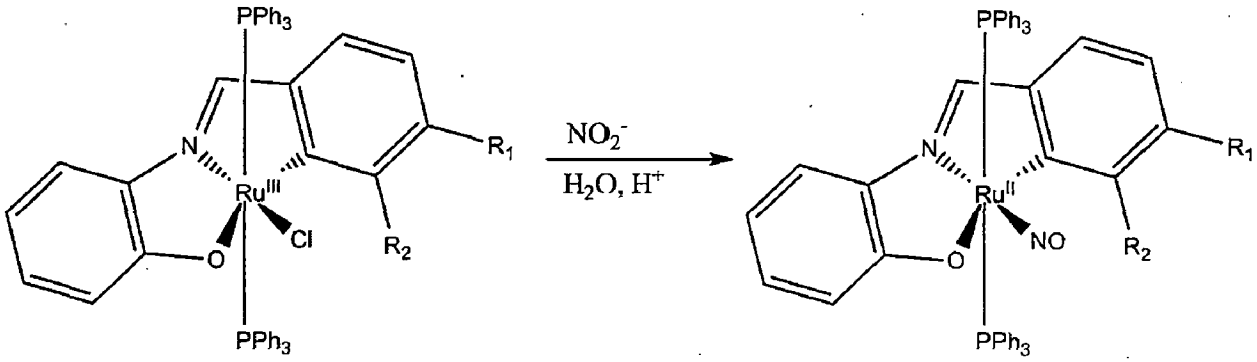

Figure 2.3: Synthesis of $Ru(PPh_3)_2L^n(NO)$

2.2.3 Synthesis of Ruthenium Nitrosyl Complexes

Synthesis of $Ru(PPh_3)_2L^n(NO)$. This complex was prepared as and when needed. A few grains of the complex $Ru(PPh_3)_2L^nCl$ (n=1-3) were dissolved in benzene to obtain a violet coloured solution. This solution was layered over distilled water mildly acidified with concentrated sulphuric acid in a 5 mL glass vial. A few grains of *sodium nitrite* were added to the vial (*Figure 2.3*). The colour of the benzene layer immediately turned orange-red due to formation of $Ru(PPh_3)_2L^n(NO)$. The benzene layer was pipetted out into an amber glass vials to protect from light. The solution was heated in a boiling water bath to completely remove benzene.

2.2.4 Testing Photolability of $Ru(PPh_3)_2L^n(NO)$

(a). *Preparation of stock solution of* $Ru(PPh_3)_2L^nCl$. 10 mg of $Ru(PPh_3)_2L^nCl$ was dissolved in benzene and the volume was made up to 10 mL in a volumetric flask.

(b). *Testing Photolability of* $Ru(PPh_3)_2L^n(NO)$. 3 mL of the above prepared stock solution was converted to $Ru(PPh_3)_2L^n(NO)$ by procedure described above. 2 mL of the orange-red benzene layer was pipetted out into a glass vial. The vial was kept in sunlight. 200 μL of sample was withdrawn at regular intervals of time and immediately analyzed for change in UV-Vis spectrum.

2.2.5 Transfer of NO to Myoglobin

(a). *Preparation of Phosphate Buffer.* 50 mM phosphate buffer of $\approx$ 6.8 pH was prepared by adding 0.4192 g of *sodium dihydrogen phosphate dihydrate* and 0.3283 g of *disodium hydrogen phosphate anhydrous* to 50 mL of MilliQ water and making the volume to 100 mL in a 100 mL volumetric flask.

(b). *Preparation of Myoglobin Stock Solution.* 5 mg equine skeletal muscle myoglobin was thoroughly suspended in 5 mL of the above prepared buffer.

(c). *Reduction of Myoglobin.* To an aliquot of the above prepared myoglobin stock solution, a few grains of *sodium dithionite* were added to reduce the iron center.

(d). *Preparation of Myoglobin-NO Adduct.* To an aliquot of the above prepared reduced myoglobin solution, a few grains of *sodium nitrite* were added to generate NO *in situ* resulting in formation of *myoglobin-NO* adduct.

(e). *Standard UV-Vis Spectra* for the above prepared solution were obtained against phosphate buffer as reference. 150 μL of myoglobin stock solution was diluted to 3000 μL in quartz cuvette and its UV-Vis spectrum was obtained. To obtain spectrum for reduced myoglobin, a few grains of *sodium dithionite* were added to the solution in the cuvette to reduce the myoglobin. A few grains of *sodium nitrite* were added to the reduced myoglobin solution in the cuvette to obtain spectrum for *myoglobin-NO* adduct.

(f). *Transfer of NO to Myoglobin.* 1 mL of $Ru(PPh_3)_2L^nCl$ stock solution was converted to $Ru(PPh_3)_2L^n(NO)$ by procedure described above. After removal of benzene, the product was dissolved in 1 mL of dichloromethane. 500 μL reduced myoglobin stock solution was layered over 500 μL of above prepared solution of $Ru(PPh_3)_2L^n(NO)$ in dichloromethane in a glass vial. The vial was kept in sunlight for 5 minutes after which 300 μL of the aqueous layer was pipetted out and immediately analyzed for change in UV-Vis spectrum.

(g). *Control Experiment.* A control experiment was run simultaneously with the transfer experiment following the same procedure as for the transfer experiment except that the vial was kept in complete darkness. 300 μL of the aqueous layer was pipetted out and immediately analyzed for change in UV-Vis spectrum.

2.3 Physical Measurements

2.3.1 Infrared Spectroscopy

Infrared spectroscopy is a technique based on the vibrations of the atoms of a molecule. An infrared spectrum is obtained by passing infrared radiation through a sample and determining what fraction of the incident radiation is absorbed at a particular energy. The energy at which any peak in an absorption spectrum appears corresponds to the

frequency of a vibration of a part of a sample molecule. IR spectroscopy thus aids in the identification of functional groups. Metal complexes or chelates are largely covalent in nature and the spectra of such compounds are dominated by the contribution of the ligand and its coordination chemistry. Organometallic compounds contain ligands that bond to metal atoms or ions through carbon bonds. Aromatic organometallic molecules show a strong band near 1430 cm^{-1}, due to benzene ring stretching for metals directly attached to the benzene ring.

IR spectra of all the compounds were recorded in the range 4000 to 400 cm^{-1} as KBr discs on Thermo Nicolet Nexus FT-IR spectrometer.

2.3.2 UV - Visible Spectrophotometry

Many complexes of metals with organic ligands absorb in the visible part of the spectrum and are important in qualitative analysis. The colours arise from $d \leftrightarrow d$ transitions within the metal ion, which usually produce absorptions of low intensity; and $n \rightarrow \pi^*$ and $\pi \rightarrow \pi^*$ transitions within the ligand. Another type of transition, known as *charge transfer*, may also operate, where an electron is transferred between an orbital in the ligand and an unfilled orbital of the metal, or vice versa. Charge transfers give rise to more intense absorption bands which are of analytical importance.

UV-Vis spectra of the complexes and myoglobin experiments were recorded on Thermo Scientific Evolution 600 spectrophotometer.

2.3.3 Gas Chromatography - Mass Spectrometry

Gas chromatography separates solutes that differ in their vapour pressure and/or intensity of solute-stationary phase interaction. The chromatogram provides information about the complexity (number of components), quantity (peak height or area) and identity (retention parameter) of the components in a mixture. A mass spectrometer produces a mass spectrum, which is histogram of the relative abundance of the ions generated by ionization of the sample and their mass-to-charge ratio *(m/z)*. The mass spectrum is a fingerprint of the molecule conveying information about its molecular weight, and if fragmentation occurs during ionization, structurally useful fragment ions characteristic of the bond order of the structure. By using gas chromatography hyphenated with mass spectrometry, the identity of the sample can be firmly established.

This technique was used to analyze the ligands on Perkin Elmer Clarus 500 Gas Chromatograph hyphenated to Perkin Elmer Clarus 500 Mass Spectrometer.

2.3.4 Nuclear Magnetic Resonance Spectroscopy

Nuclear magnetic resonance (NMR) detects signals from the absorption of radio frequency energy by nuclei placed in a strong and homogeneous magnetic field. The circulation of electrons around the nucleus creates local magnetic environments, resulting in characteristic chemical shifts suitable for functional group identification. The presence of coupling between pairs of nuclei extending over 1 to 3 bonds establishes the connectivity between atoms and provides a powerful tool for structure determination including stereochemical information. Thus, the particular strengths of NMR are its ability to differentiate between most structural, conformational, and optical isomers, and the possibility of complete structural elucidation of unknown compounds with a known molecular mass.

The ^{1}H nucleus is the most commonly studied nucleus by NMR spectroscopy because of its high natural abundance (99.98%) and the fact that it is invariably present in majority of compounds. Proton magnetic resonance spectrum provides information about the number of different types of protons and the nature of the immediate environment of each of them.

The ^{13}C nucleus has low natural abundance (1.1%) and is important because carbon forms the backbone of all organic compounds and valuable structural information can be derived by ^{13}C NMR spectroscopy. It is usually possible to get good proton decoupled ^{13}C NMR spectra from most organometallic complexes in a reasonable time. Unfortunately, integration of carbon spectra is rarely reliable, in part because of the wide range of relaxation times encountered.

^{31}P NMR spectroscopy is very useful in studying phosphine complexes. Normally all the ligand protons are decoupled so as to simplify the spectra. The *cis-* or *trans-* configuration of two triphenylphosphine ligands present in a complex can easily be determined by ^{31}P NMR spectrum.

NMR spectra were recorded on Bruker Avance 500 MHz NMR Spectrometer for ligands and ruthenium nitrosyl complexes.

Chapter 3

Results and Discussion

3.1 Characterization of Ligands

The ligands L^1, L^2 and L^3 were characterized by IR spectroscopy, GC-MS and NMR spectroscopy. In the IR spectra of all three ligands (*Figures 3.1-3.3*), C=N stretching frequency was observed ~1625 cm^{-1}, suggesting the formation of the ligands. The OH stretching was observed in the region 3300 to 3350 cm^{-1}. Well resolved gas chromatograms (*Figures 3.4-3.9*) were obtained for all the ligands with retention times ranging from 13 to 18 minutes. The base and molecular ion peaks in the mass spectra established the formation of the ligands. An account of the above characteristics of the ligands is summarized in *Table 3.1.* The NMR spectra for the ligands are as shown in *Figures 3.10-3.13.*

Table 3.1: Characteristics of Ligands

Ligand	$\nu_{C=N}$ cm^{-1}	ν_{OH} cm^{-1}	*Retention Time* minutes	*m/z Base Peak*	*m/z Molecular Ion Peak*
L^1	1625	3329	13.26	120	197
L^2	1626	3308	14.60	120	232
L^3	1629	3346	17.63	240	242

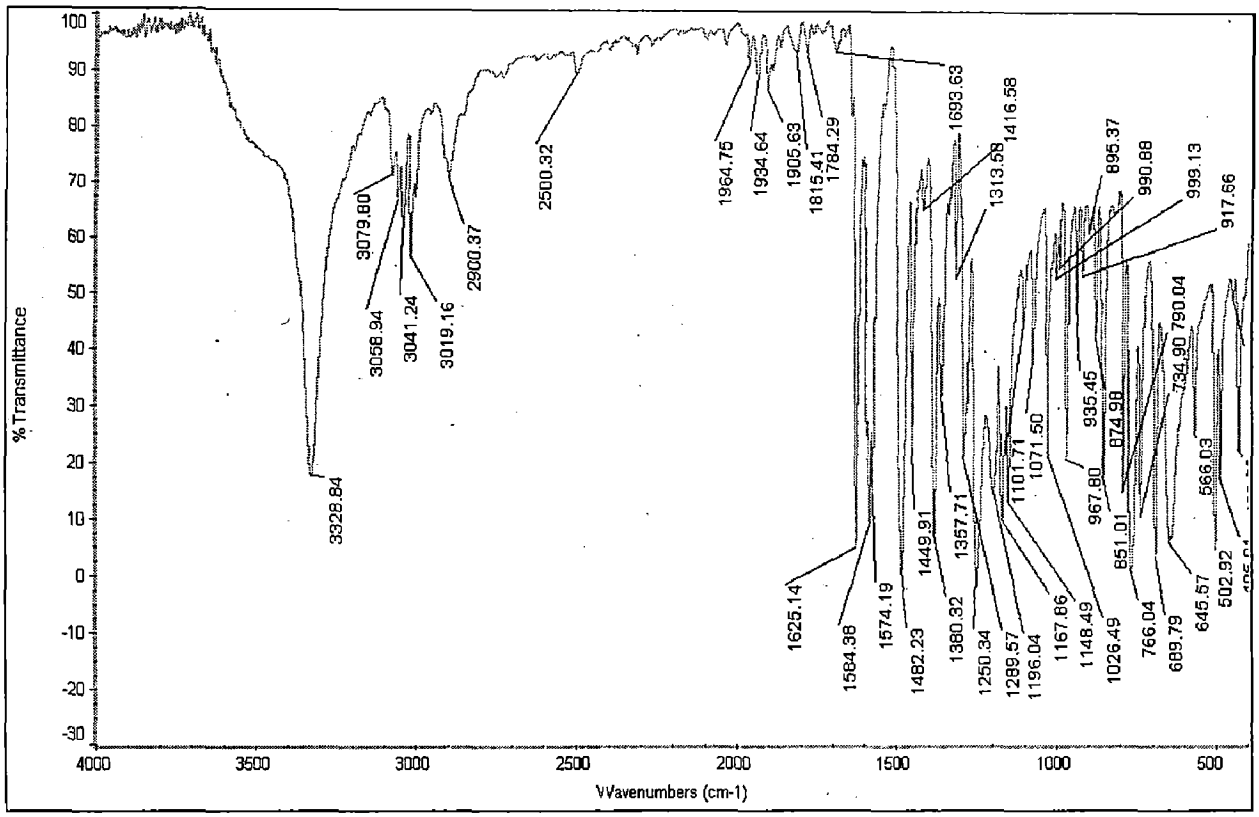

Figure 3.1: IR Spectrum of Ligand L^1

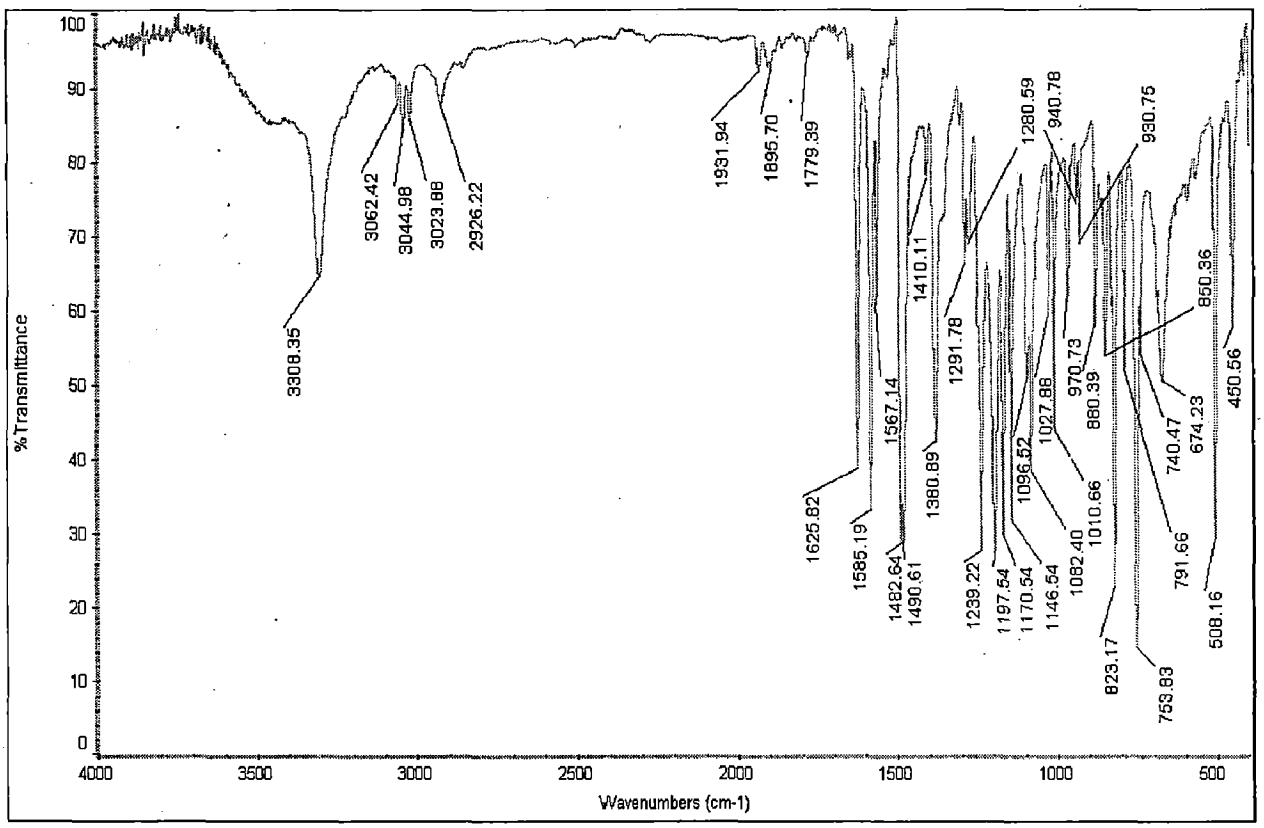

Figure 3.2: IR Spectrum of Ligand L^2

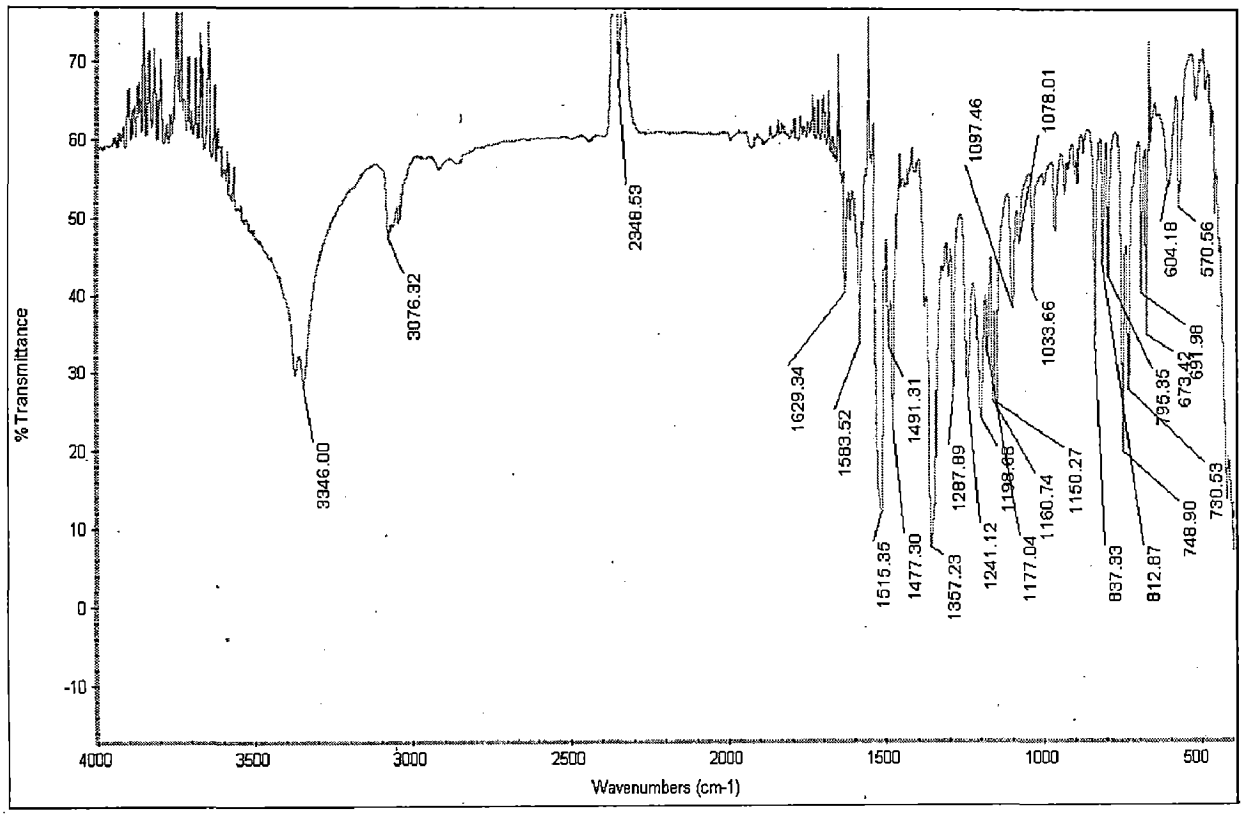

Figure 3.3: IR Spectrum of Ligand L^3

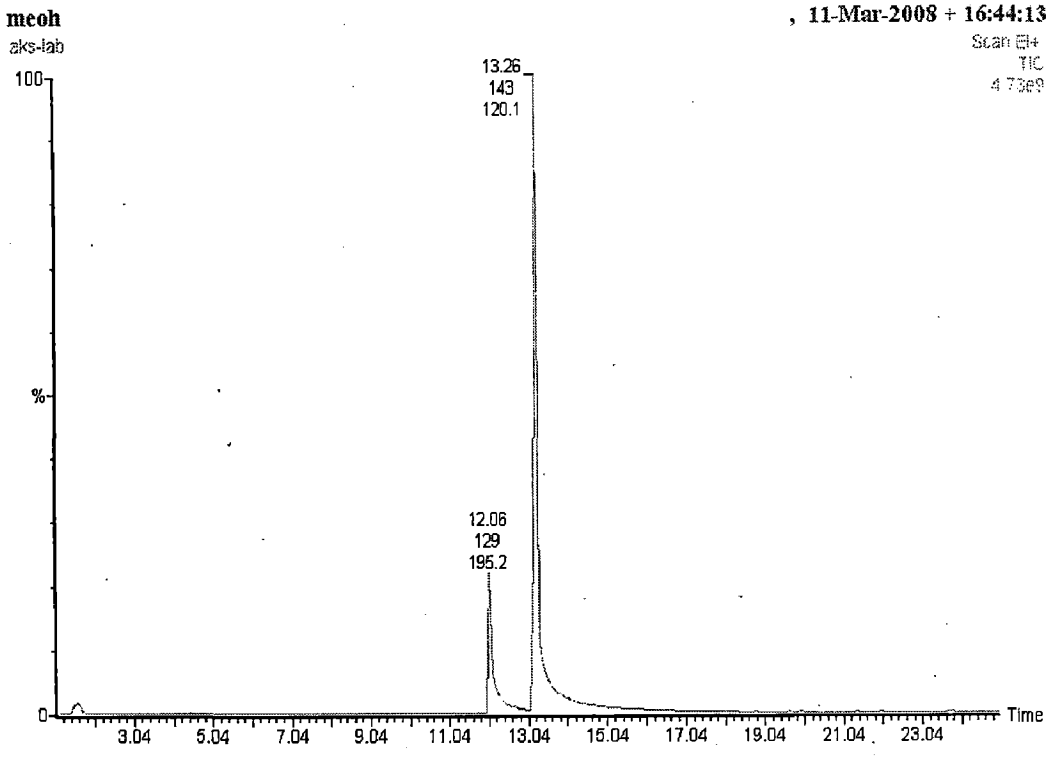

Figure 3.4: Gas Chromatogram of Ligand L^1

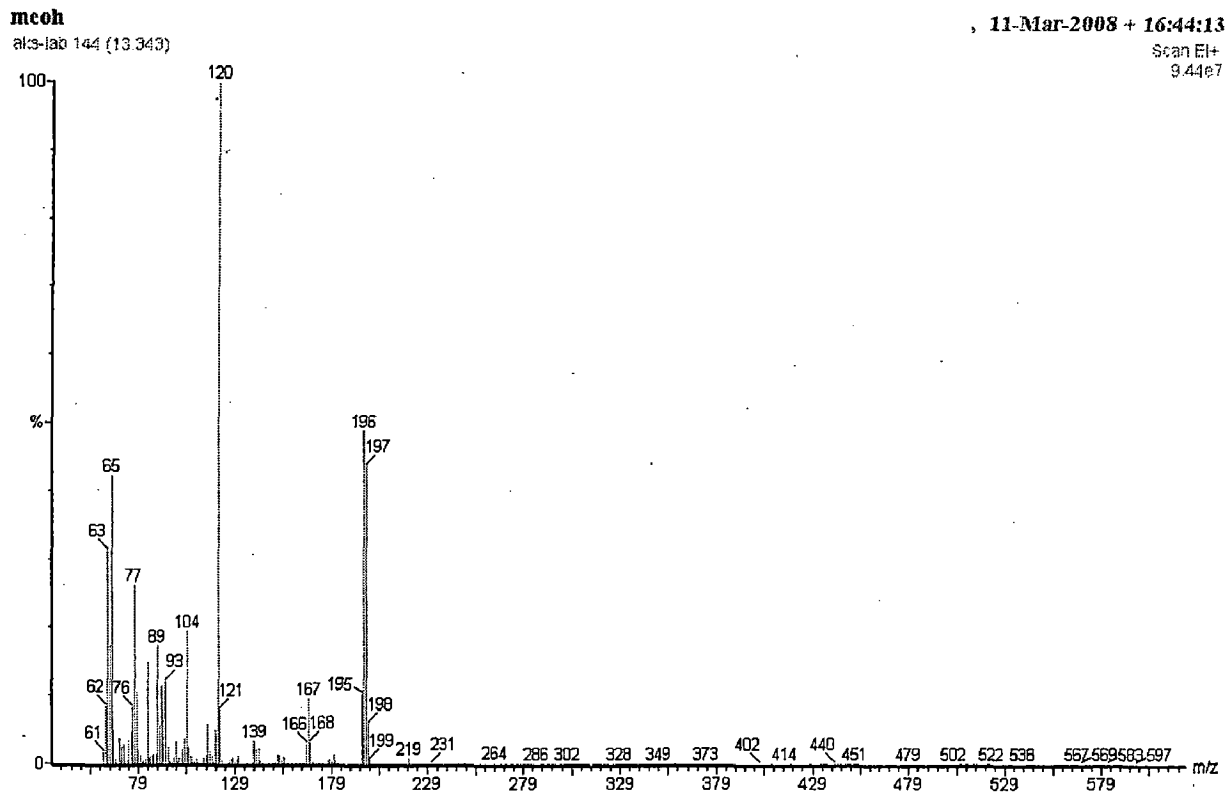

Figure 3.5: Mass Spectrum of Ligand L^1

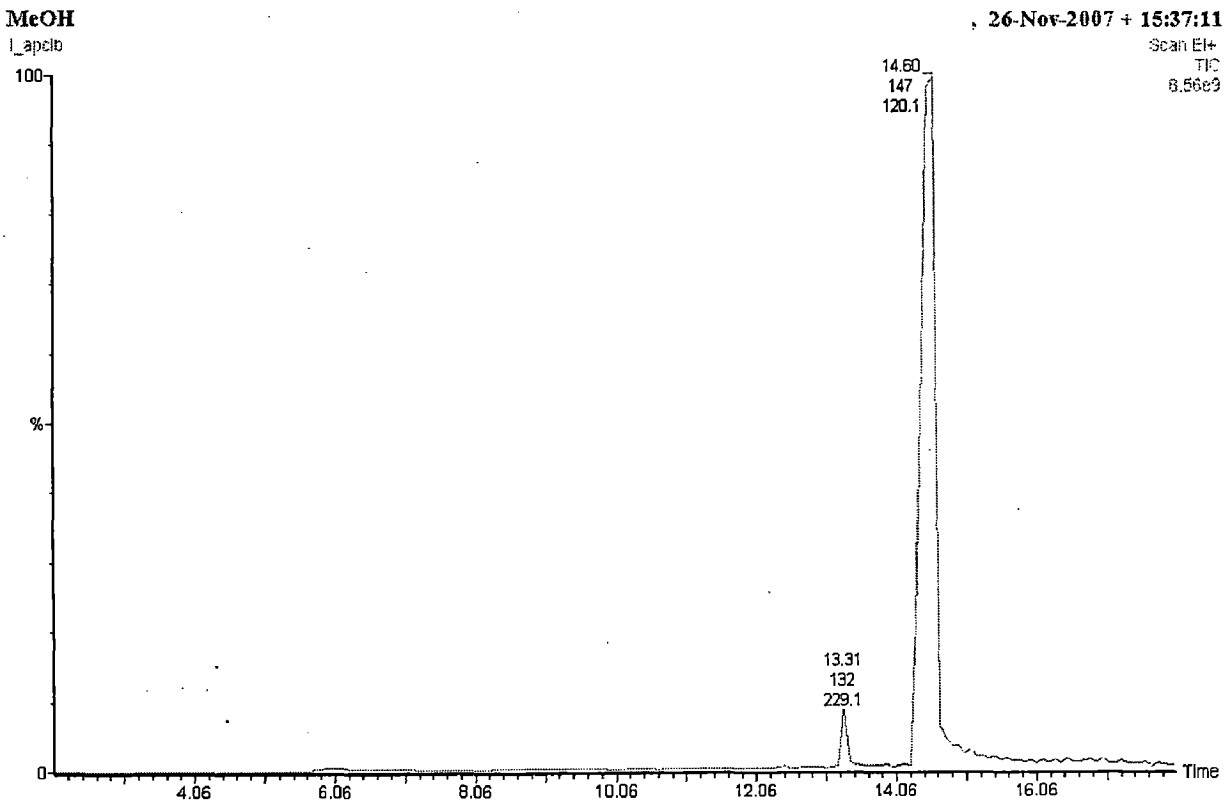

Figure 3.6: Gas Chromatogram of Ligand L^2

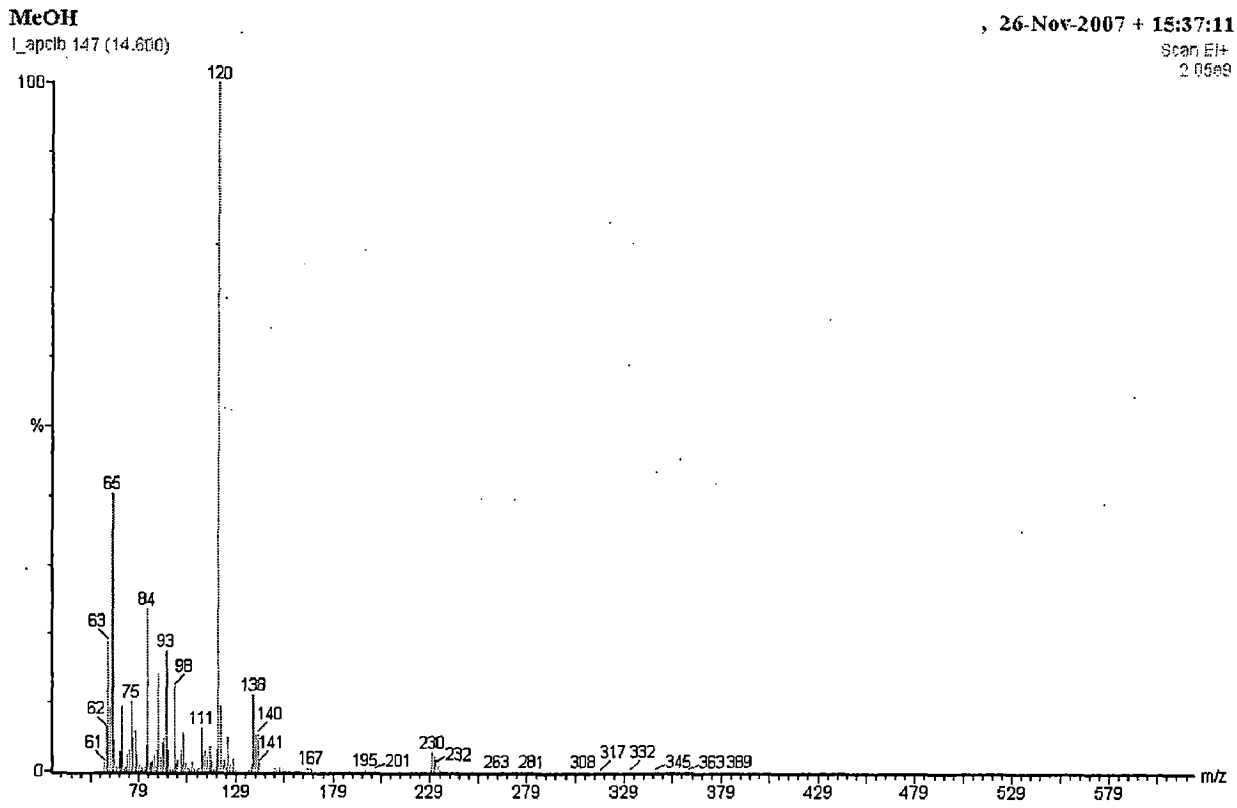

Figure 3.7: Mass Spectrum of Ligand L^2

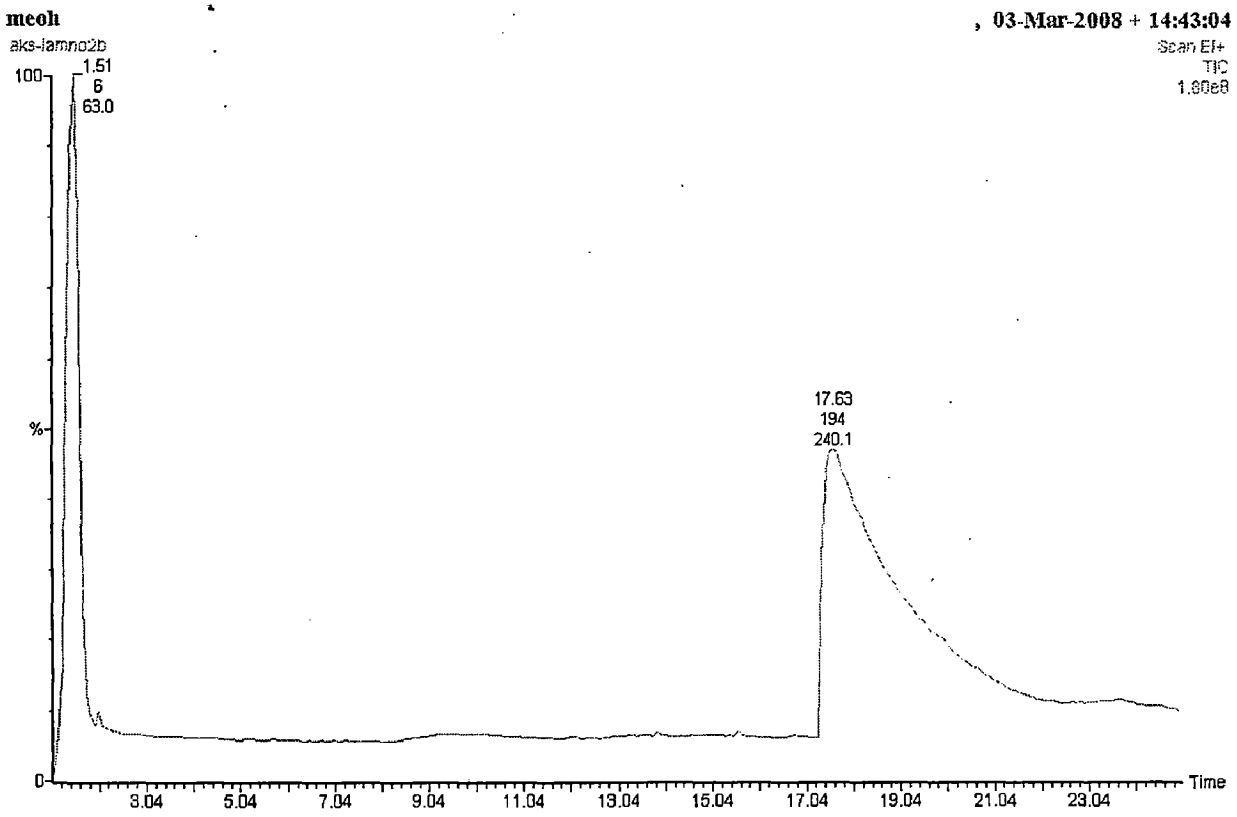

Figure 3.8: Gas Chromatogram of Ligand L^3

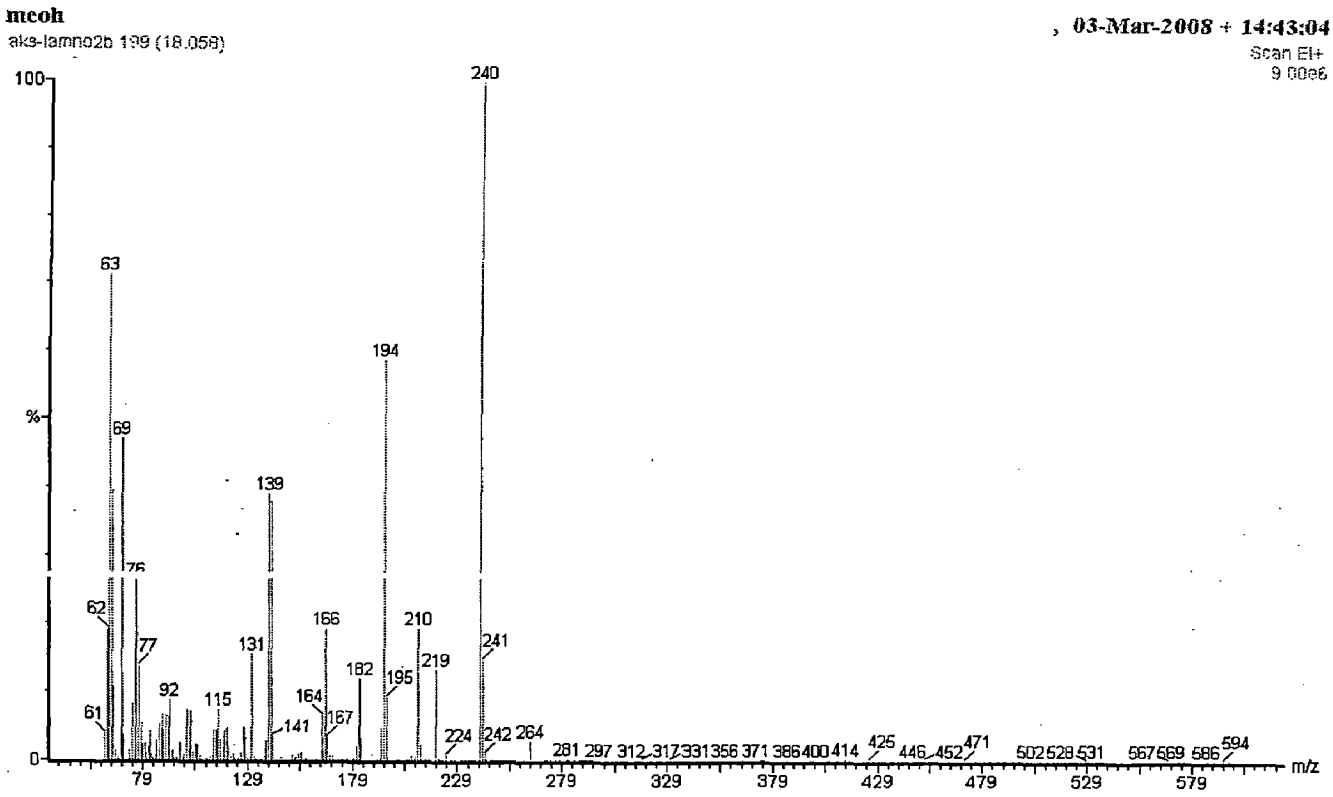

Figure 3.9: Mass Spectrum of Ligand L^3

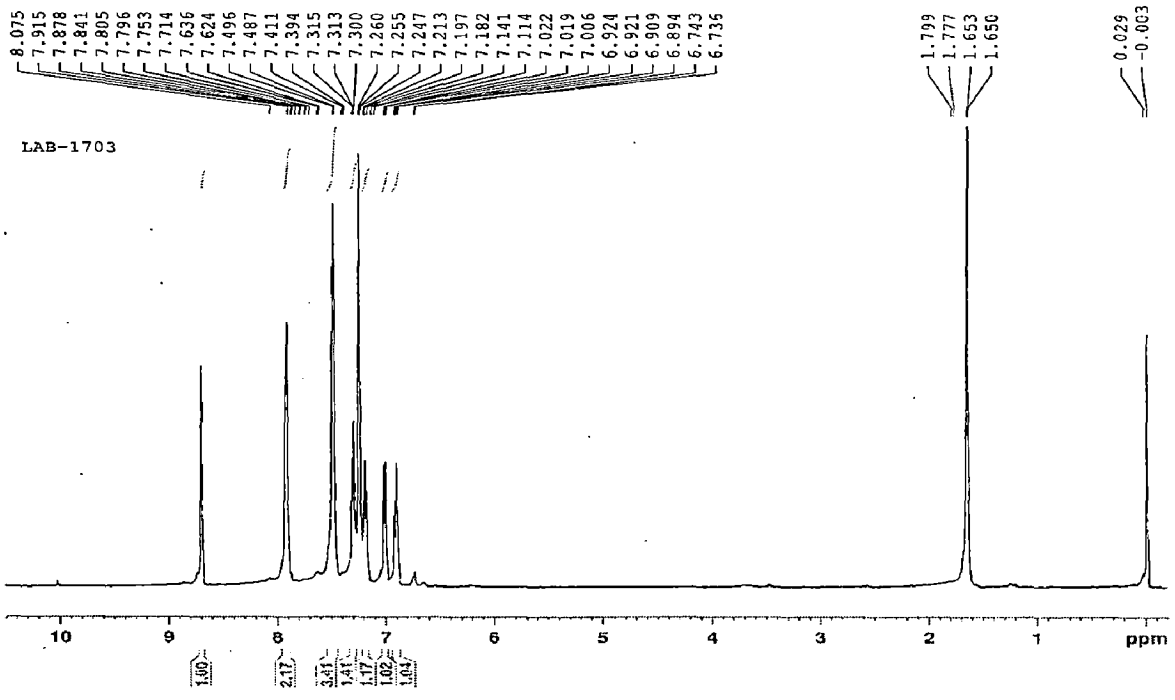

Figure 3.10: ^1H NMR Spectrum of Ligand L^1

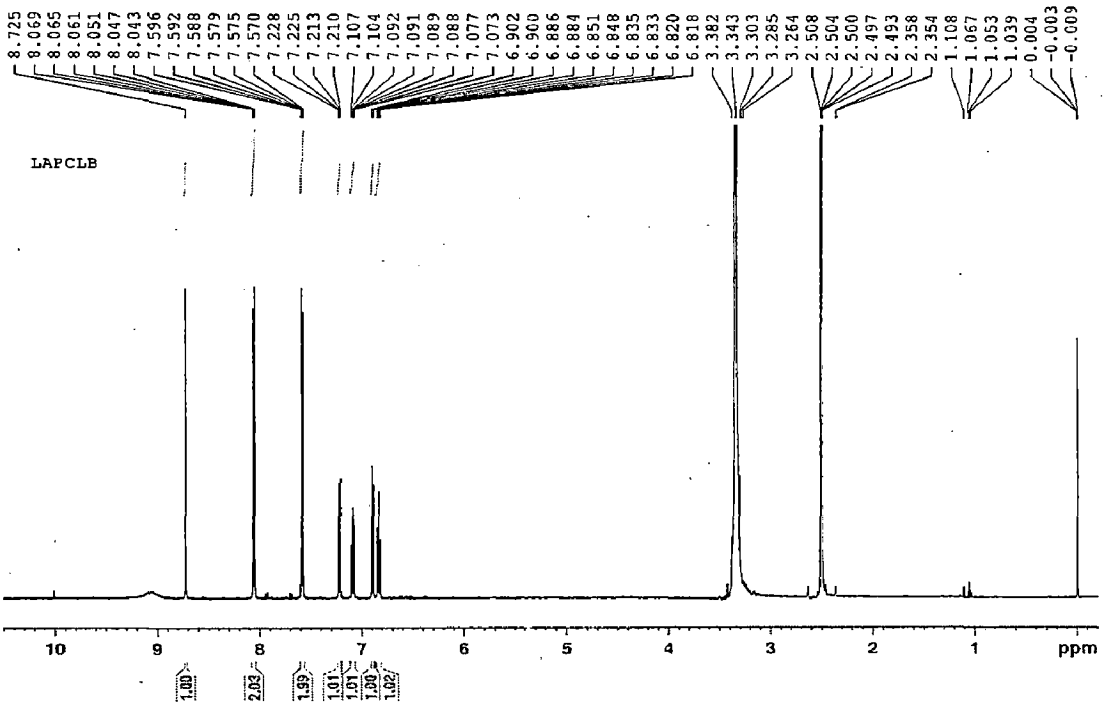

Figure 3.11: ^1H NMR Spectrum of Ligand L^2

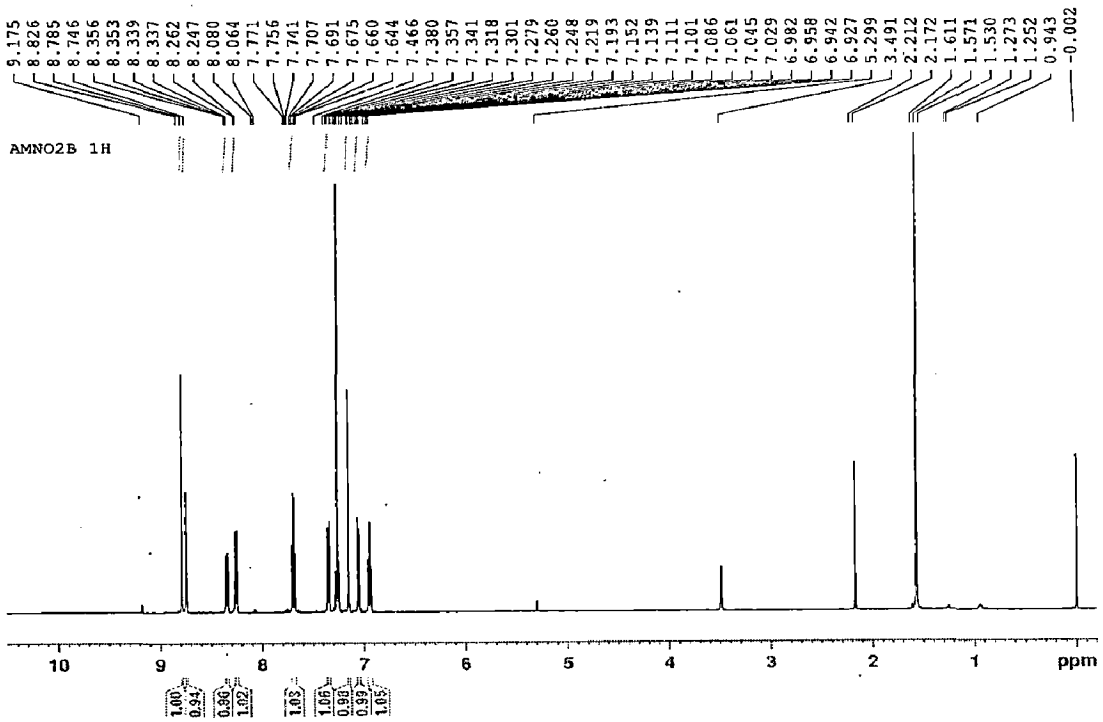

Figure 3.12: ^1H NMR Spectrum of Ligand L^3

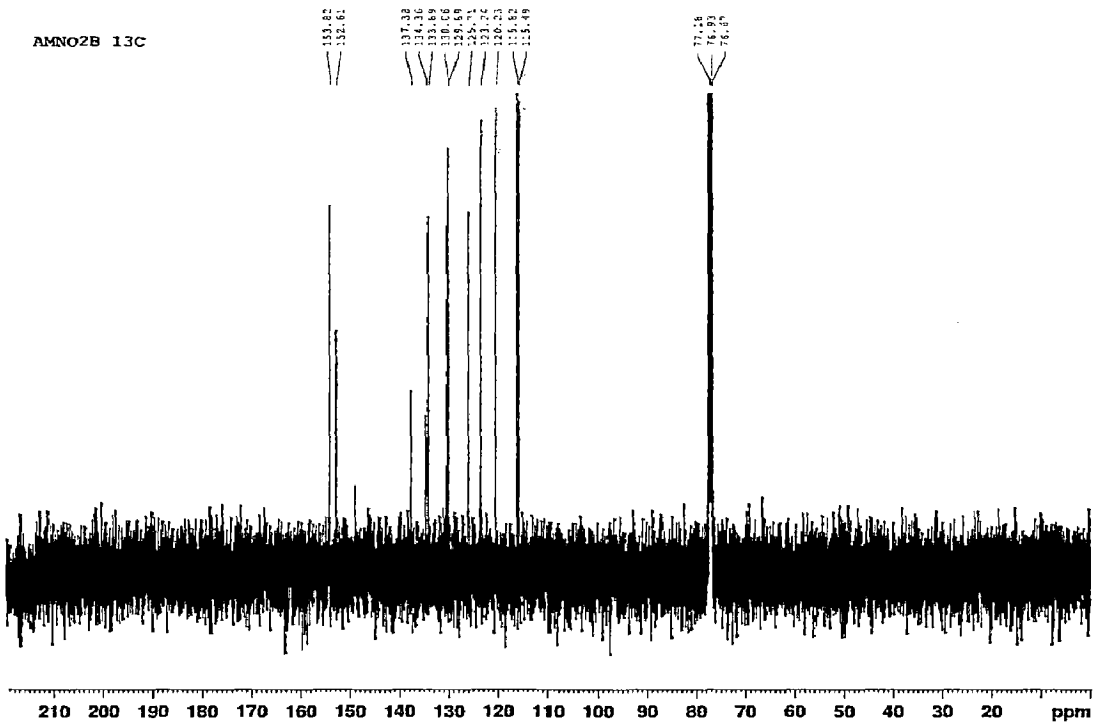

Figure 3.13: ^{13}C NMR Spectrum of Ligand L^3

3.2 Characterization of $Ru(PPh_3)_2L^nCl$ Complexes

The complexes $Ru(PPh_3)_2L^nCl$ (n=1-3) were characterized by IR spectroscopy and UV-Visible spectrophotometry. These complexes being paramagnetic did not afford NMR spectra. The C=N stretching in the complexes is observed ~1636 cm^{-1} (*Table 3.2* and *Figures 3.14-3.16*) which is also present in the IR spectra of the ligands. The OH stretching band is absent in the spectra of these complexes as is expected. The electronic spectra show three bands ~553 nm, ~400 nm, ~277 nm. These complexes absorb moderately in the visible region as is shown by UV-Visible spectral data (*Table 3.2* and *Figures 3.17-3.19*). Also. this data shows that the complexes strongly absorb UV radiation. The IR and UV-Vis spectral data is characteristic of these compounds.

Table 3.2: IR and UV-Vis Spectral Data for $Ru(PPh_3)_2L^nCl$ Complexes

Complex	$\nu_{C=N}$ cm^{-1}	λ(nm)	ϵ ($M^{-1}cm^{-1}$)
$Ru(PPh_3)_2L^1Cl$	1637	554	1301
		374	2226
		277	12108
$Ru(PPh_3)_2L^2Cl$	1637	554	1852
		373	3438
		278	17512
$Ru(PPh_3)_2L^3Cl$	1635	553	3244
		445	5083
		371	6886
		278	26534

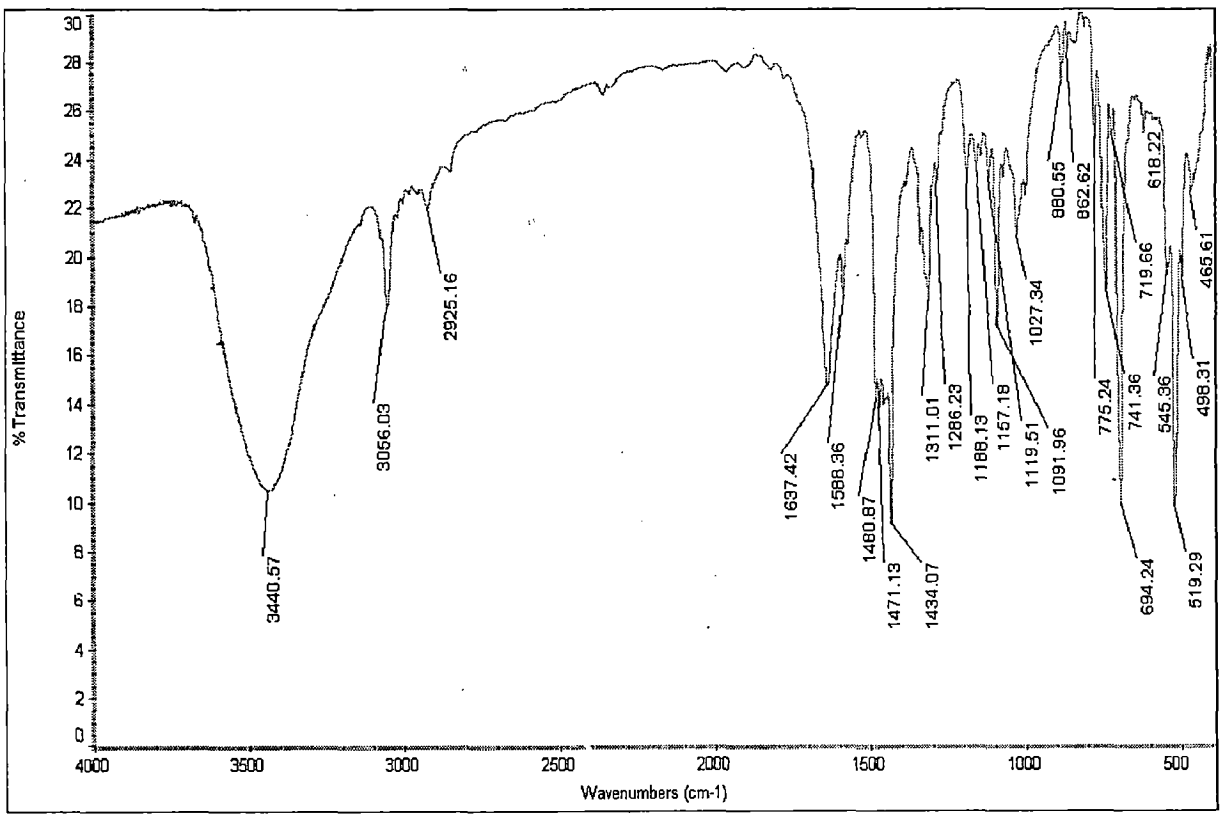

Figure 3.14: IR Spectrum of $Ru(PPh_3)_2L^1Cl$

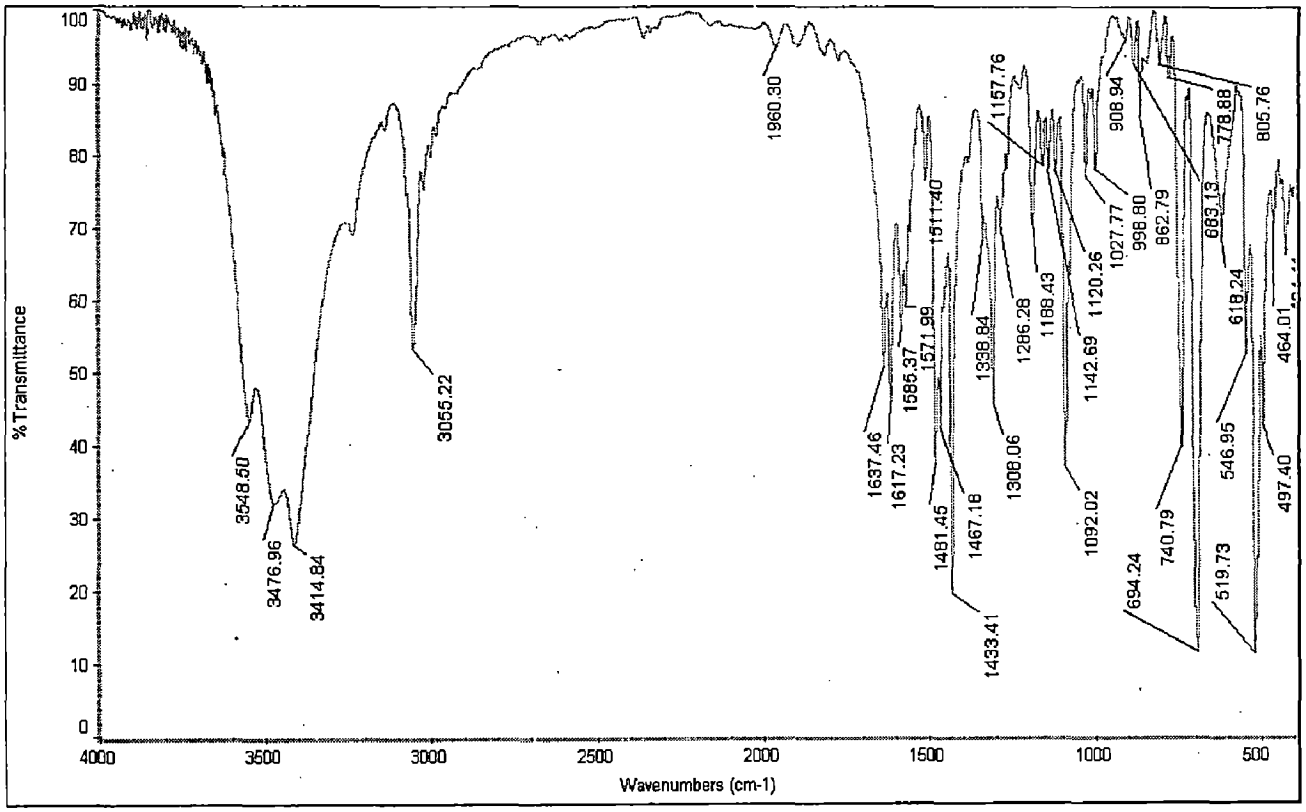

Figure 3.15: IR Spectrum of $Ru(PPh_3)_2L^2Cl$

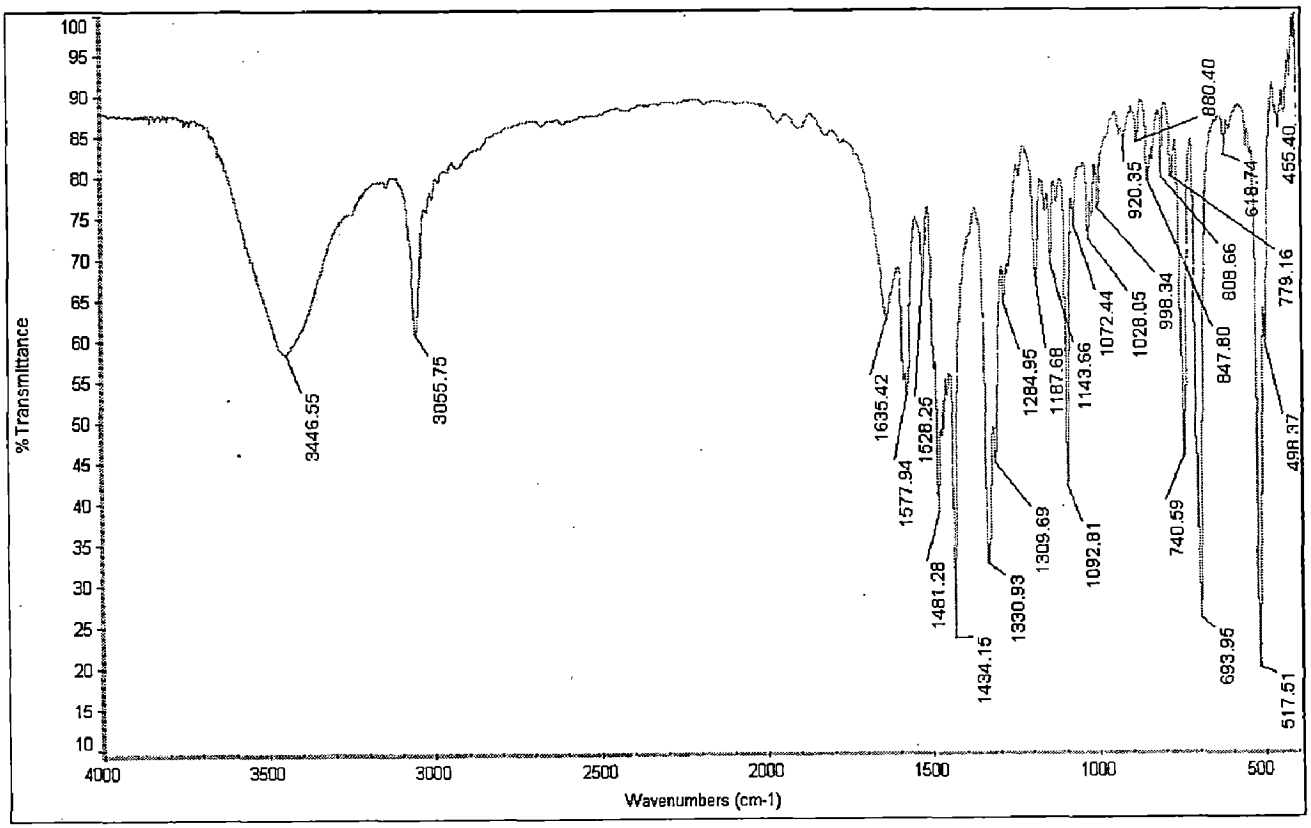

Figure 3.16: IR Spectrum of $Ru(PPh_3)_2L^3Cl$

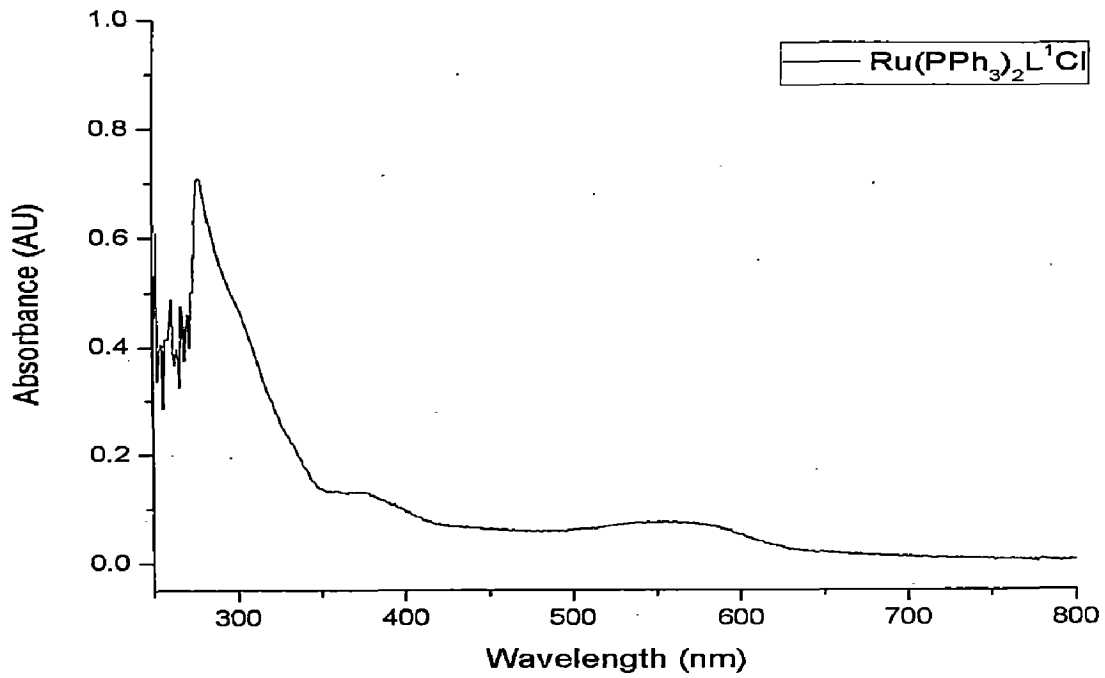

Figure 3.17: UV-Vis Spectrum of $Ru(PPh_3)_2L^1Cl$

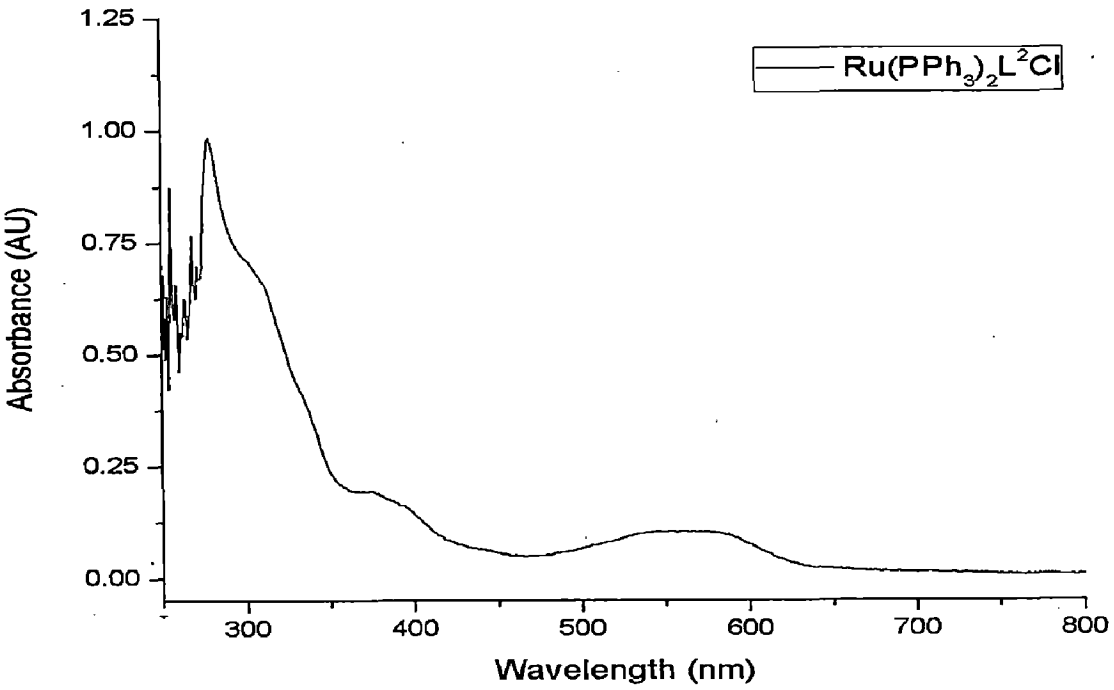

Figure 3.18: UV-Vis Spectrum of $Ru(PPh_3)_2L^2Cl$

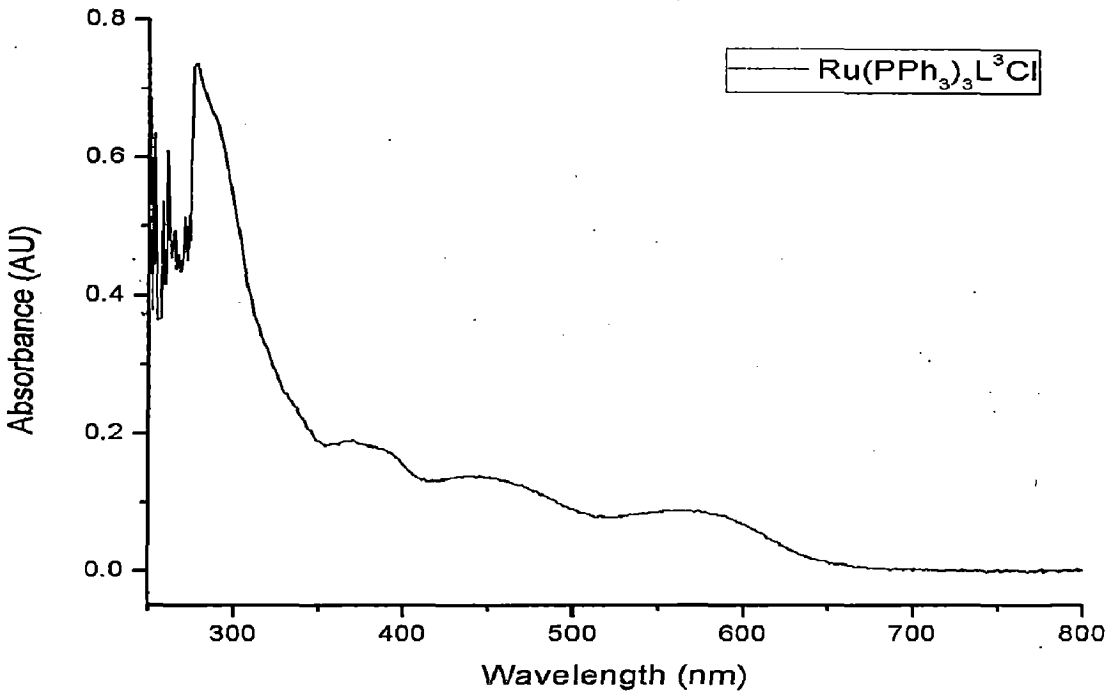

Figure 3.19: UV-Vis Spectrum of $Ru(PPh_3)_2L^3Cl$

3.3 Characterization of $Ru(PPh_3)_2L^n(NO)$ Complexes

The complexes $Ru(PPh_3)_2L^n(NO)$ (n=1-3) were characterized by IR spectroscopy, UV-Visible spectrophotometry and NMR spectroscopy. The C=N stretching in the complexes is observed ~1636 cm^{-1} (*Table 3.3* and *Figures 3.20-3.22*) which is also present in the IR spectra of the initial paramagnetic complexes and ligands. In the case of ruthenium, a $\{Ru-NO\}^6$ unit could represent one of two possible combinations of formal oxidation states of the metal center and NO, namely $\{Ru(III)-NO^{\cdot}\}^6$ and $\{Ru(II)-NO^+\}^6$. The NO stretching frequency for the ruthenium nitrosyl complexes was observed in the range 1820-1870 cm^{-1} which in ruthenium chemistry is generally accepted as NO^+ bound to a Ru(II) center denoted by $\{Ru-NO\}^6$ as per Enemark and Feltham notation [29,46]. Thus, reductive nitrosylation yielded diamagnetic $\{Ru-NO\}^6$ complexes from initial paramagnetic Ru(III) complexes. Ghosh and Mascharak have explained the above in a more involved fashion as to how one can ascribe a particular resonance structure to the complex at hand [25].

The electronic spectra show three bands in the ranges 430-530 nm, 370-410 nm

Table 3.3: IR and UV-Vis Spectral Data for $Ru(PPh_3)_2L^n(NO)$ Complexes

Complex	$\nu_{C=N}$ cm^{-1}	ν_{NO} cm^{-1}	λ(nm)	ϵ ($M^{-1}cm^{-1}$)
$Ru(PPh_3)_2L^1(NO)$	1637	1854	432	2775
			378	2552
			280	8966
$Ru(PPh_3)_2L^2(NO)$	1636	1824	527	1294
			409	5112
			281	19421
$Ru(PPh_3)_2L^3(NO)$	1635	1869	445	5160
			372	9532
			279	24905

and a band ~280 nm (*Table 3.3* and *Figures 3.23-3.25*). These complexes absorb moderately in the visible region but show strong absorption in the UV region as is evident from the UV-Visible spectral data. The IR and UV-Vis spectral data is characteristic of these compounds.

The diamagnetic behaviour of these compounds was exploited to characterize them by ^1H, ^{13}C and ^{31}P NMR spectroscopy (*Figures 3.26-3.29*). The spectra were recorded in $CDCl_3$. ^1H NMR spectra were recorded for $Ru(PPh_3)_2L^1(NO)$ and $Ru(PPh_3)_2L^2(NO)$. The aromatic protons in the benzene rings of triphenylphosphine, and the tridentate ligand and the CH=N proton appeared in the region δ= 7-8 ppm in accordance with values reported in literature [47]. Since, the signals were clustered together, it was difficult to integrate the peak areas. In the ^{13}C NMR spectrum for $Ru(PPh_3)_2L^3(NO)$, 17 signals in the range δ= 123.36-133.16 ppm were observed, clearly indicating that the ligand frame is intact. ^{31}P NMR spectrum for $Ru(PPh_3)_2L^3(NO)$ showed just one signal at δ= 29.10 ppm implying the presence of *trans* configuration of the two triphenylphosphines in these complexes which is as expected from steric point of view as suggested by Lahiri and coworkers [48].

All the above data clearly indicate the formation of the diamagnetic ruthenium nitrosyl complexes.

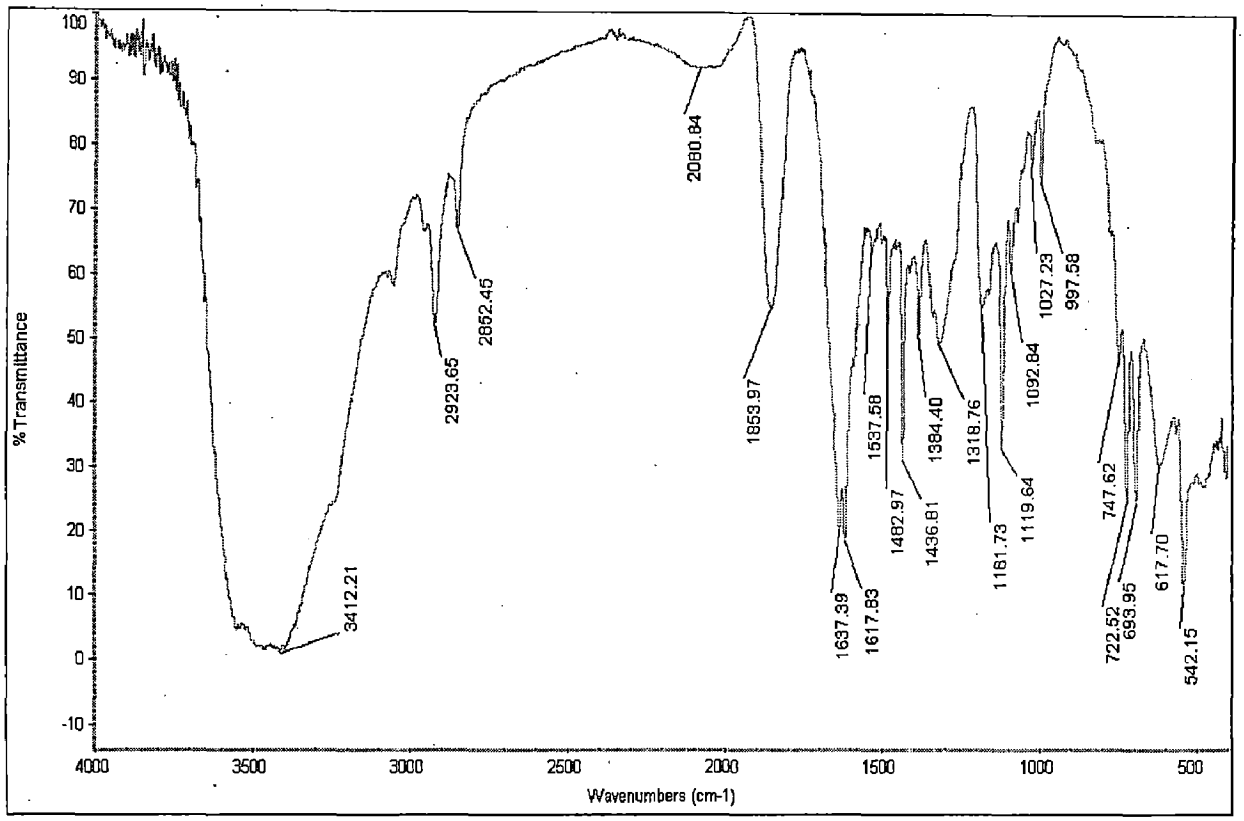

Figure 3.20: IR Spectrum of $Ru(PPh_3)_2L^1(NO)$

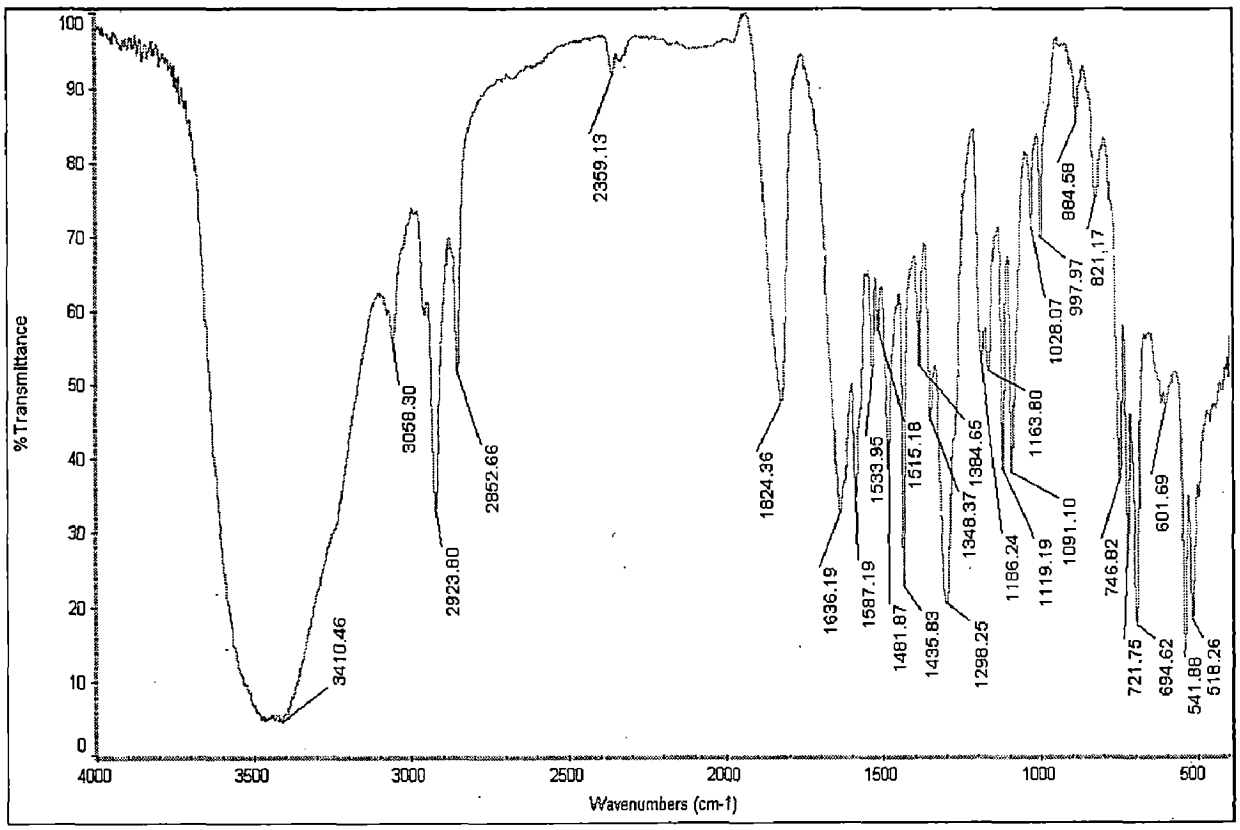

Figure 3.21: IR Spectrum of $Ru(PPh_3)_2L^2(NO)$

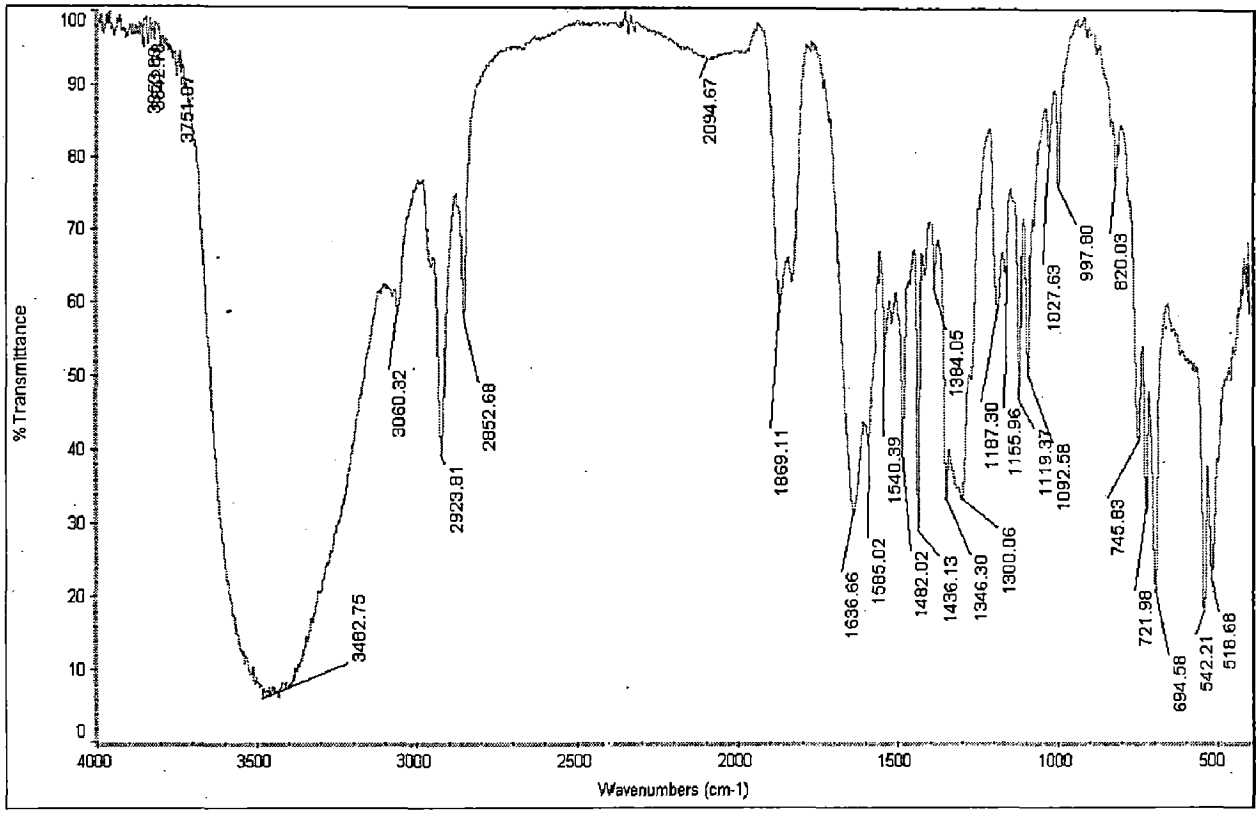

Figure 3.22: IR Spectrum of $Ru(PPh_3)_2L^3(NO)$

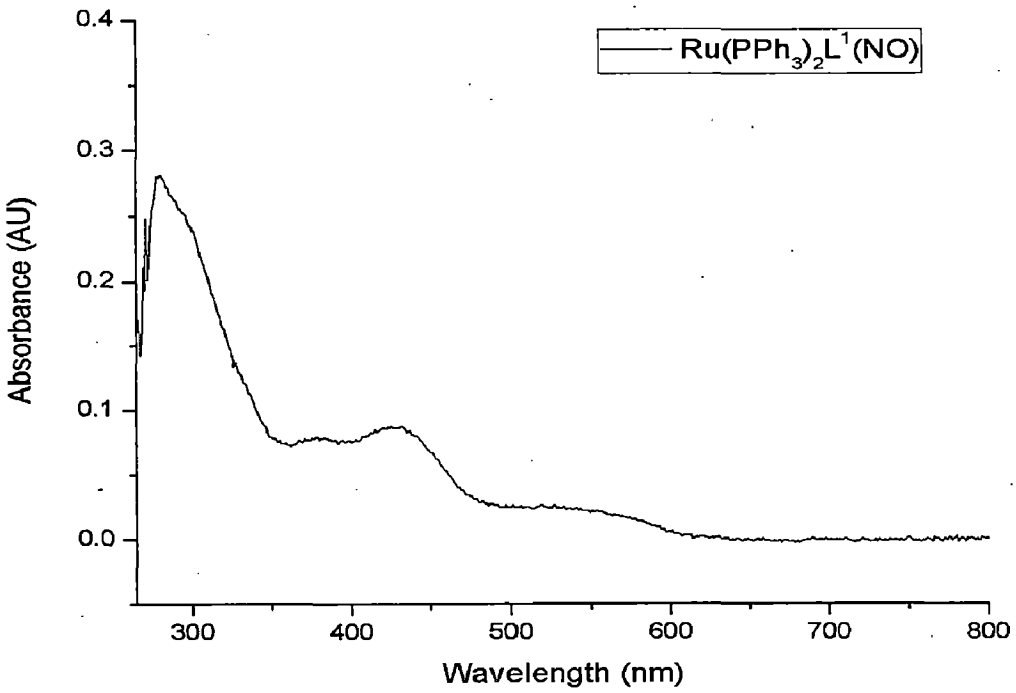

Figure 3.23: UV-Vis Spectrum of $Ru(PPh_3)_2L^1(NO)$

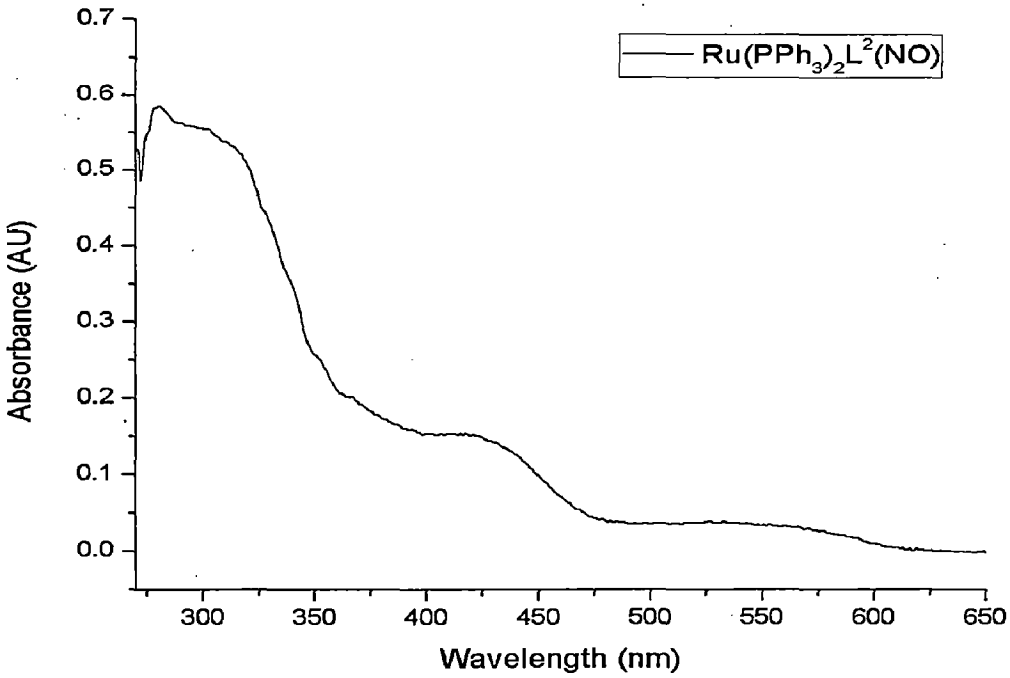

Figure 3.24: UV-Vis Spectrum of $Ru(PPh_3)_2L^2(NO)$

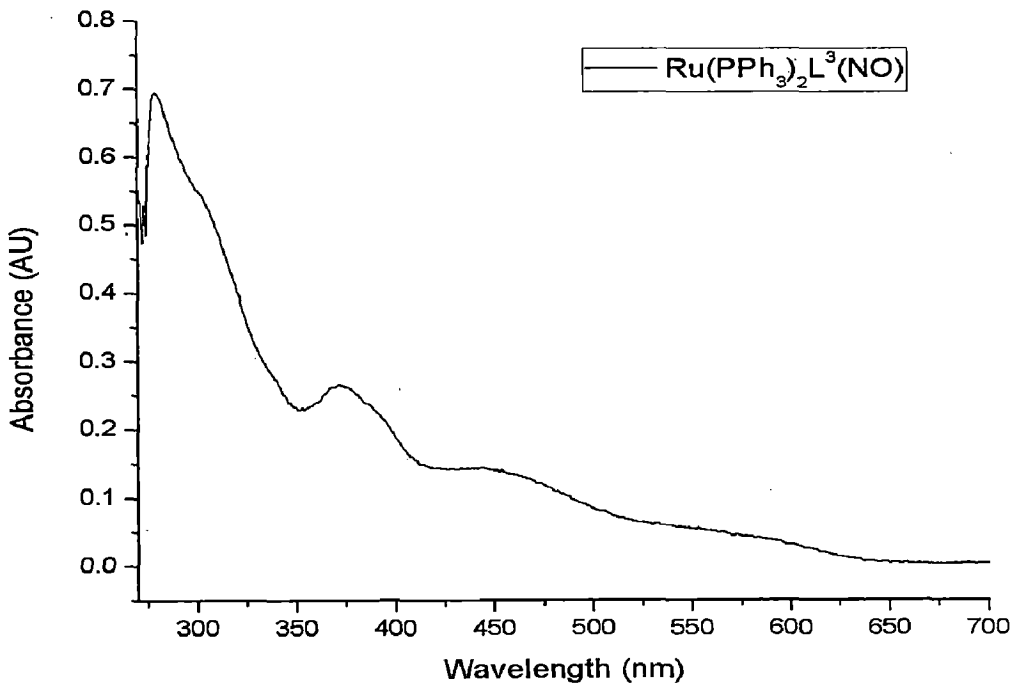

Figure 3.25: UV-Vis Spectrum of $Ru(PPh_3)_2L^3(NO)$

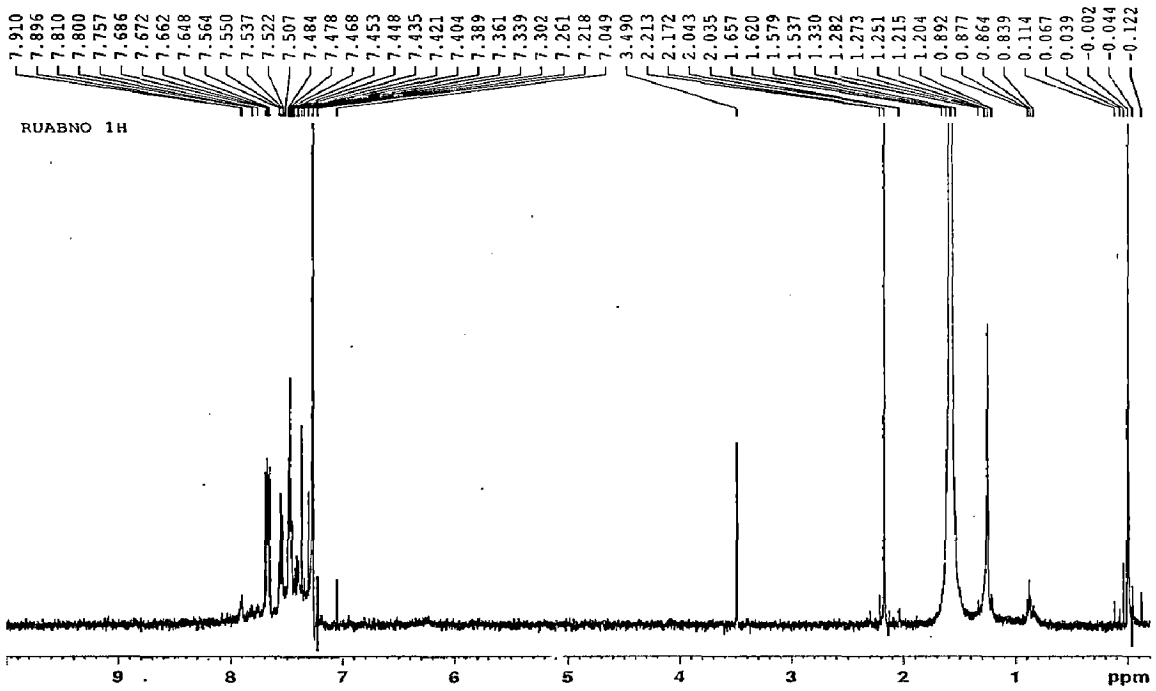

Figure 3.26: ^1H NMR Spectrum of $Ru(PPh_3)_2L^1(NO)$

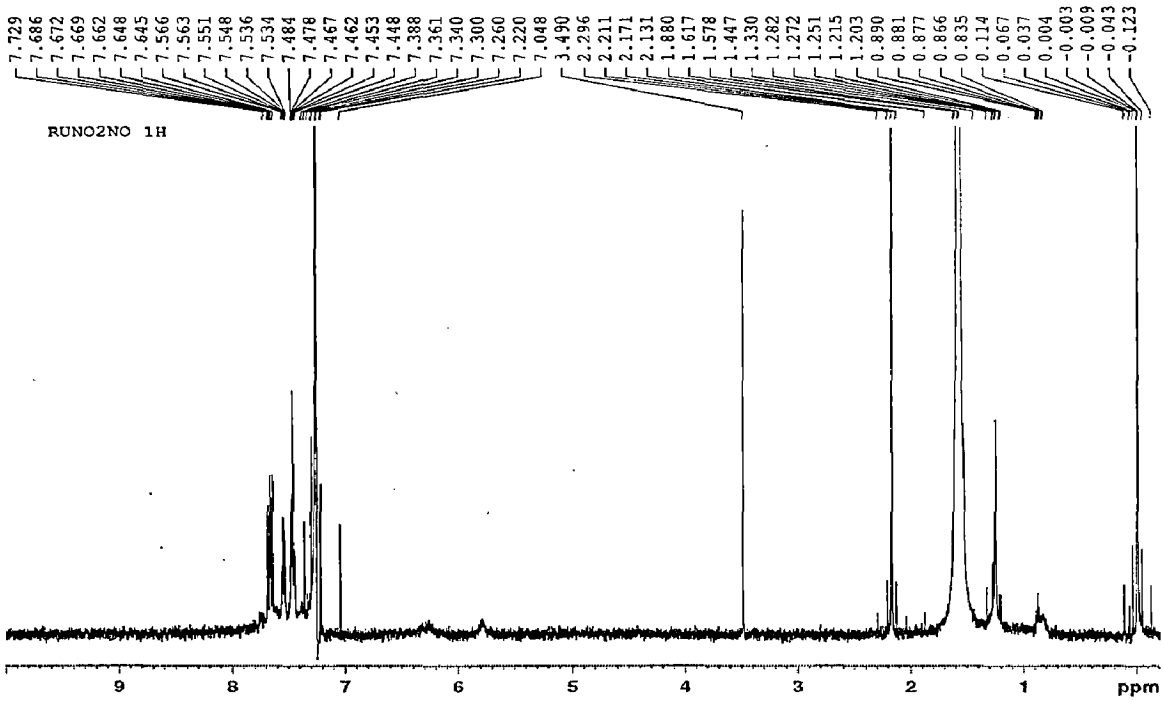

Figure 3.27: ^1H NMR Spectrum of $Ru(PPh_3)_2L^3(NO)$

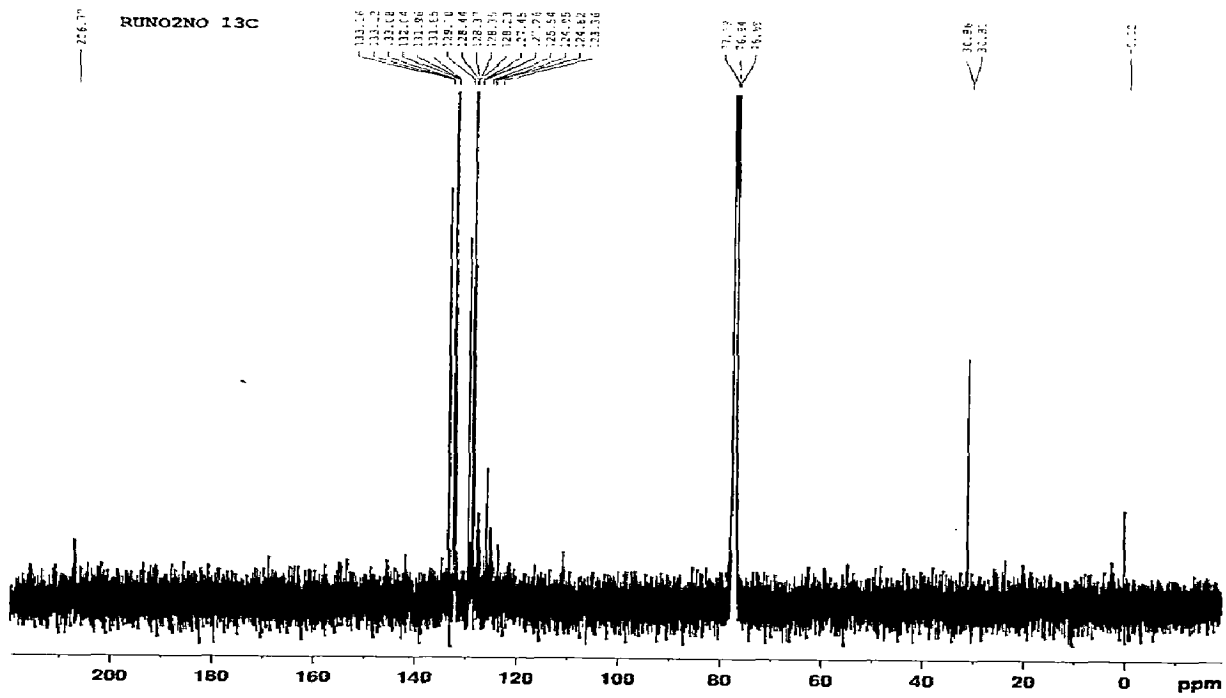

Figure 3.28: ^{13}C NMR Spectrum of $Ru(PPh_3)_2L^3(NO)$

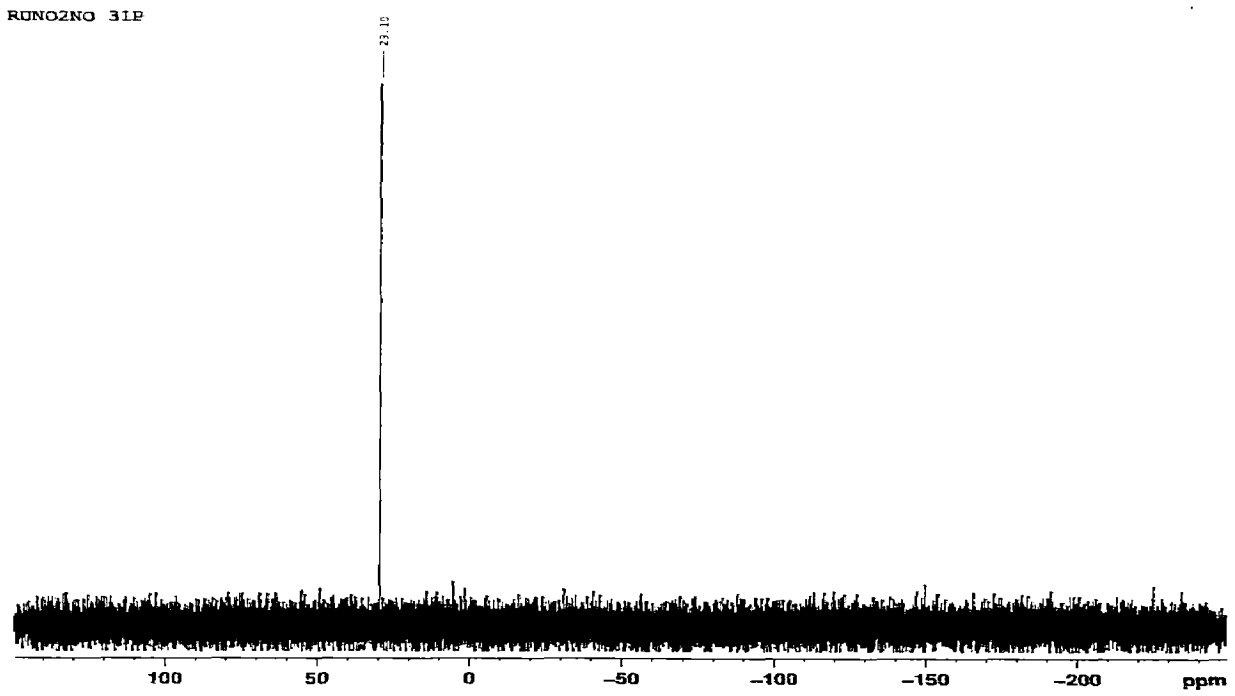

Figure 3.29: ^{31}P NMR Spectrum of $Ru(PPh_3)_2L^3(NO)$

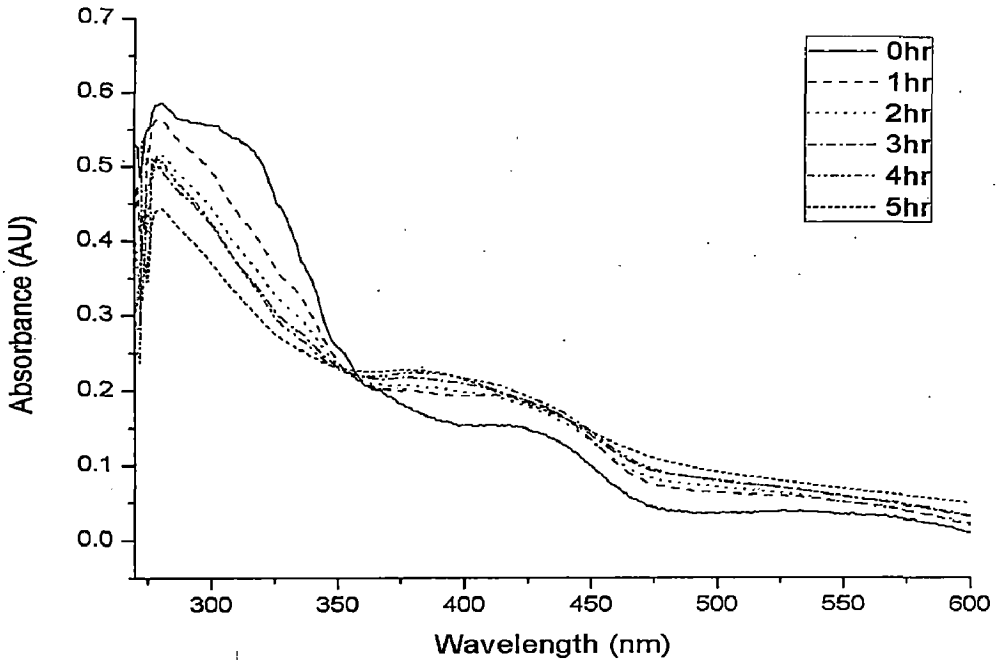

Figure 3.32: Photolability of $Ru(PPh_3)_2L^2(NO)$

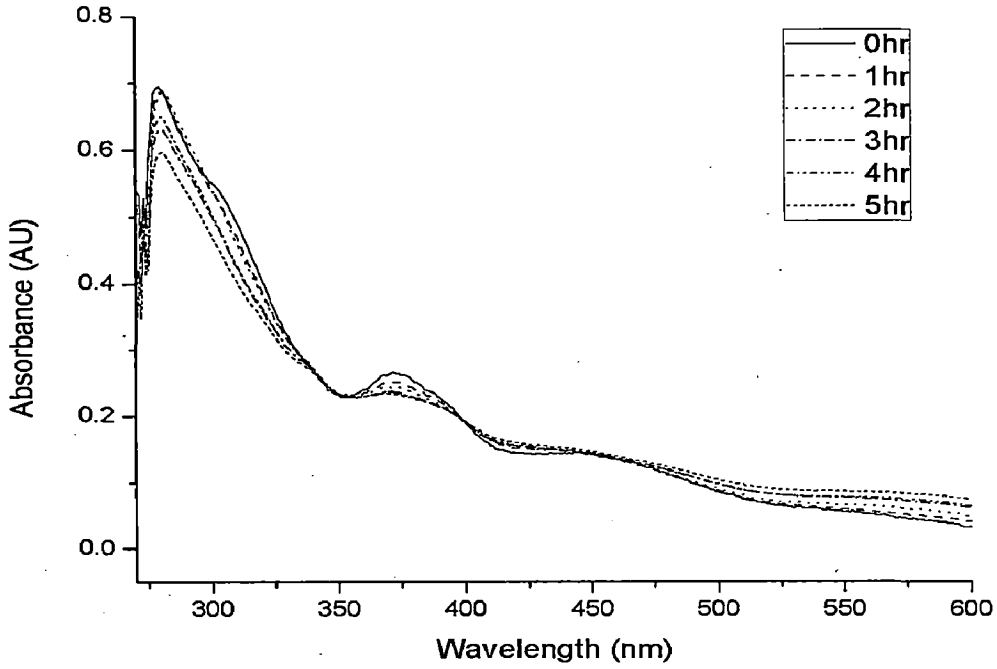

Figure 3.33: Photolability of $Ru(PPh_3)_2L^3(NO)$

3.5 Transfer of NO to Reduced Myoglobin

In order to prove that NO is photoreleased, a NO trapping experiment with reduced myoglobin was designed. In the standardization experiment, Söret band was observed at 409 nm for myoglobin, at 418 nm for reduced myoglobin and at 411 nm for myoglobin-NO adduct (*Figure 3.34*).

In the experiment carried out in visible light involving transfer of NO from $Ru(PPh_3)_2L^n(NO)$ complexes to reduced myoglobin the Söret band was observed ~409 nm and in the control experiment carried out in absence of light, the Söret band was observed ~415 nm (*Table 3.4* and *Figures 3.35-3.37*).

Table 3.4: Söret band in NO Transfer Experiments

Complex	*Experiment in Light*	*Experiment in Dark*
$Ru(PPh_3)_2L^1(NO)$	409 nm	415
$Ru(PPh_3)_2L^2(NO)$	409 nm	417
$Ru(PPh_3)_2L^3(NO)$	410 nm	415

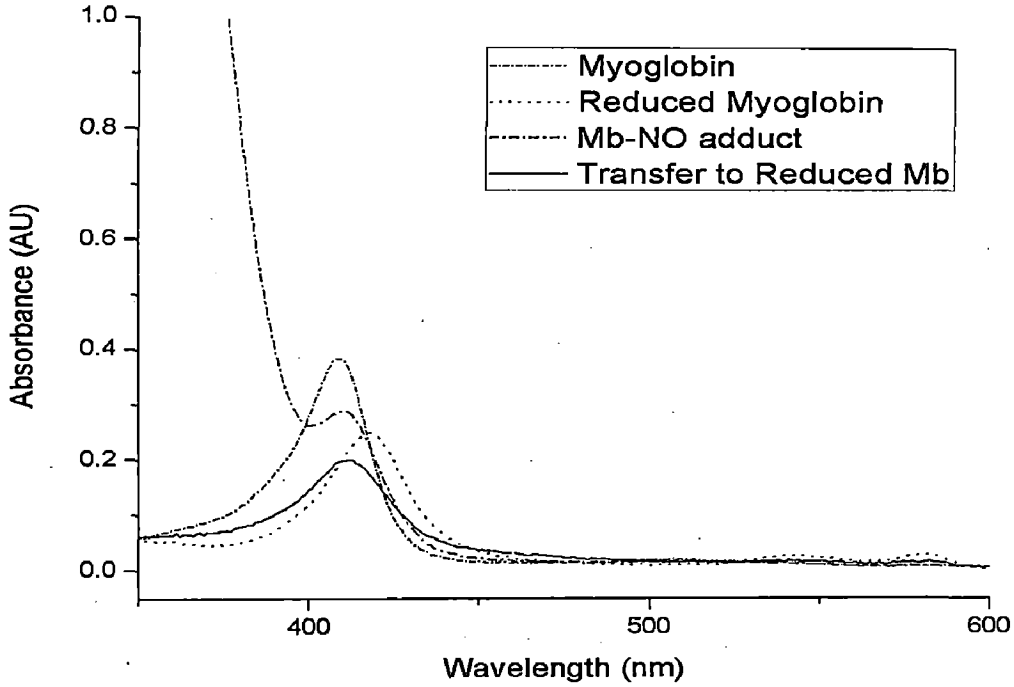

Figure 3.34: Transfer of NO from $Ru(PPh_3)_2L^2(NO)$ to Reduced Myoglobin

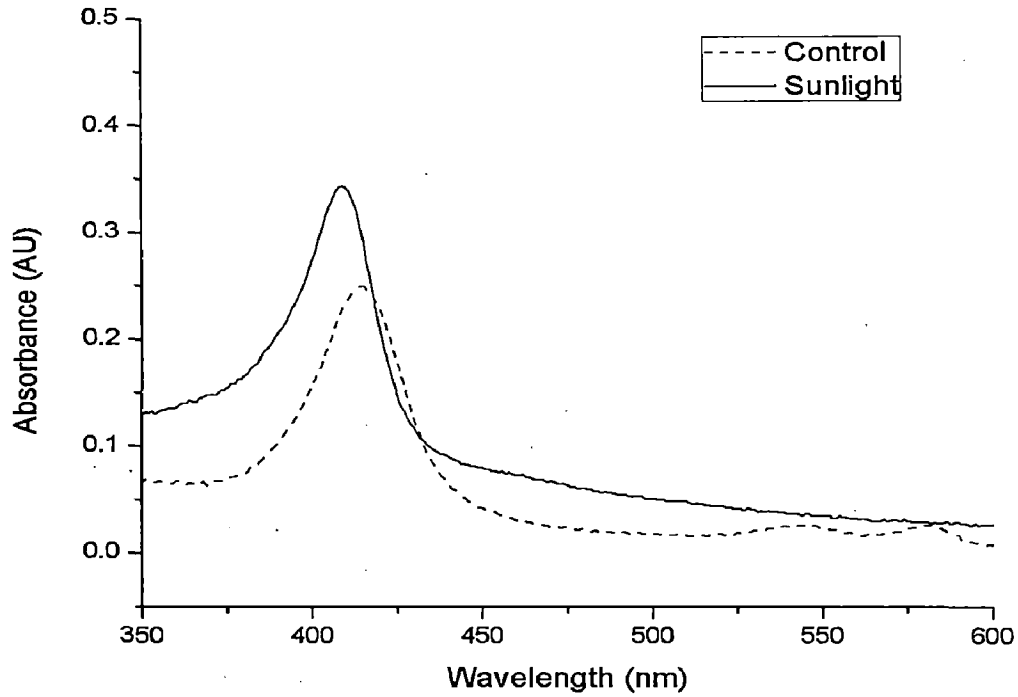

Figure 3.35: Transfer of NO from $Ru(PPh_3)_2L^1(NO)$ to Reduced Myoglobin

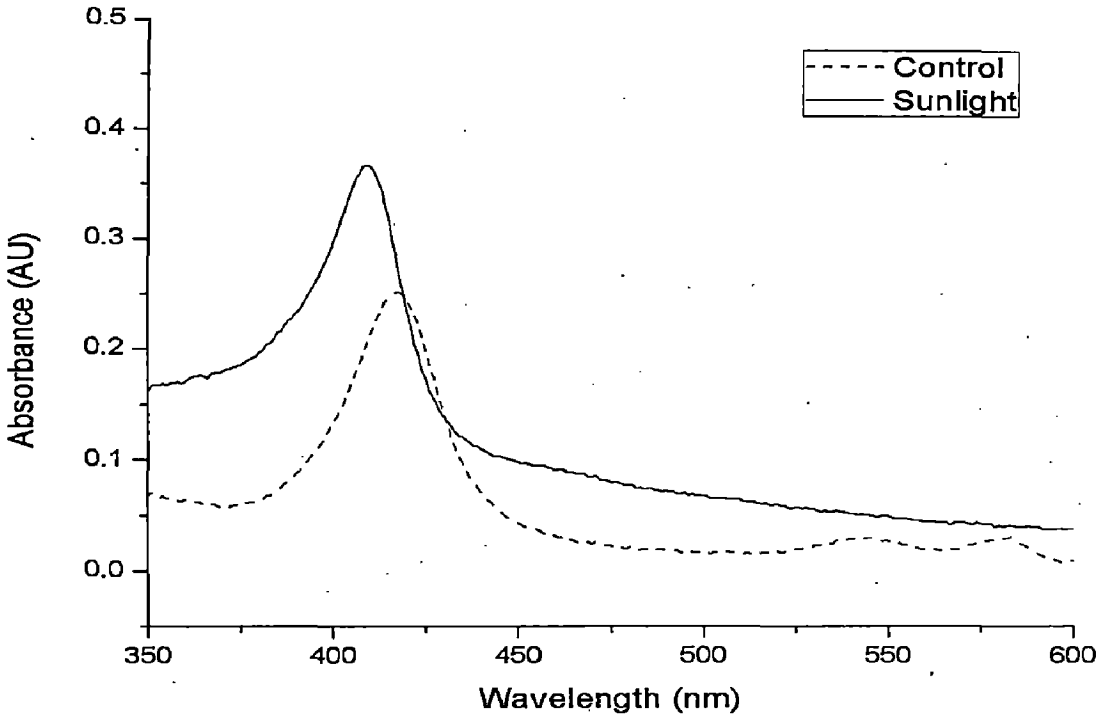

Figure 3.36: Transfer of NO from $Ru(PPh_3)_2L^2(NO)$ to Reduced Myoglobin

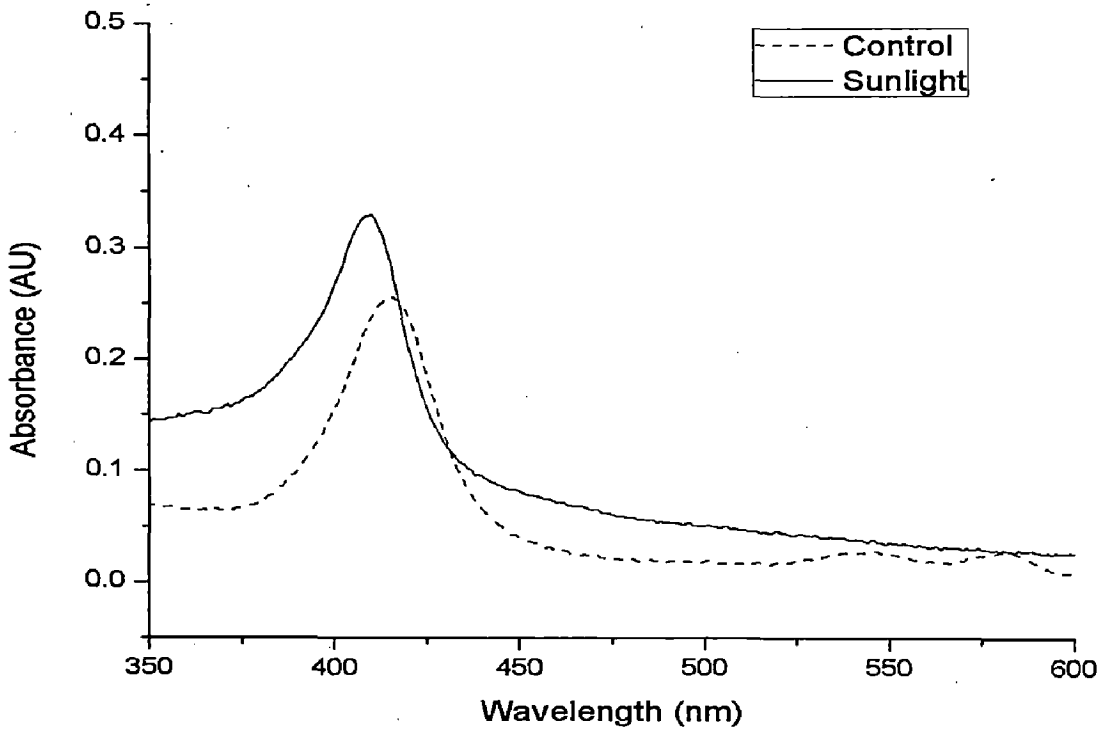

Figure 3.37: Transfer of NO from $Ru(PPh_3)_2L^3(NO)$ to Reduced Myoglobin

Chapter 4

Conclusions

The following are the principal findings and conclusions of the present study.

1. Organometallic Ru(III) compounds were synthesized and characterized by IR spectroscopy and UV-Vis spectrophotometry.

2. Nitric oxide was reacted with these compounds to synthesize corresponding ruthenium nitrosyl complexes.

3. In the starting compounds, ruthenium was in the formal oxidation state (III). However, reaction with NO afforded $\{Ru-NO\}^6$ diamagnetic species. Due to the diamagnetic nature of resultant ruthenium nitrosyl complexes ^1H, ^{13}C and ^{31}P NMR were investigated. All the data show the presence of ligand frame with *trans-* orientation of triphenylphosphine groups around the metal center.

4. ν_{NO} in range 1820-1870 cm^{-1} clearly indicate the presence of $\{Ru(II)-NO^+\}^6$ which means that between the possible $\{Ru(III)-NO\}^6$ and $\{Ru(II)-NO^+\}^6$ we are proposing the later resonating structure. There was a strong effect on the NO stretching frequency due to substituents on the aryl ring. Huge delocalization of electrons from NO to Ru to aryl ring is evidenced here.

5. We have found that the coordinated NO is photolabile.

6. Photolability of NO has been confirmed by trapping NO with reduced myoglobin.

References

1. Koshland, D.E., Jr. *Science*, **1992**, *258*, 1861.
2. Furchgott, R.F. *Angew. Chem. Int. Ed.*, **1999**, *38*, 1870.
3. Ignarro, L.J. *Angew. Chem. Int. Ed.*, **1999**, *38*, 1882.
4. Murad, F. *Angew. Chem. Int. Ed.*, **1999**, *38*, 1856.
5. Lundberg, J.O.; Weitzberg, E.; Galdwin, M.T. *Nature Reviews Drug Discovery*, **2008**, *Advanced Online Publication*, doi:10.1038/nrd2466.
6. Palmer, R.M.J.; Ferrige, A.J.; Moncada, S. *Nature*, **1987**, *327*, 524.
7. Ignarro, L.J.; Buga, G.M.; Wood, K.S.; Byrns, R.E.; Chaudhuri, G. *Proc. Natl. Acad. Sci. USA*, **1987**, *84*, 9265.
8. Radomski, M.W.; Palmer, R.M.J.; Moncada, S. *Proc. Natl. Acad. Sci. USA*, **1990**, *87*, 5193.
9. Bredt, D.S.; Snyder, S.H. *Proc. Natl. Acad. Sci. USA*, **1989**, *86*, 9030.
10. Marsden, P.A.; Ballermann, B.J. *J. Exp. Med.*, **1990**, *172*, 1843.
11. Stuehr, D.J.; Nathan, C.F. *J. Exp. Med.*, **1989**, *169*, 1543.
12. Gracia, X.; Stein, F. *Semin. Pediatr. Infect. Dis.*, **2006**, *17*, 55.
13. Pal, B.; Kitagawa, T. *J. Inorg. Biochem.*, **2005**, *99*, 267.
14. Endo, I.; Odaka, M.; Yohda, M. *Trends Biotechnol.*, **1999**, *77*, 244.
15. Gaston, B. *Biochim. Biophys. Acta*, **1998**, *1411*, 323.
16. Szacilowski, K.; Chmura, A.; Stasicka, Z. *Coord. Chem. Rev.*, **2005**, *249*, 2408.
17. Wink, D.A.; Mitchell, J.B. *Free Radical Biol. Med.*, **1998**, *25*, 434.
18. Rose, M.J.; Mascharak, P.K. *Curr. Opin. Chem. Biol.*, **2008**, *12*, 1.
19. Ford, P. C.; Bourassa, J.; Miranda, K.; Lee, B.; Lorkovic, I.; Boggs, S.; Kudo, S.; Laverman, L. *Coord. Chem. Rev.*, **1998**, *171*, 185.
20. Stochel, G.; Wanat, A.; Kulis, E.; Stasicka, Z. *Coord. Chem. Rev.*, **1998**, *171*, 203.

21. Fortney, C.F.; Shepherd, R.E. *Inorg. Chem. Commun.*, **2004**, *7*, 1065.

22. Wang, P.G.; Xian, M.; Tang, X.; Wu, X.; Wen, Z.; Cai, T.; Janczuk, A.J. *Chem. Rev.*, **2002**, *102*, 1091.

23. Patra, A.K.; Afshar, R.; Olmstead, M.M.; Mascharak, P.K. *Angew. Chem. Int. Ed.*, **2002**, *41*, 2512.

24. Afshar, R.K.; Patra, A.K.; Olmstead, M.M.; Mascharak, P.K. *Inorg. Chem.*, **2004**, *43*, 5736.

25. Ghosh, K.; Eroy-Reveles, A.A.; Avila, B.; Holman, T.R.; Olmstead, M.M.; Mascharak, P.K. *Inorg. Chem.*, **2004**, *43*, 2988.

26. Patra, A.K.; Mascharak, P.K. *Inorg. Chem.*, **2003**, *42*, 7363.

27. Rose, M.J.; Olmstead, M.M.; Mascharak, P.K. *Polyhedron*, **2007**, *26*, 4713.

28. Rose, M.J.; Patra, A.K.; Alcid, E.A.; Olmstead, M.M.; Mascharak, P.K. *Inorg. Chem.*, **2007**, *46*, 2328.

29. Rose, M.J.; Mascharak, P.K. *Coord. Chem. Rev.*, **2007**, *Article in Press*, doi:10.1016/j.ccr.2007.11.011.

30. Patra, A.K.; Rose, M.J.; Murphy, K.M.; Olmstead, M.M.; Mascharak, P.K. *Inorg. Chem.*, **2004**, *43*, 4487.

31. Rose, M.J.; Olmstead, M.M.; Mascharak, P.K. *J. Am. Chem. Soc.*, **2007**, *129*, 5342.

32. Oliveira,F.S.; Ferreira, K.Q.; Bonaventura, D.; Bendhack, L.M.; Tedesco, A.C.; Machado, S.P.; Tfouni, E.; da Silva, R.S. *J. Inorg. Biochem.*, **2007**, *101*, 313.

33. de Lima, R.G.; Sauaia, M.G.; Bonaventura, D.; Tedesco, A.C.; Bendhack, L.M.; da Silva, R.S. *Inorg. Chim. Acta*, **2006**, *359*, 2543.

34. Sauaia, M.G.; de Lima, R.G.; Tedesco, A.C.; da Silva, R.S. *J. Am. Chem. Soc.*, **2003**, *125*, 14718.

35. Sauaia, M.G.; de Lima, R.G.; Tedesco, A.C.; da Silva, R.S. *Inorg. Chem.*, **2005**, *44*, 9946.

36. Tfouni, E.; Krieger, M.; McGarvey, B.R.; Franco, D.W. *Coord. Chem. Rev.*, **2003**, *236*, 57.

37. Carlos,R.M.; Ferro, A.A.; Silva, H.A.S.; Gomes, M.G.; de Borges, S.S.S.; Ford, P.C.; Tfouni, E.; Franco, D.W. *Inorg. Chim. Acta*, **2004**, *357*, 1381.

38. Works, C.F.; Jocher, C.J.; Bart, G.D.; Bu, X.; Ford, P.C. *Inorg. Chem.*, **2002**, *41*, 3728.

39. Works, C.F.; Ford, P.C. *J. Am. Chem. Soc.*, **2000**, *122*, 7592.

40. Toma,H.E.; Alexiou, A.D.P.; Formiga, A.L.B.; Nakamura, M.; Dovidauskas, S.; Eberlin, M.N.; Tomazela, D.M. *Inorg. Chim. Acta*, **2005**, *358*, 2891.

41. Maji, S.; Sarkar, B.; Patra, M.; Das, A.K.; Mobin, S.M.; Kalm, W.; Lahiri, G.K. *Inorg. Chem.*, **2008**, *47*, 3218.

42. Lopes, L.G.F.; Wieraszko, A.; El-Sherif, Y.; Clarke, M.J. *Inorg. Chim. Acta*, **2001**, *312*, 15.

43. Holanda, A.K.M.; da Silva, F.O.N.; Sousa, J.R.; Diogenes, I.C.N.; Carvalho, I.M.M.; Moreira, I.S.; Clarke, M.J.; Lopes, L.G.F. *Inorg. Chim. Acta*, **2008**, *Article in Press*, doi:10.1016/j.ica.2008.02.052.

44. Stephenson, T.A.; Wilkinson, G. *J. Inorg. Nucl. Chem.*, **1966**, *28*, 945.

45. Ghosh, P.; Pramanik, A.; Bag, N.; Lahiri, G.K.; Chakravorty, A. *J. Organomet. Chem.*, **1993**, *454*, 237.

46. Enemark, J.H.; Feltham, R.D. *Coord. Chem. Rev.*, **1974**, *13*, 339.

47. Ghosh, P. *Polyhedron*, **1997**, *16*, 1343.

48. Hariram, R.; Santra, B.K.; Lahiri, G.K. *J. Organomet. Chem.*, **1997**, *540*, 155.

Appendices

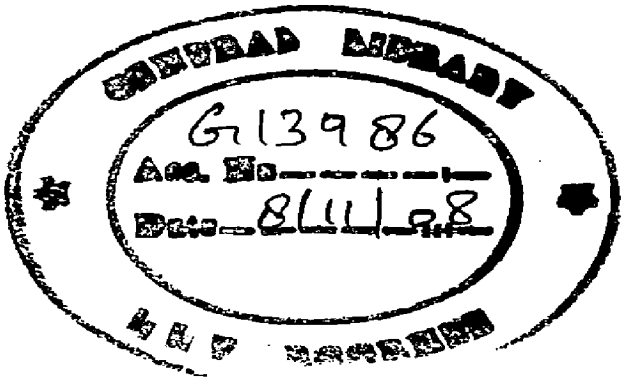

Appendix A

IR Spectra

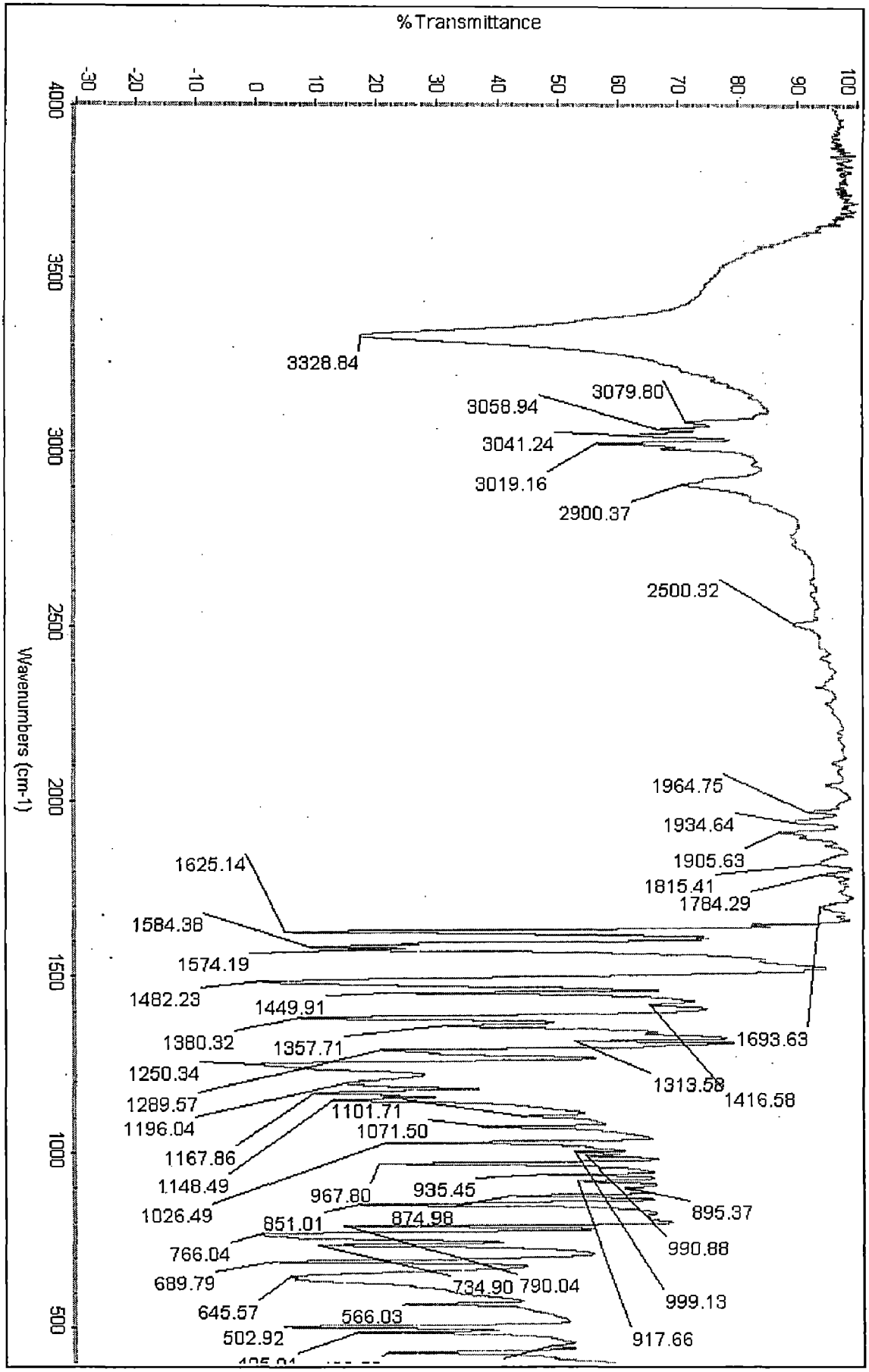

Figure A.1: IR Spectrum of Ligand L^1

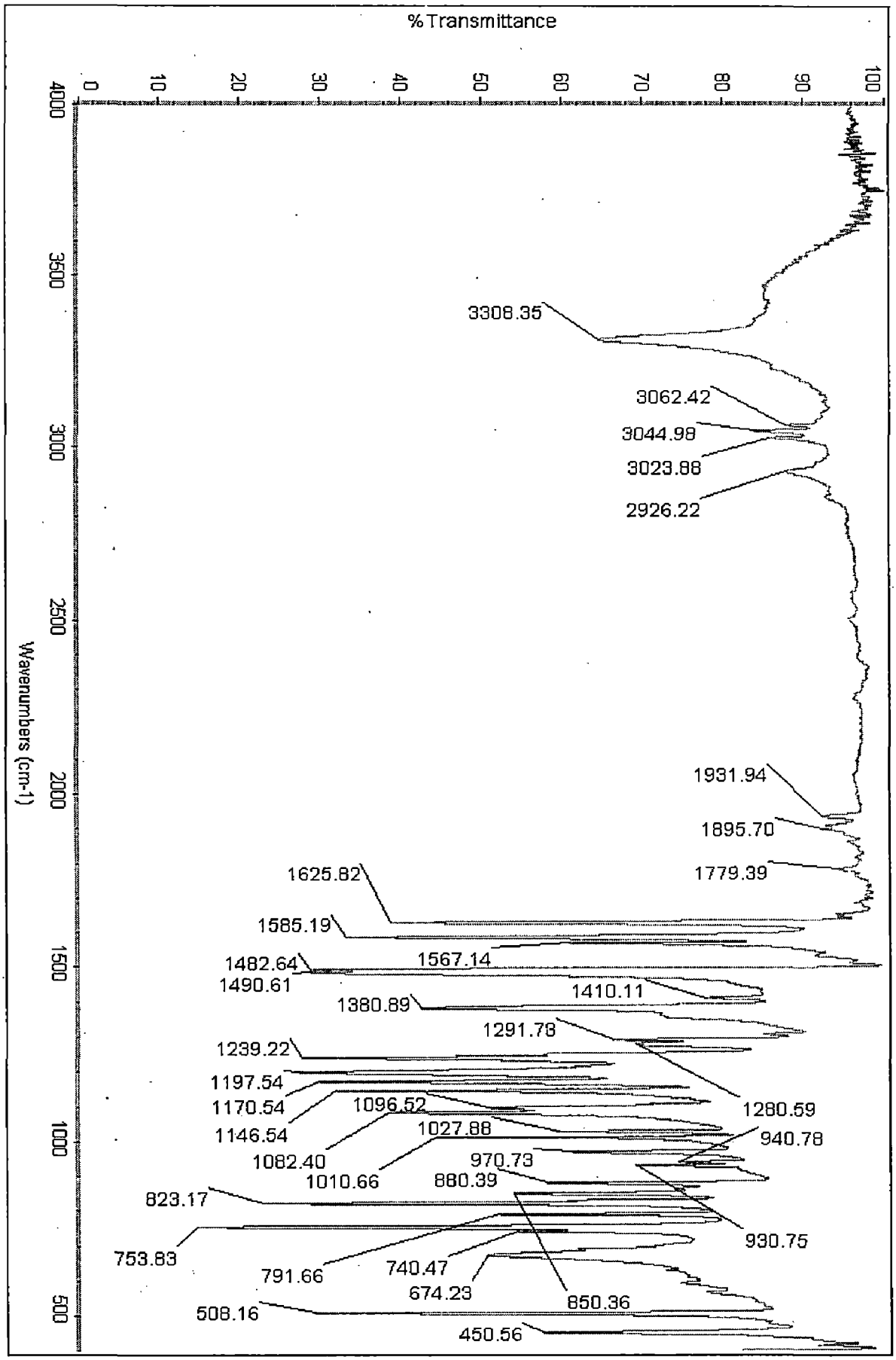

Figure A.2: IR Spectrum of Ligand L^2

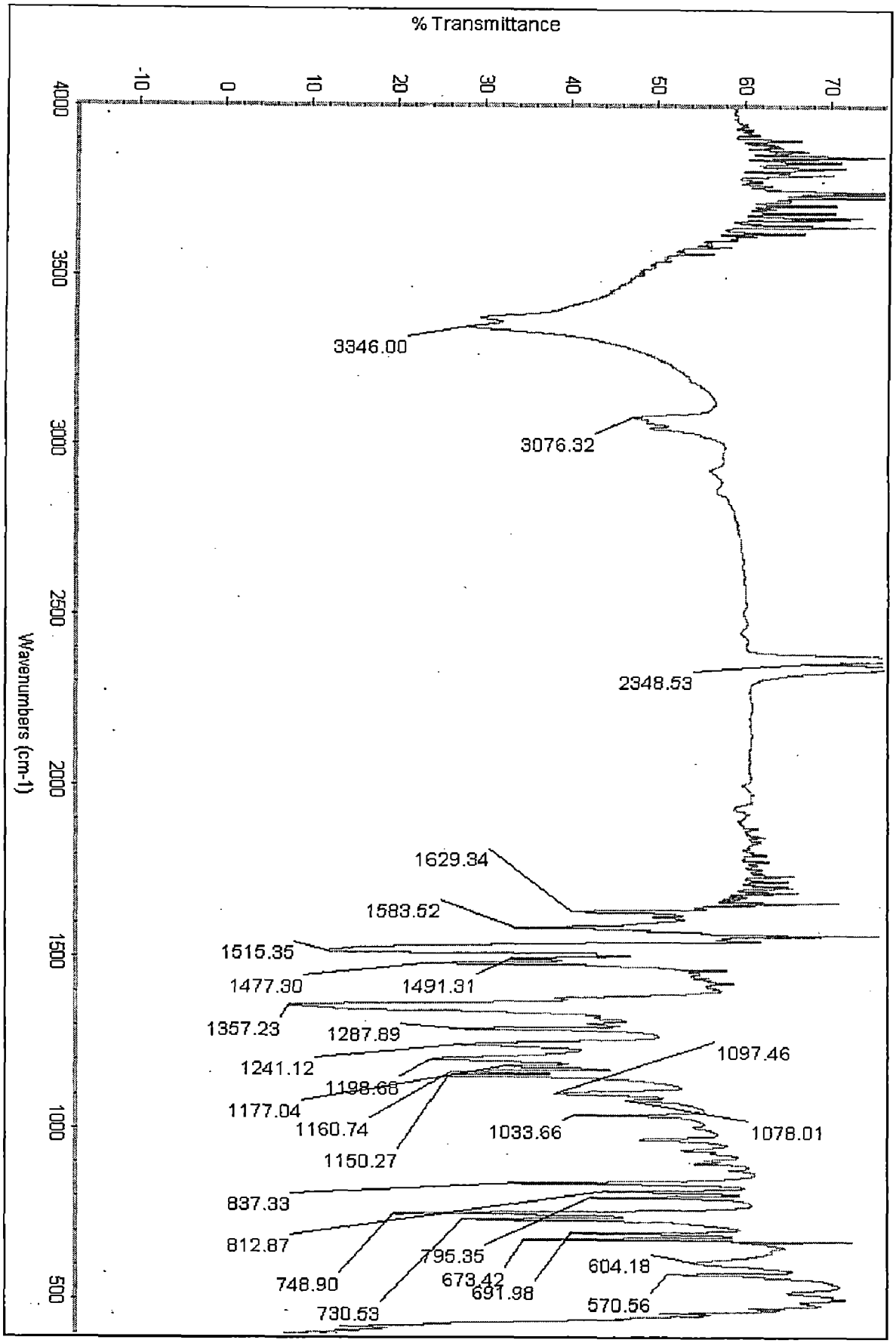

Figure A.3: IR Spectrum of Ligand L^3

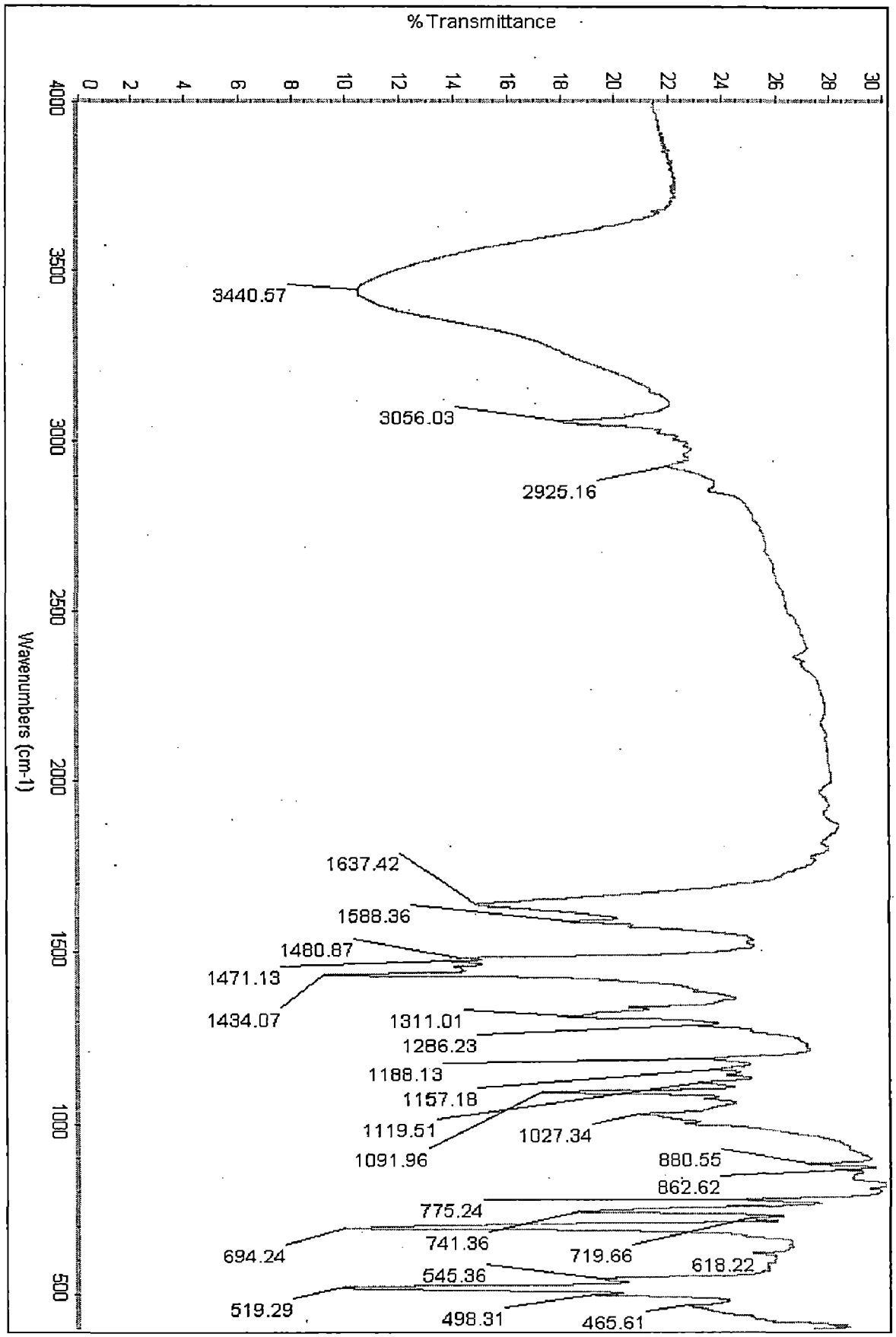

Figure A.4: IR Spectrum of $Ru(PPh_3)_2L^1Cl$

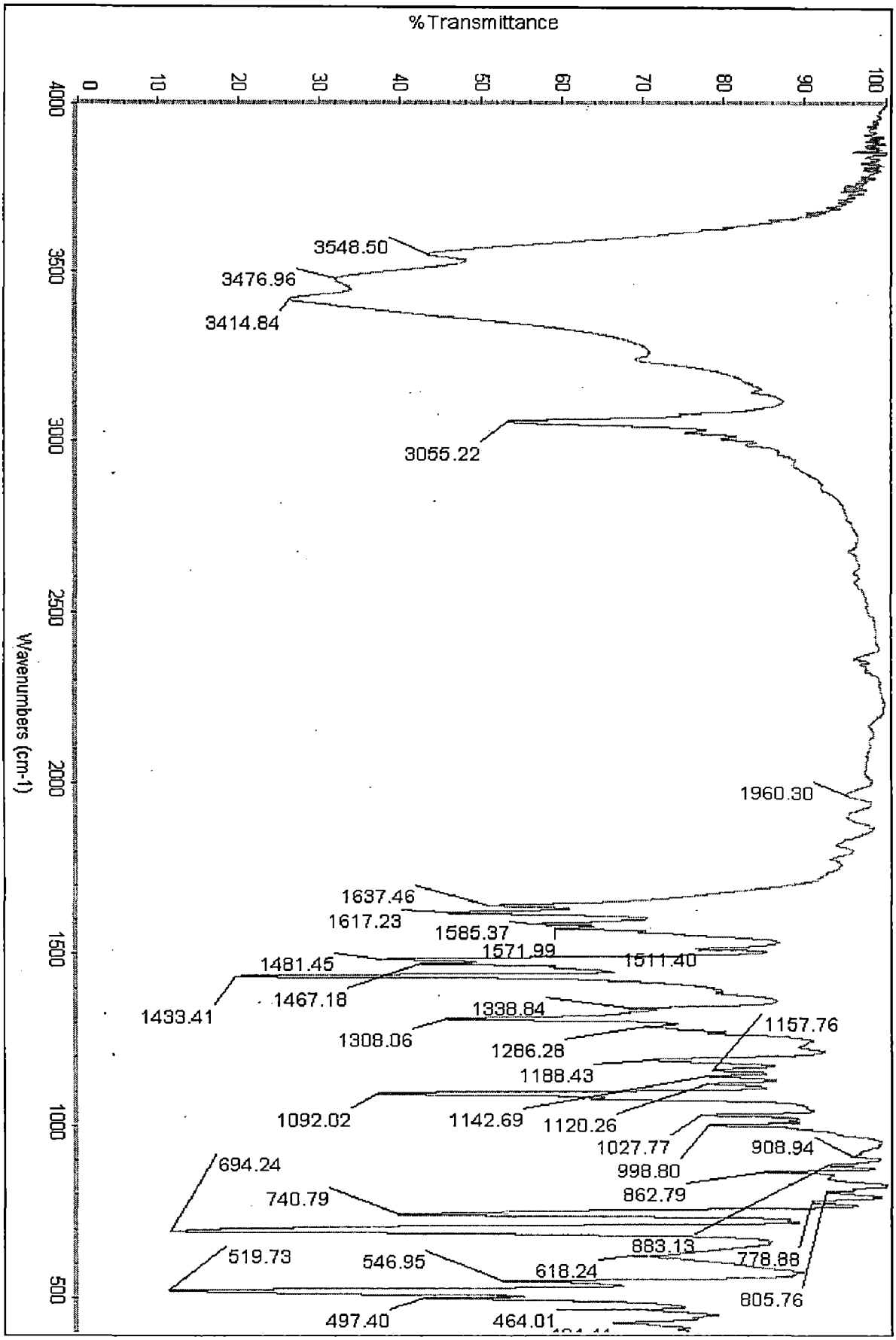

Figure A.5: IR Spectrum of $Ru(PPh_3)_2L^2Cl$

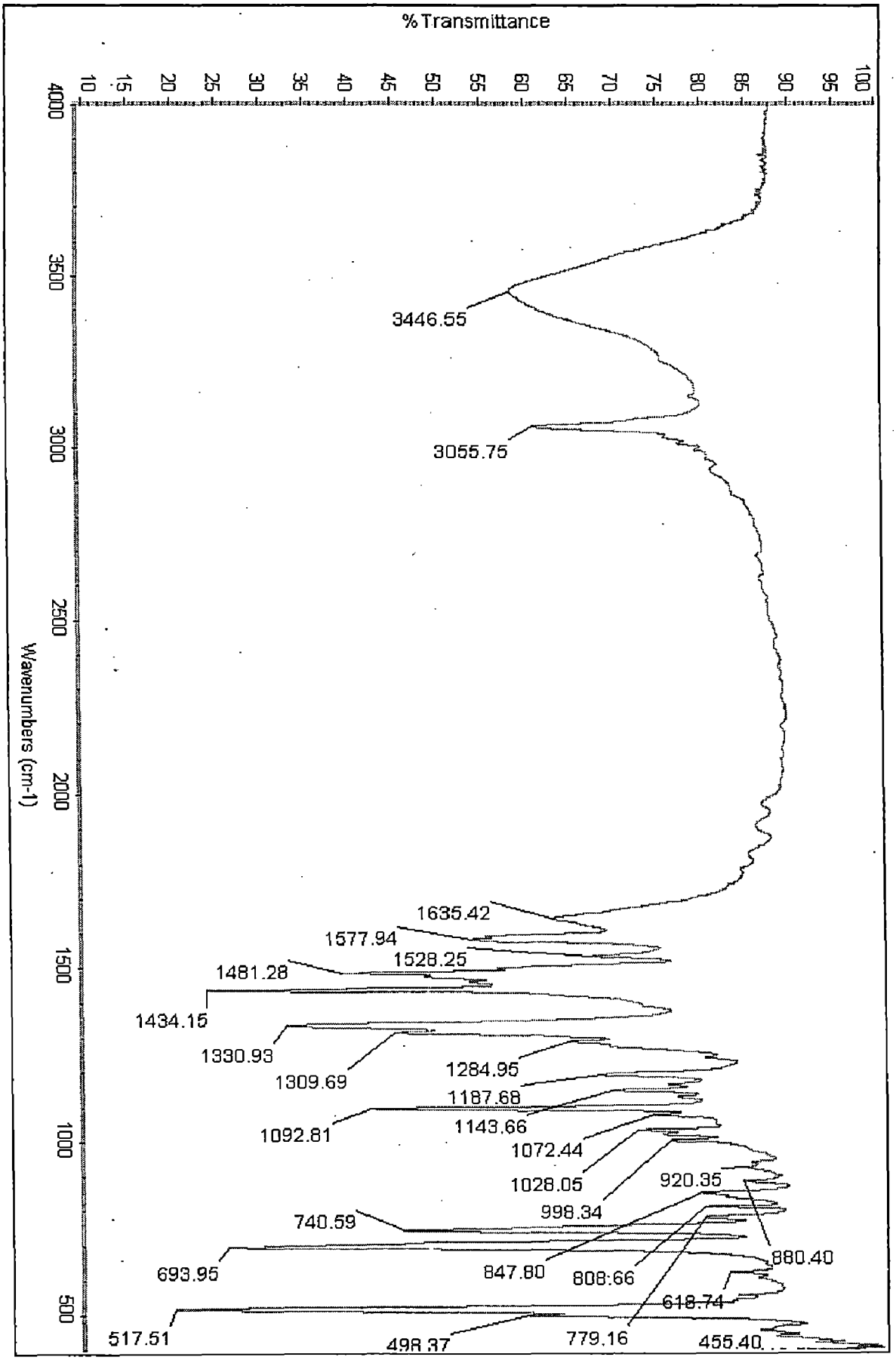

Figure A.6: IR Spectrum of $Ru(PPh_3)_2L^3Cl$

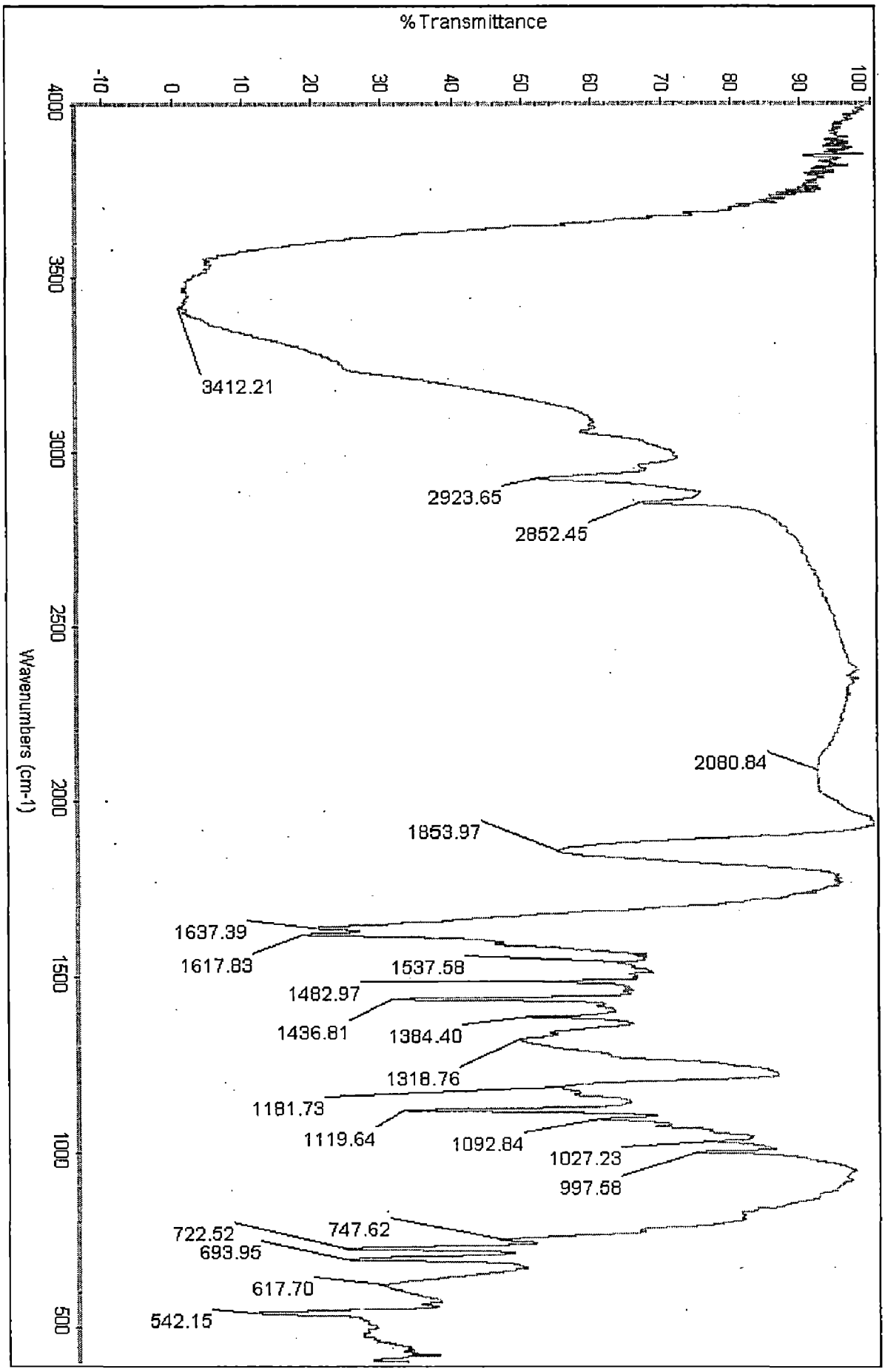

Figure A.7: IR Spectrum of $Ru(PPh_3)_2L^1(NO)$

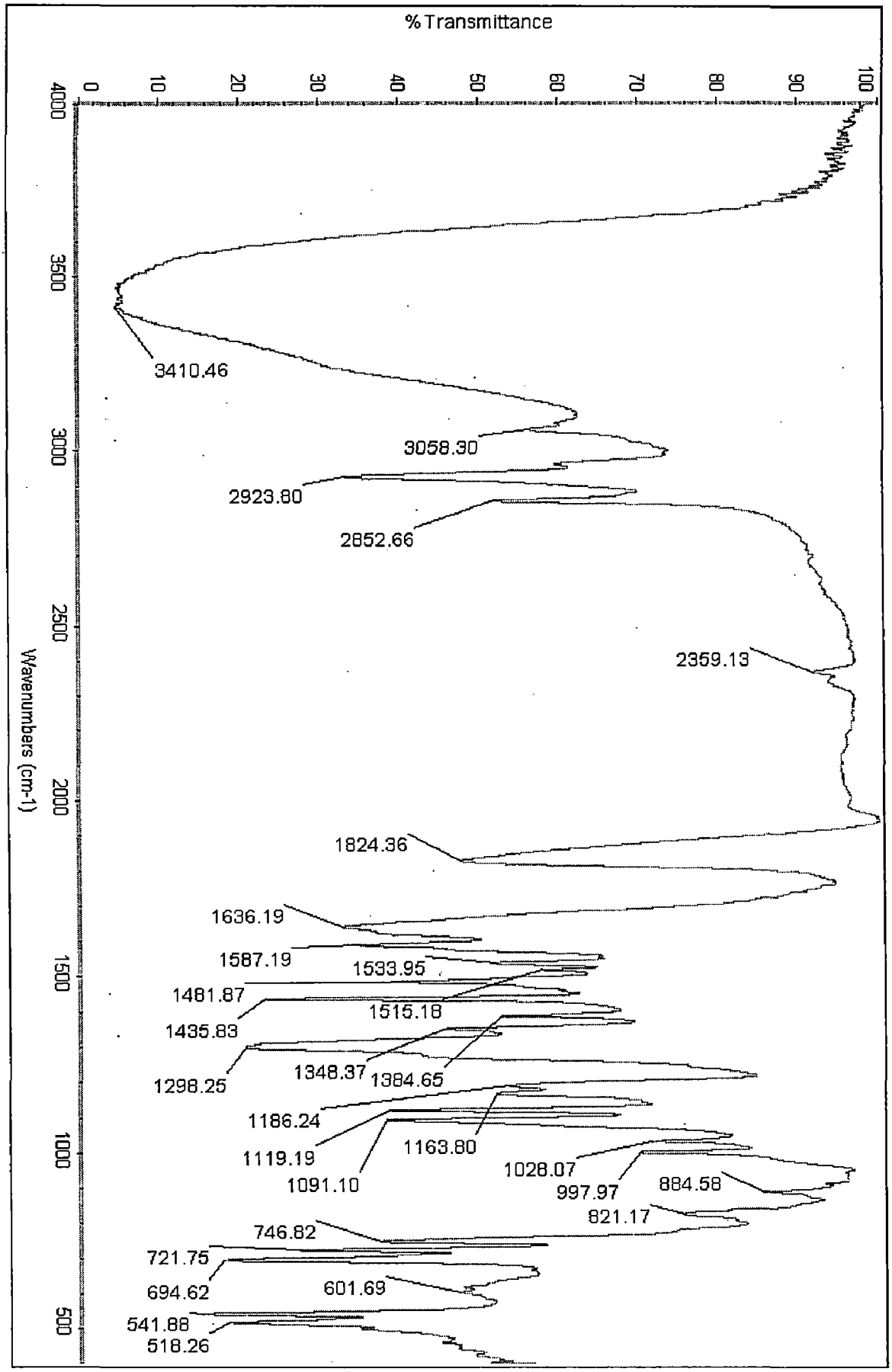

Figure A.8: IR Spectrum of $Ru(PPh_3)_2L^2(NO)$

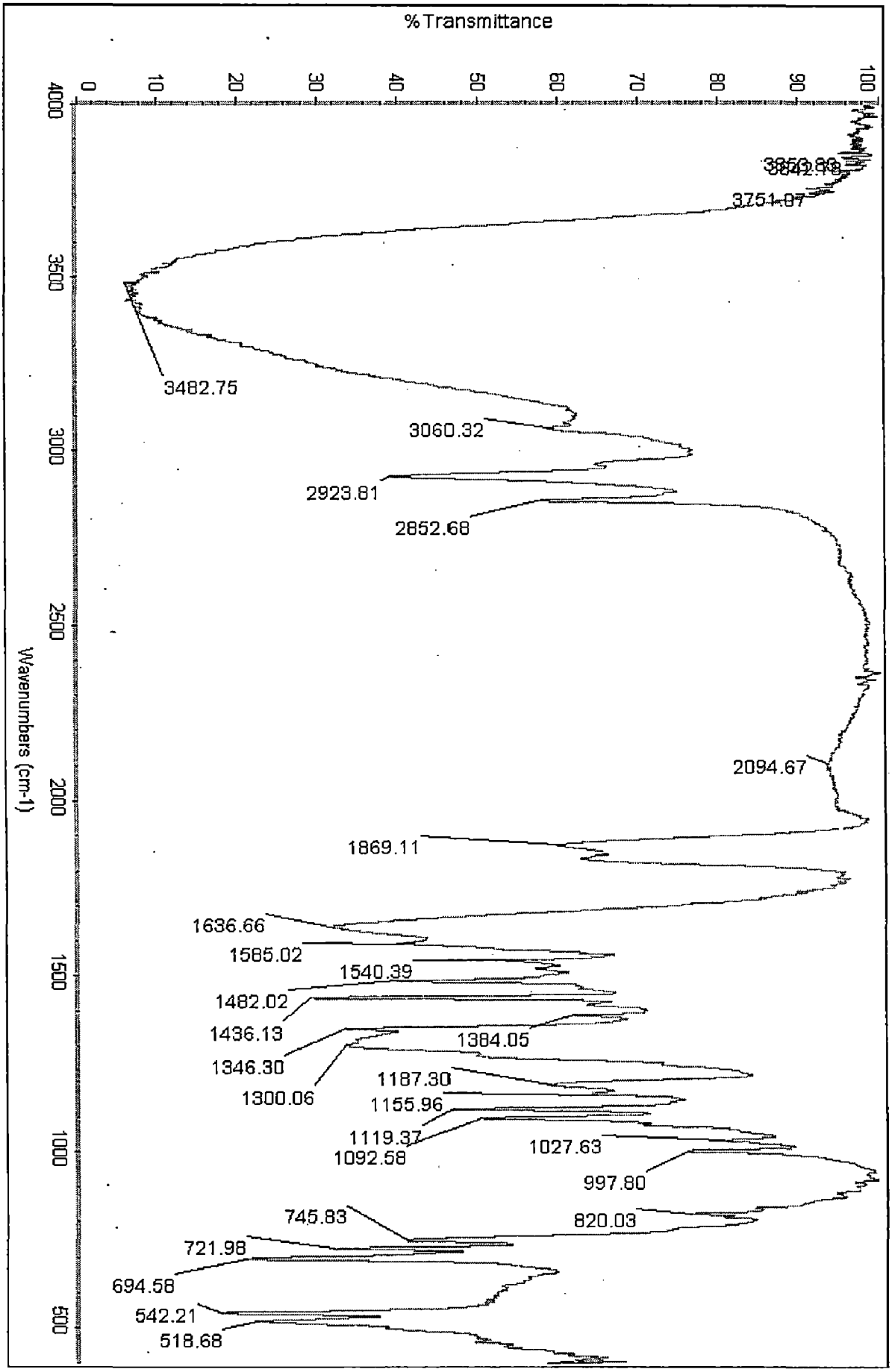

Figure A.9: IR Spectrum of $Ru(PPh_3)_2L^3(NO)$

Appendix B

Gas Chromatograms and Mass Spectra

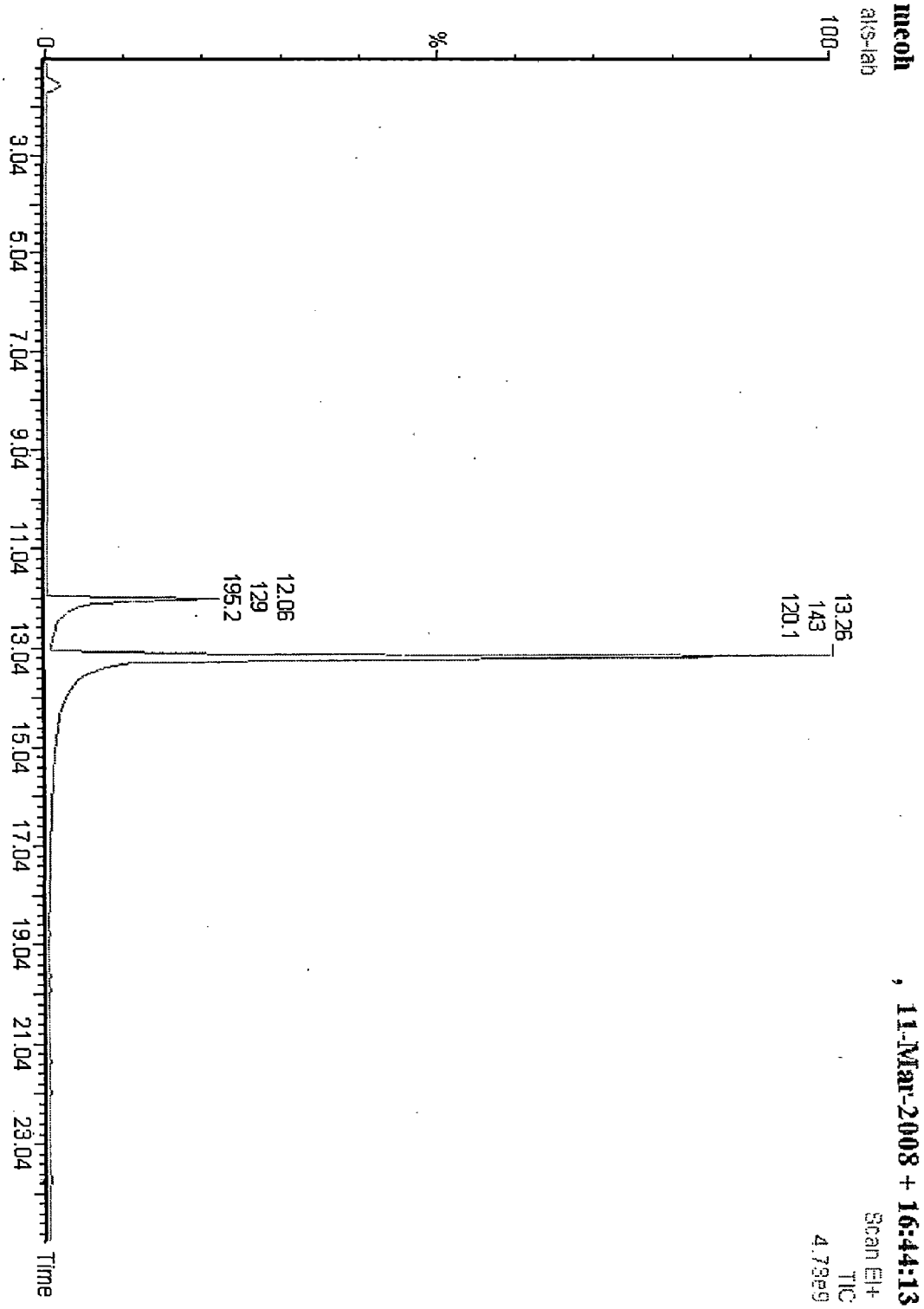

Figure B.1: Gas Chromatogram of Ligand L^1

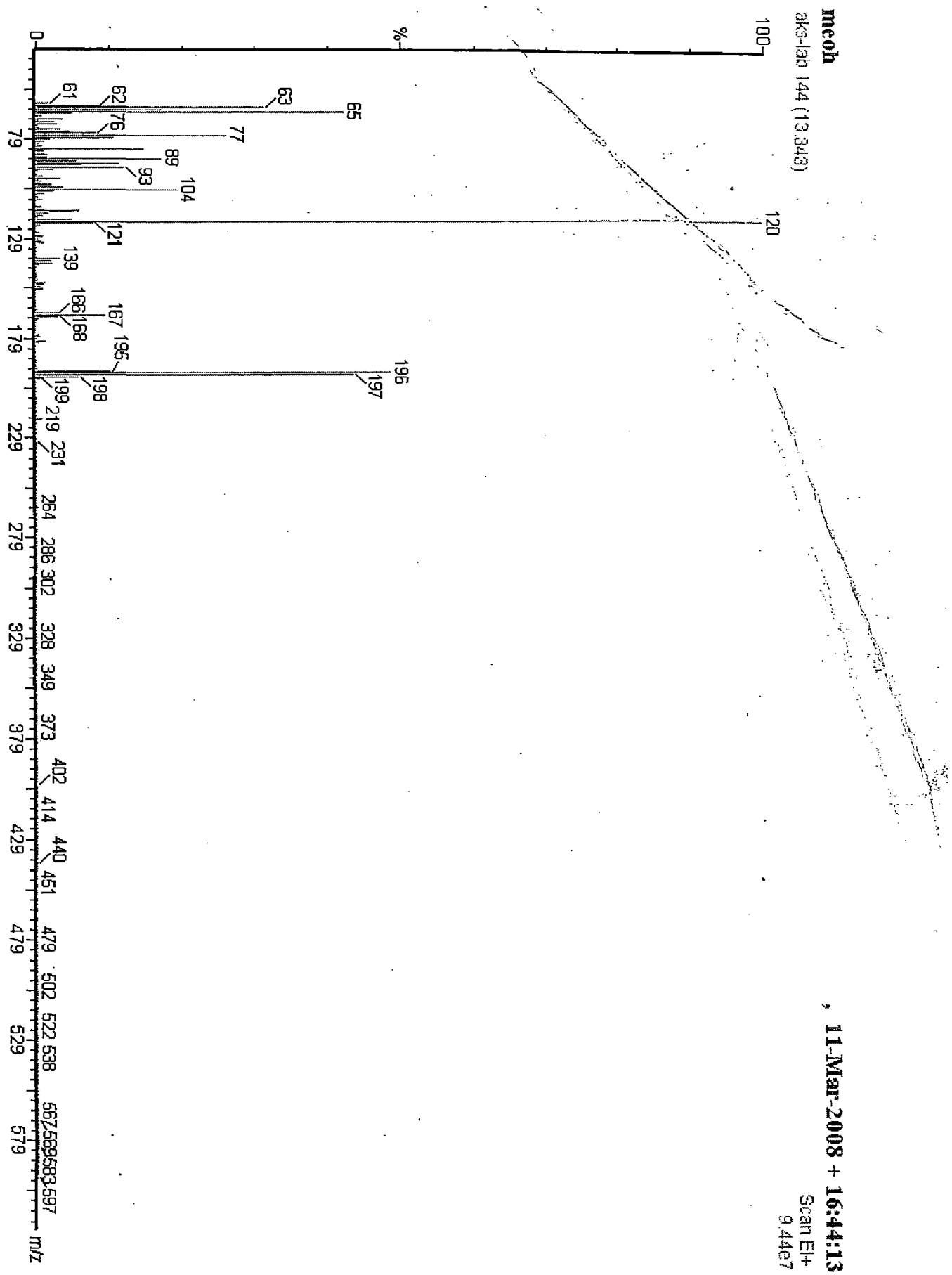

Figure B.2: Mass Spectrum of Ligand L^1

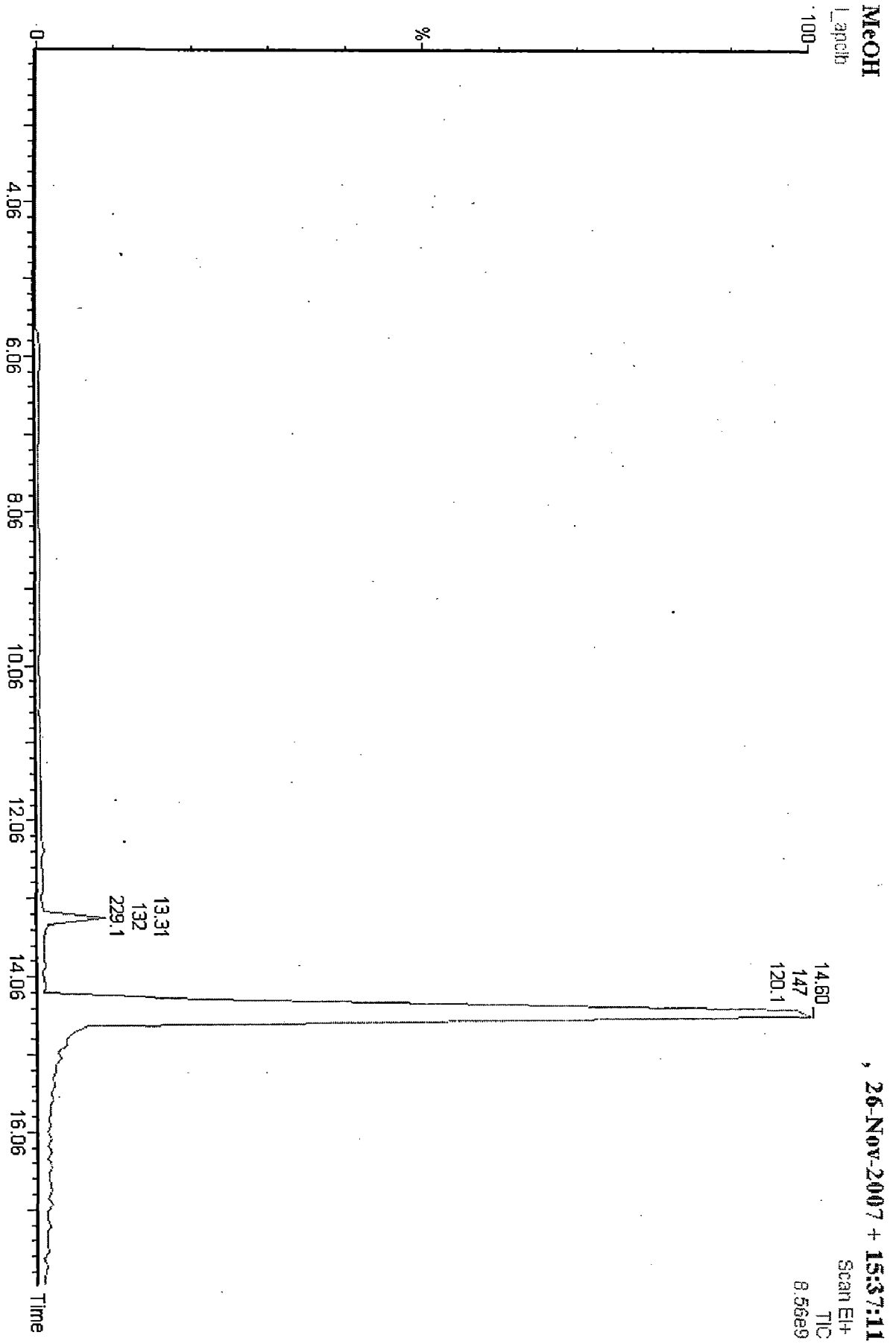

Figure B.3: Gas Chromatogram of Ligand L^2

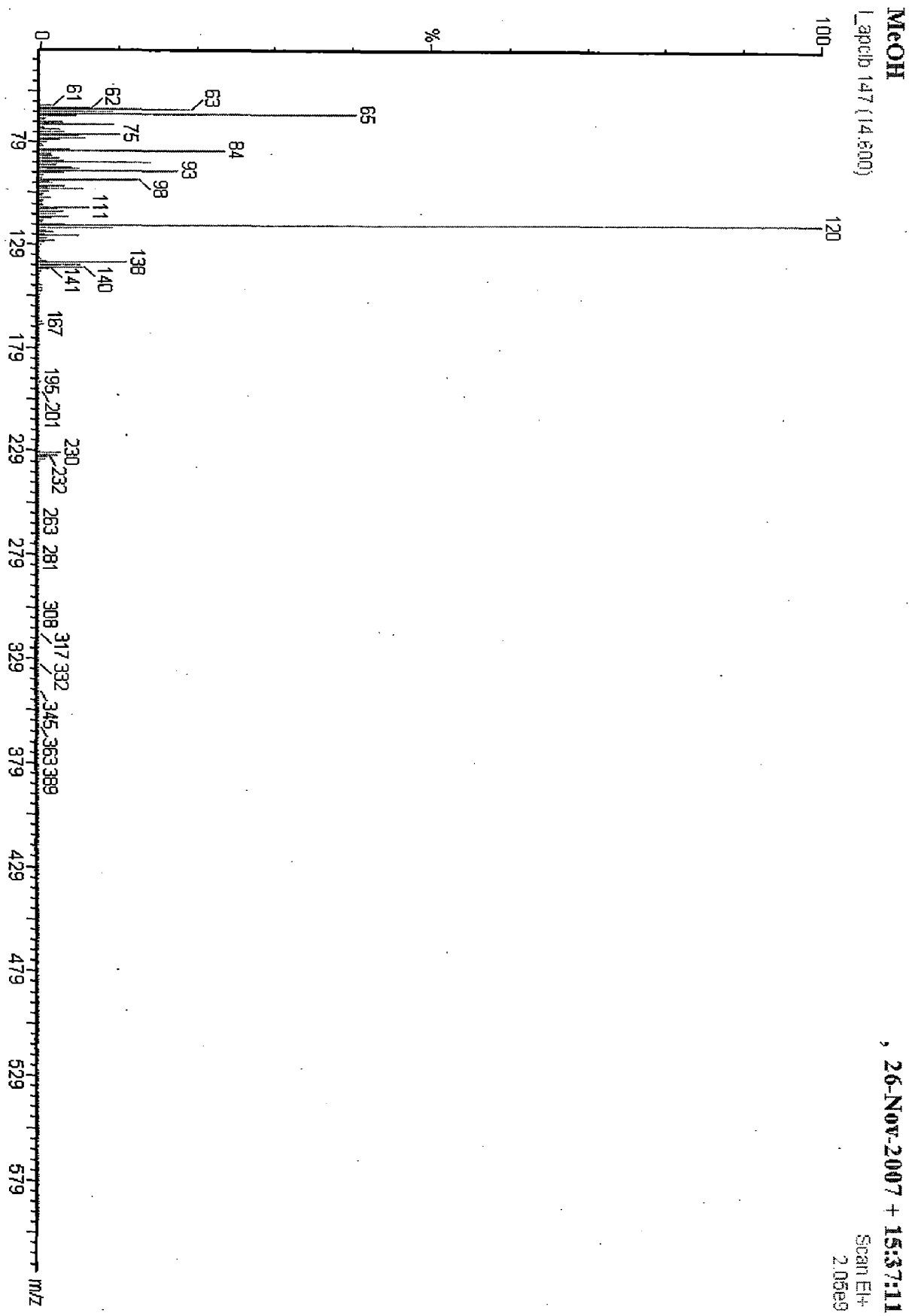

Figure B.4: Mass Spectrum of Ligand L^2

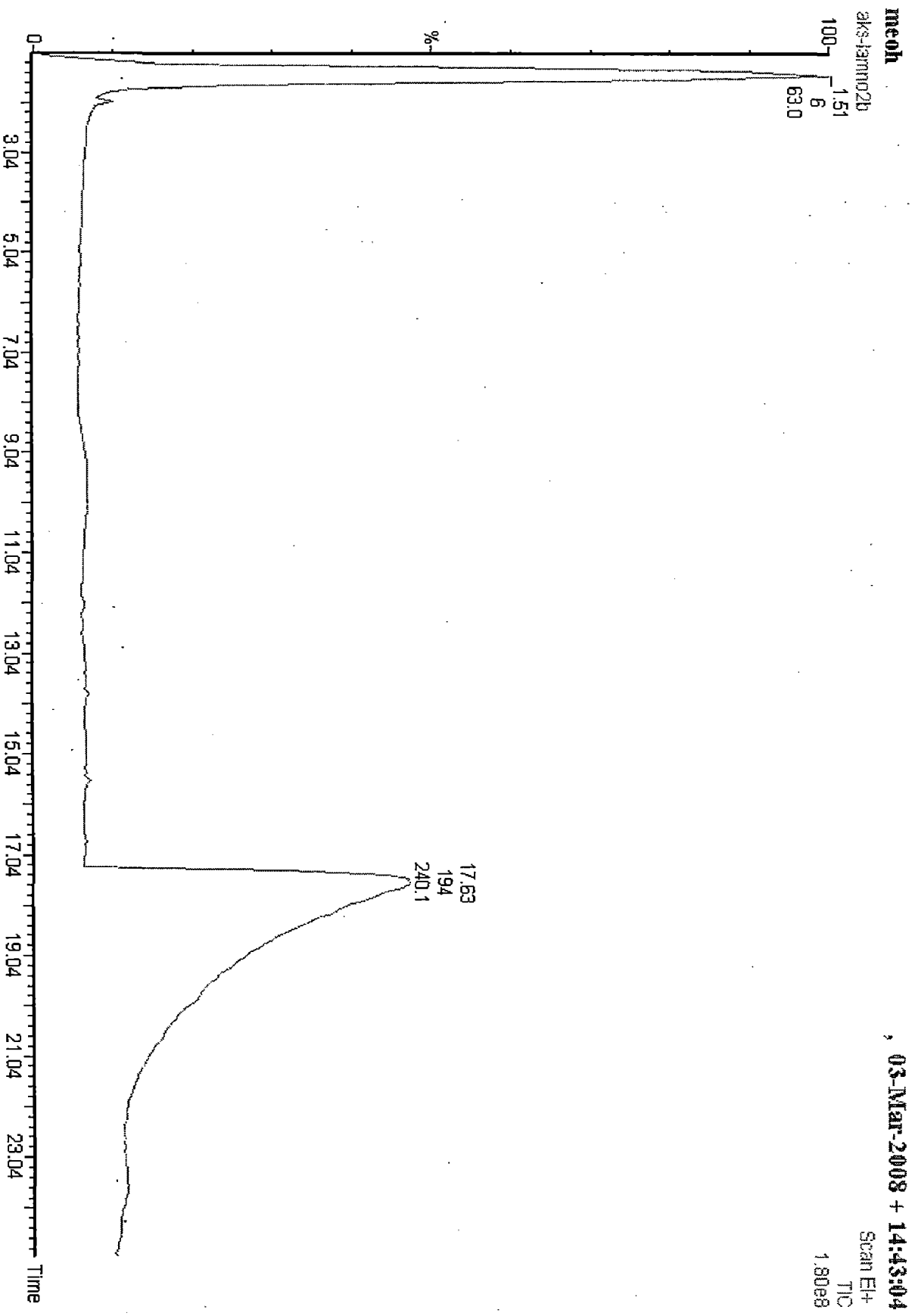

Figure B.5: Gas Chromatogram of Ligand L^3

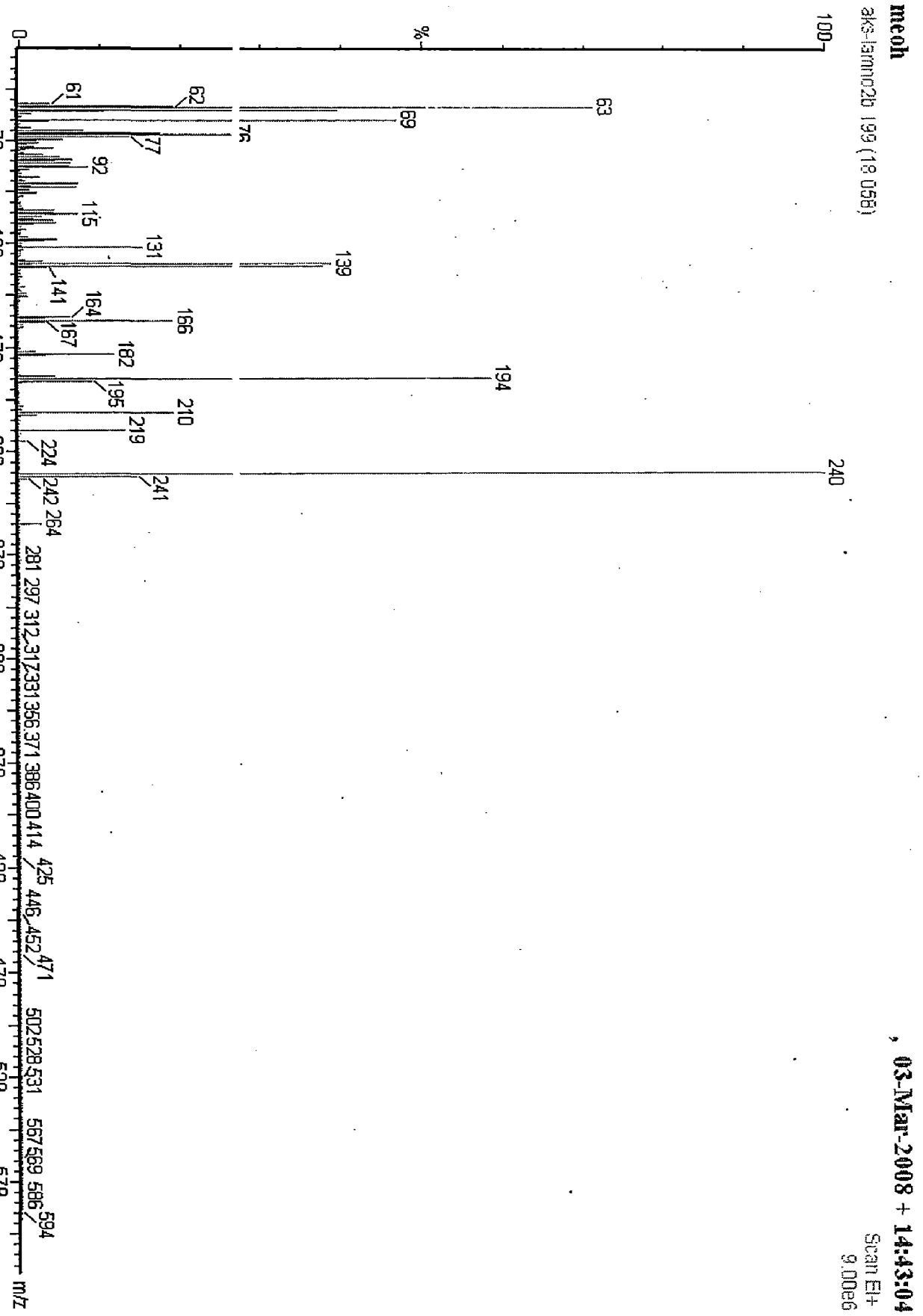

Figure B.6: Mass Spectrum of Ligand L^3

Appendix C

NMR Spectra

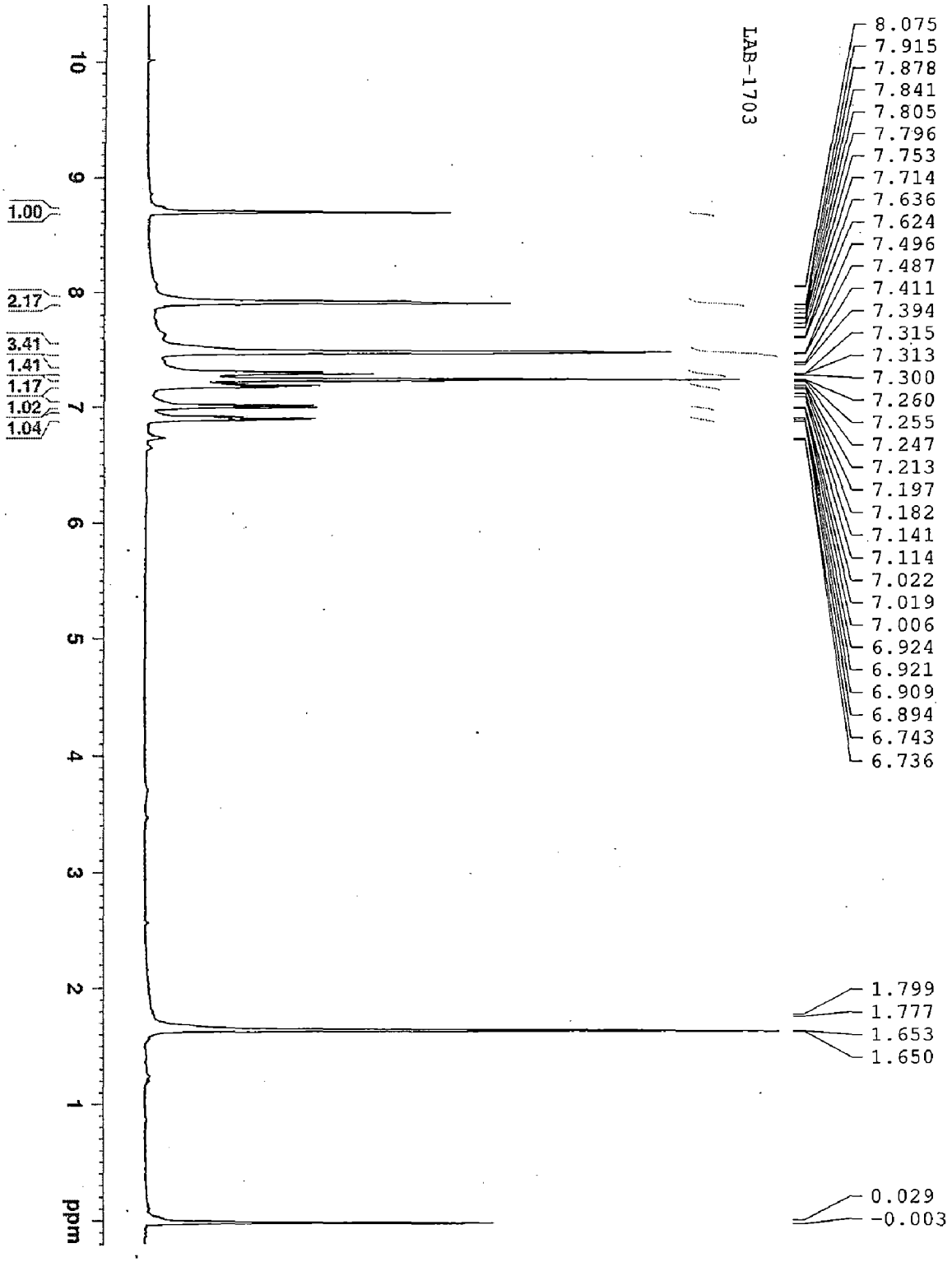

Figure C.1: ^1H NMR Spectrum of Ligand L^1

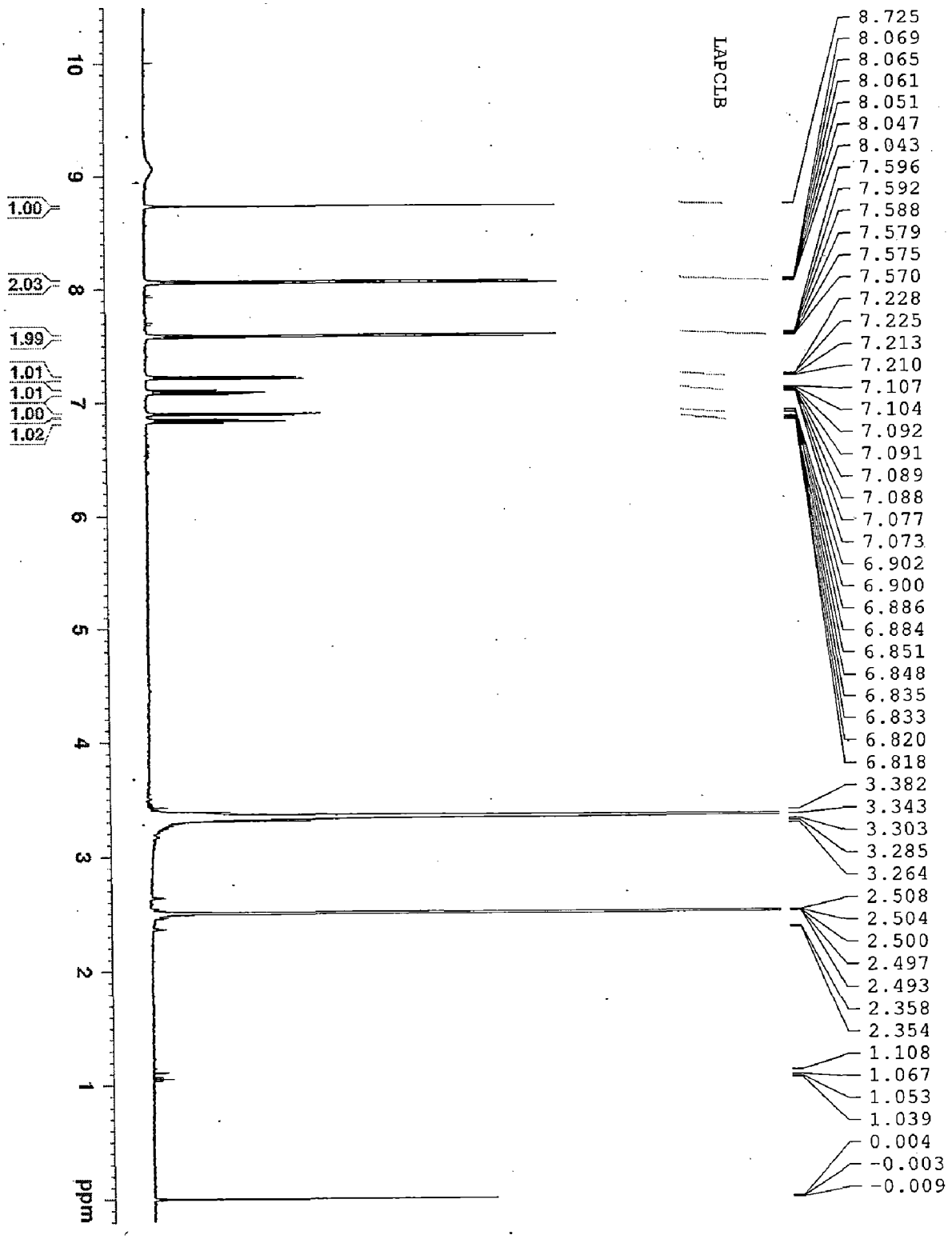

Figure C.2: ^1H NMR Spectrum of Ligand L^2

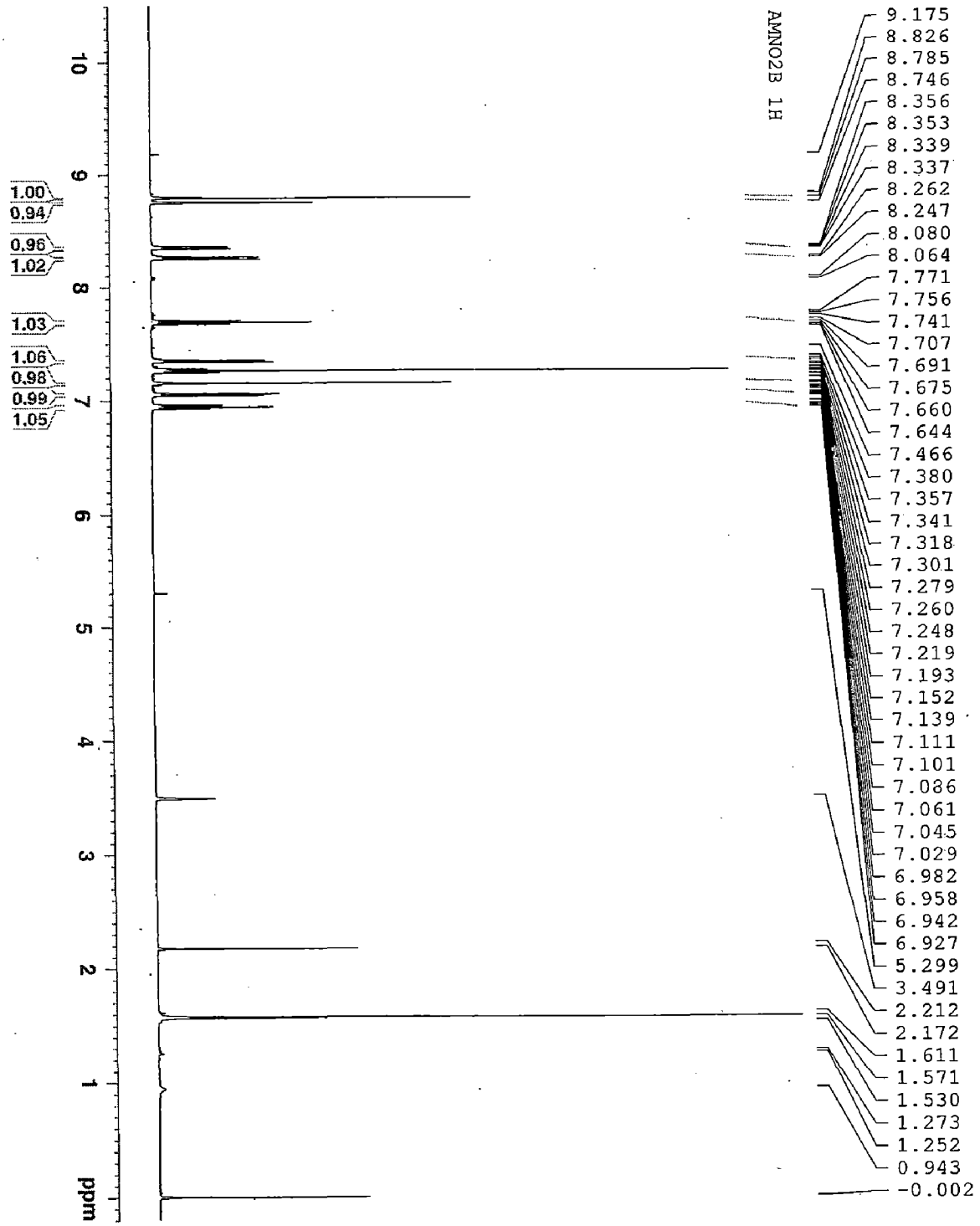

Figure C.3: ^1H NMR Spectrum of Ligand L^3

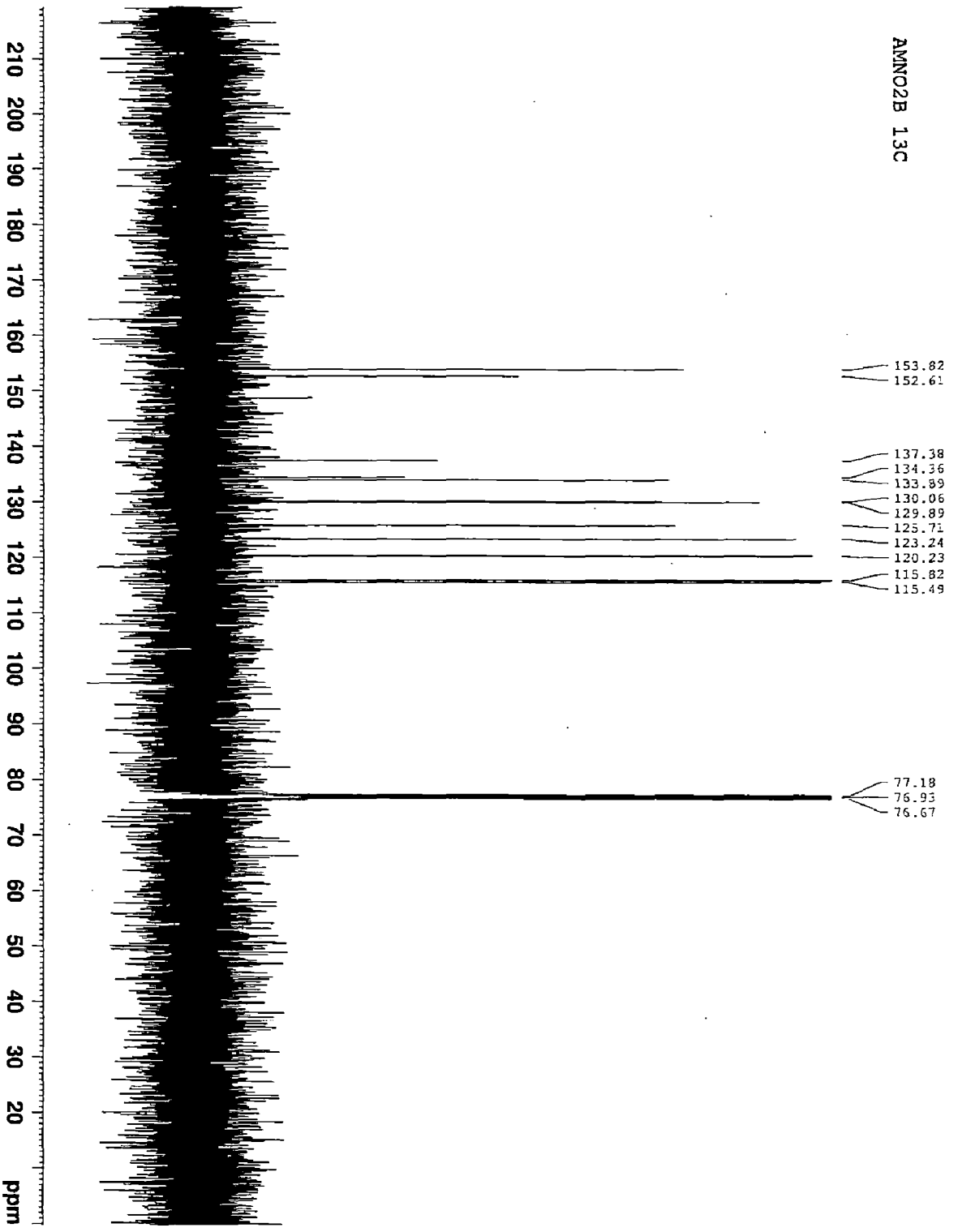

Figure C.4: ^{13}C NMR Spectrum of Ligand L^3

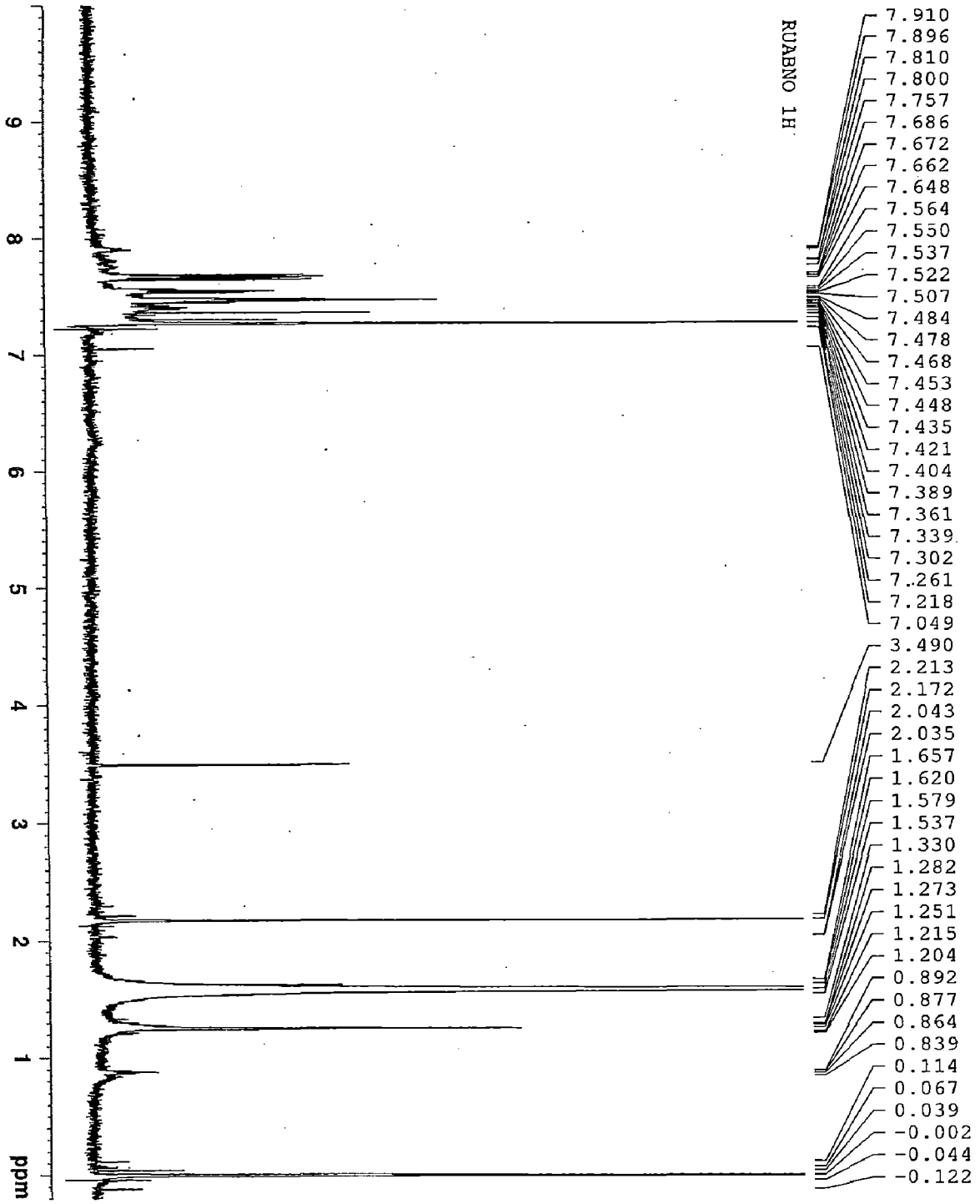

Figure C.5: ^1H NMR Spectrum of $Ru(PPh_3)_2L^1(NO)$

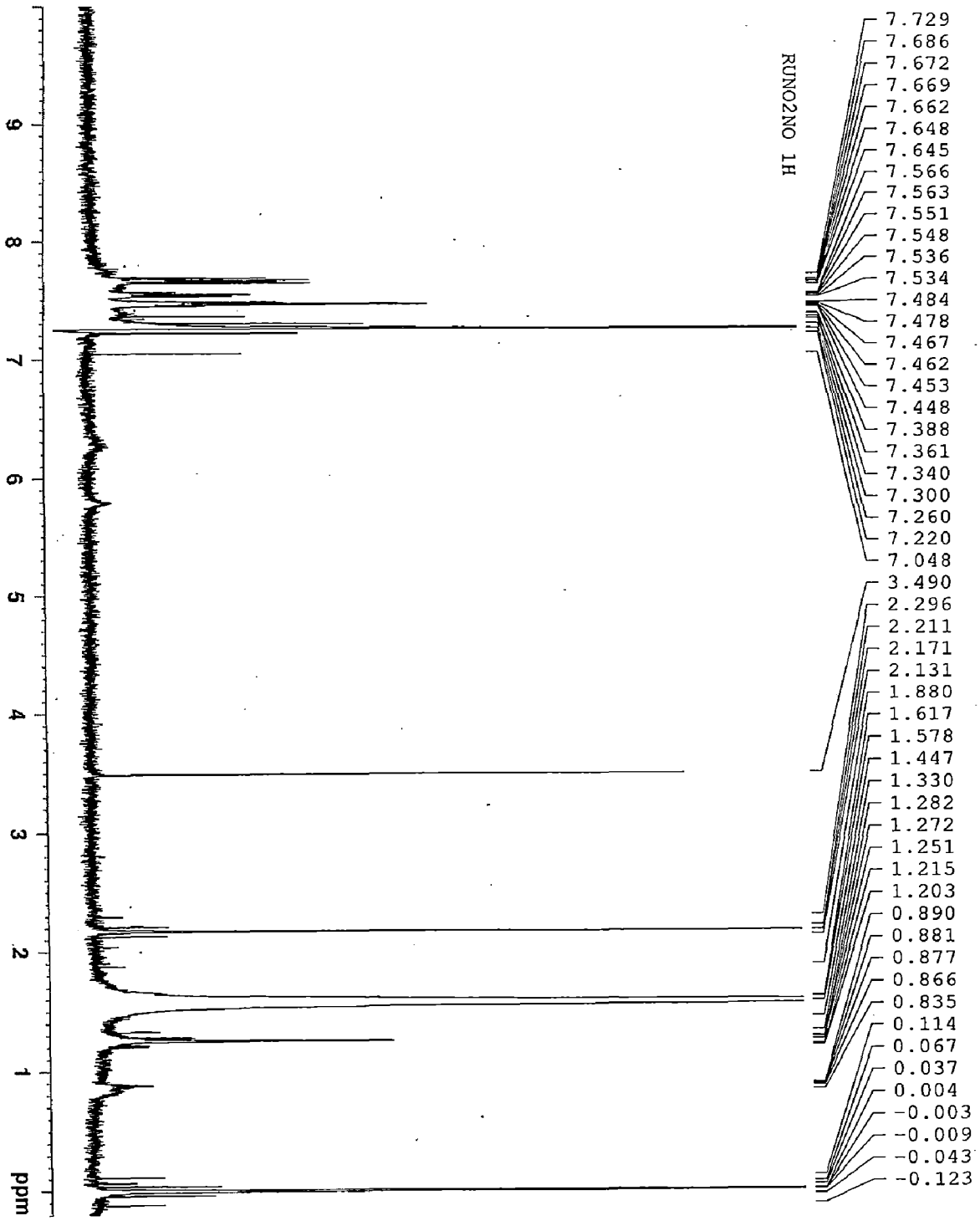

Figure C.6: ^1H NMR Spectrum of $Ru(PPh_3)_2L^3(NO)$

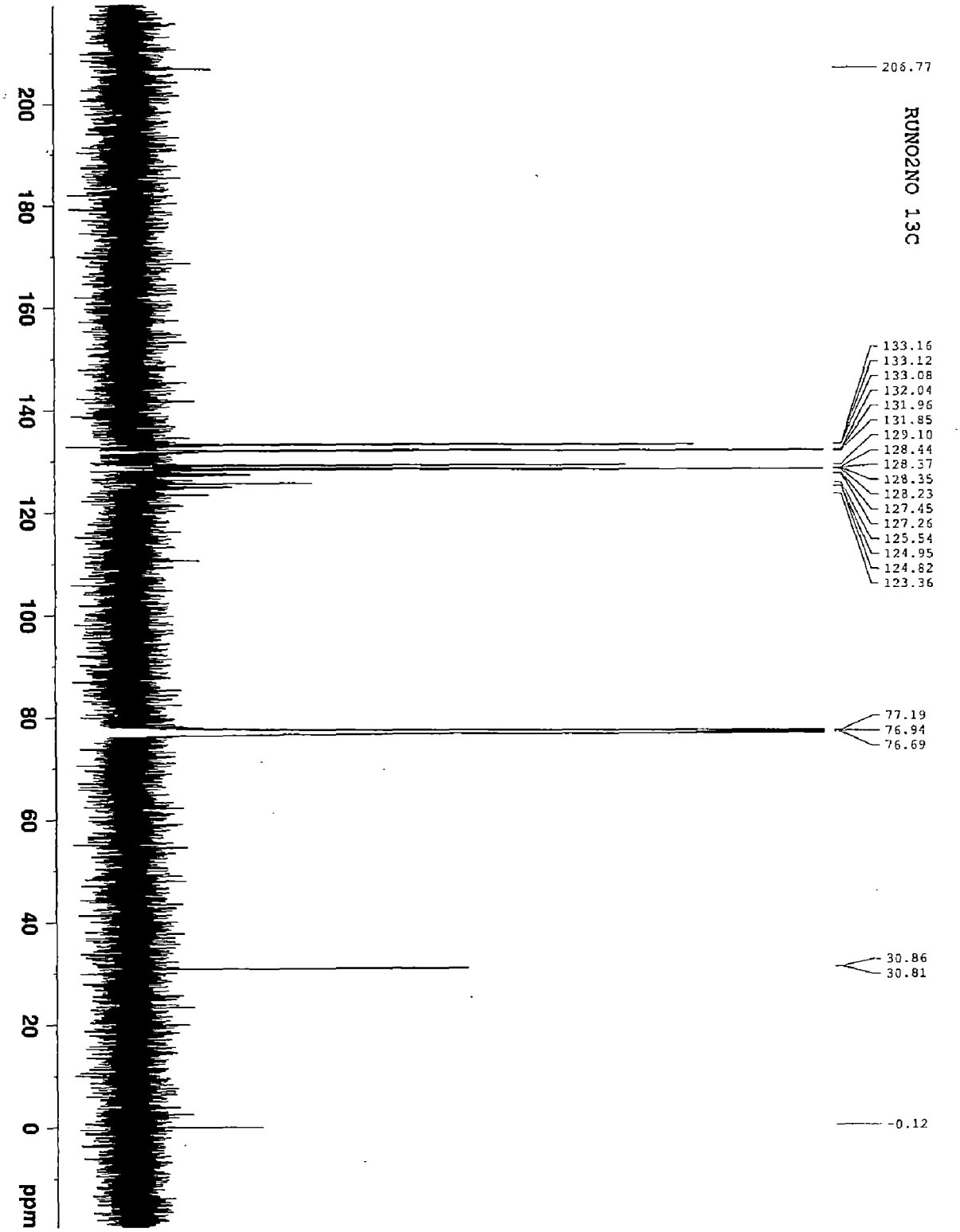

Figure C.7: ^{13}C NMR Spectrum of $Ru(PPh_3)_2L^3(NO)$

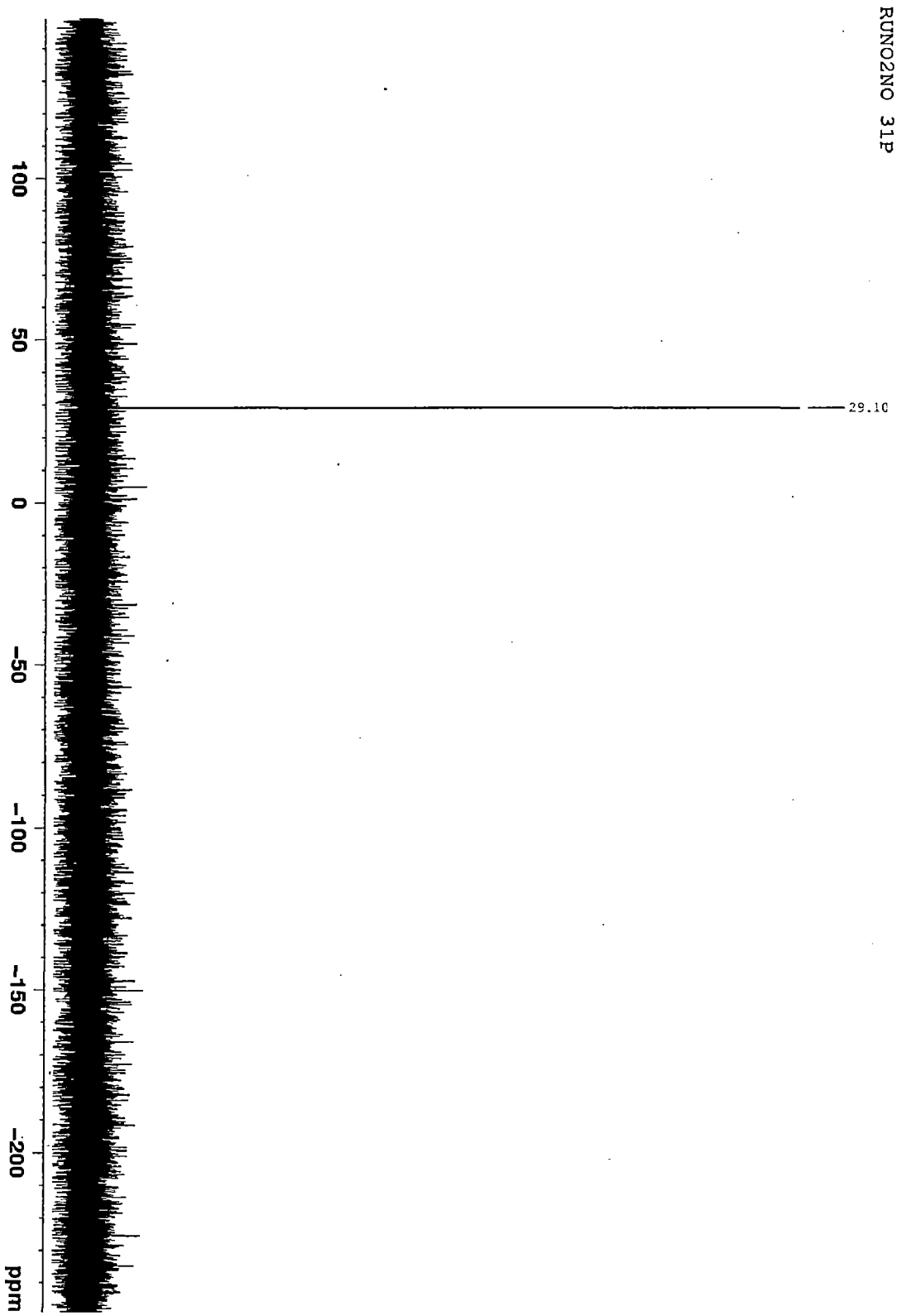

Figure C.8: ^{31}P NMR Spectrum of $Ru(PPh_3)_2L^3(NO)$

Appendix D

UV-Vis Spectra

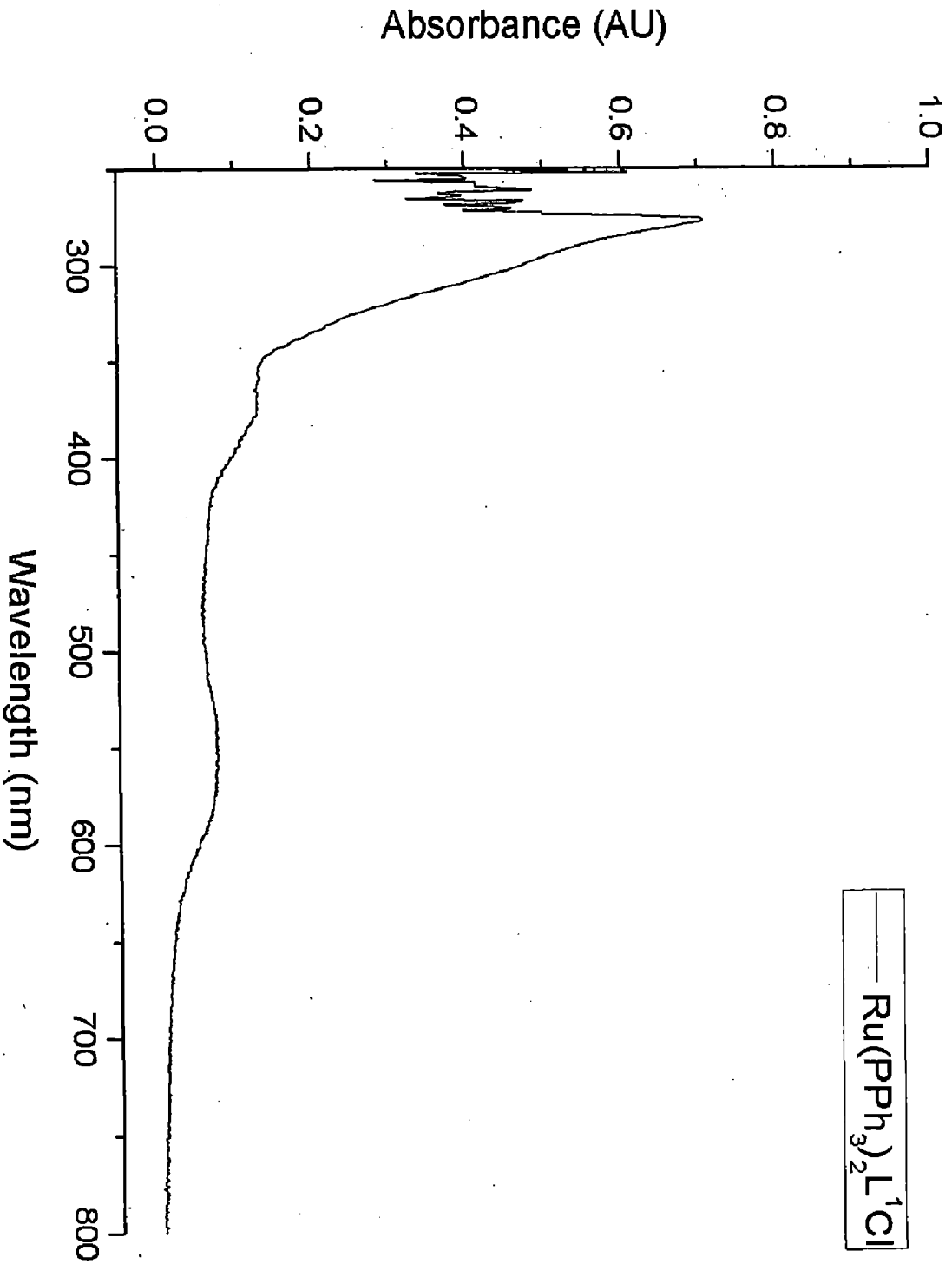

Figure D.1: UV-Vis Spectrum of $Ru(PPh_3)_2L^1Cl$

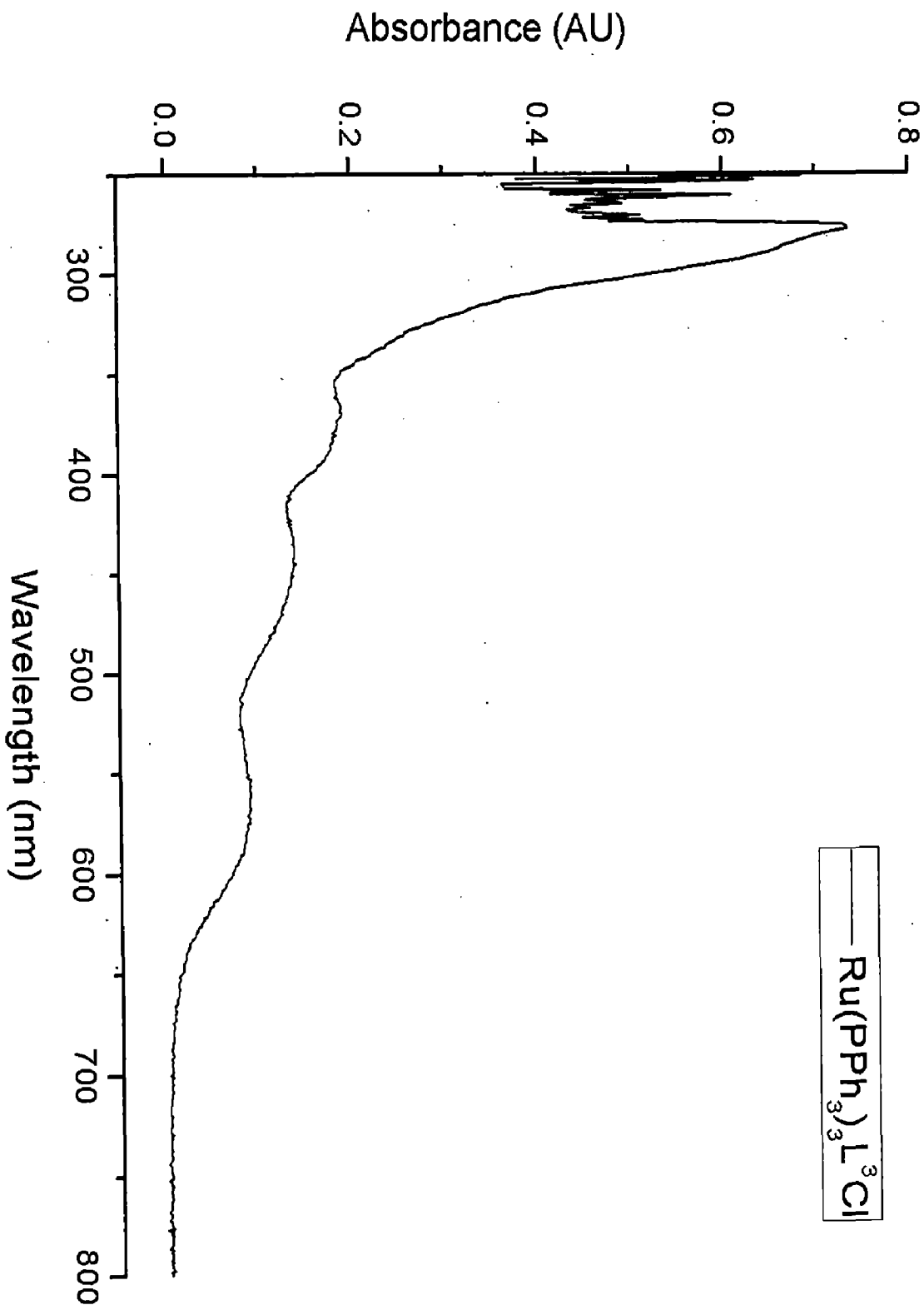

Figure D.3: UV-Vis Spectrum of $Ru(PPh_3)_2L^3Cl$

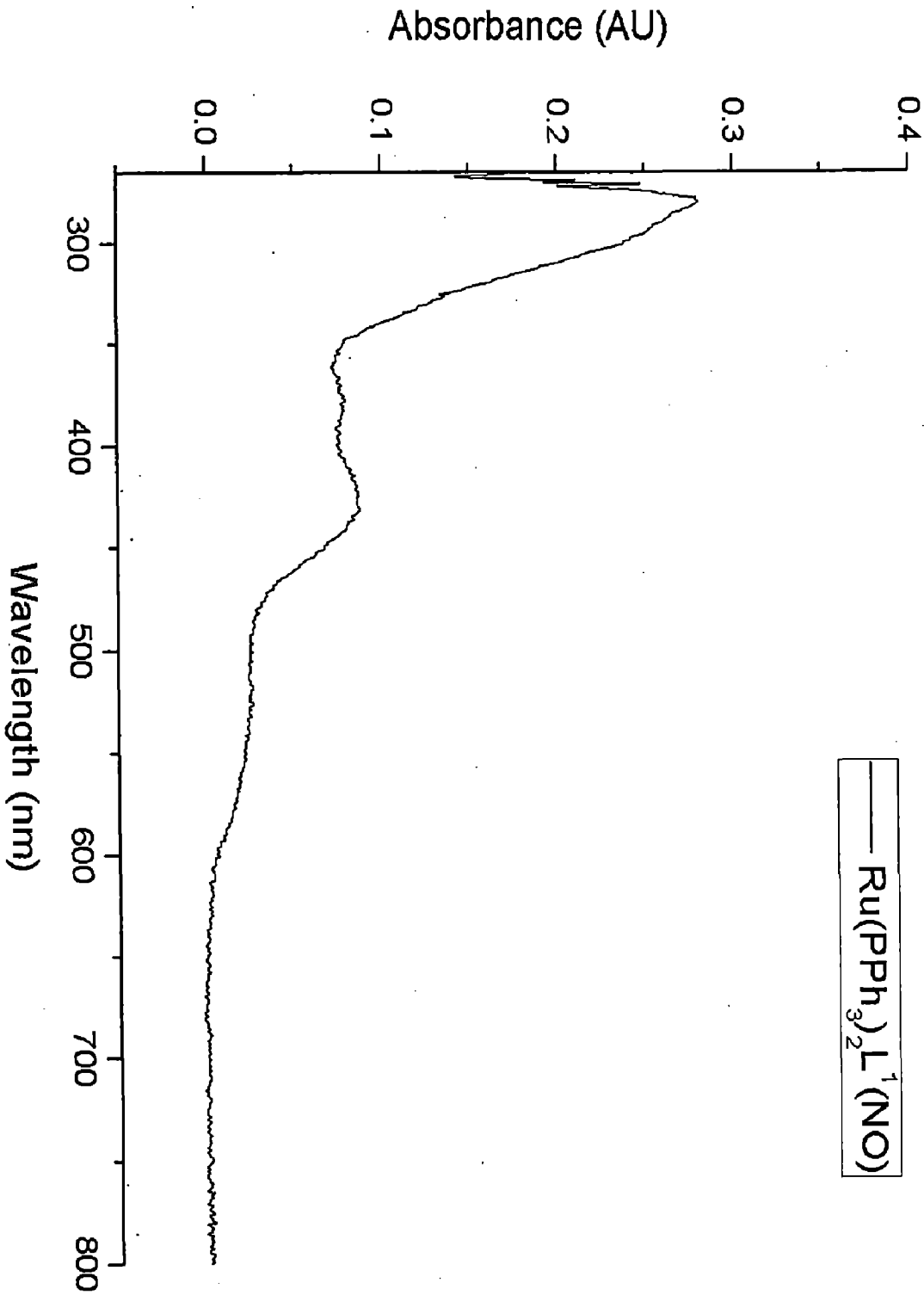

Figure D.4: UV-Vis Spectrum of $Ru(PPh_3)_2L^1(NO)$

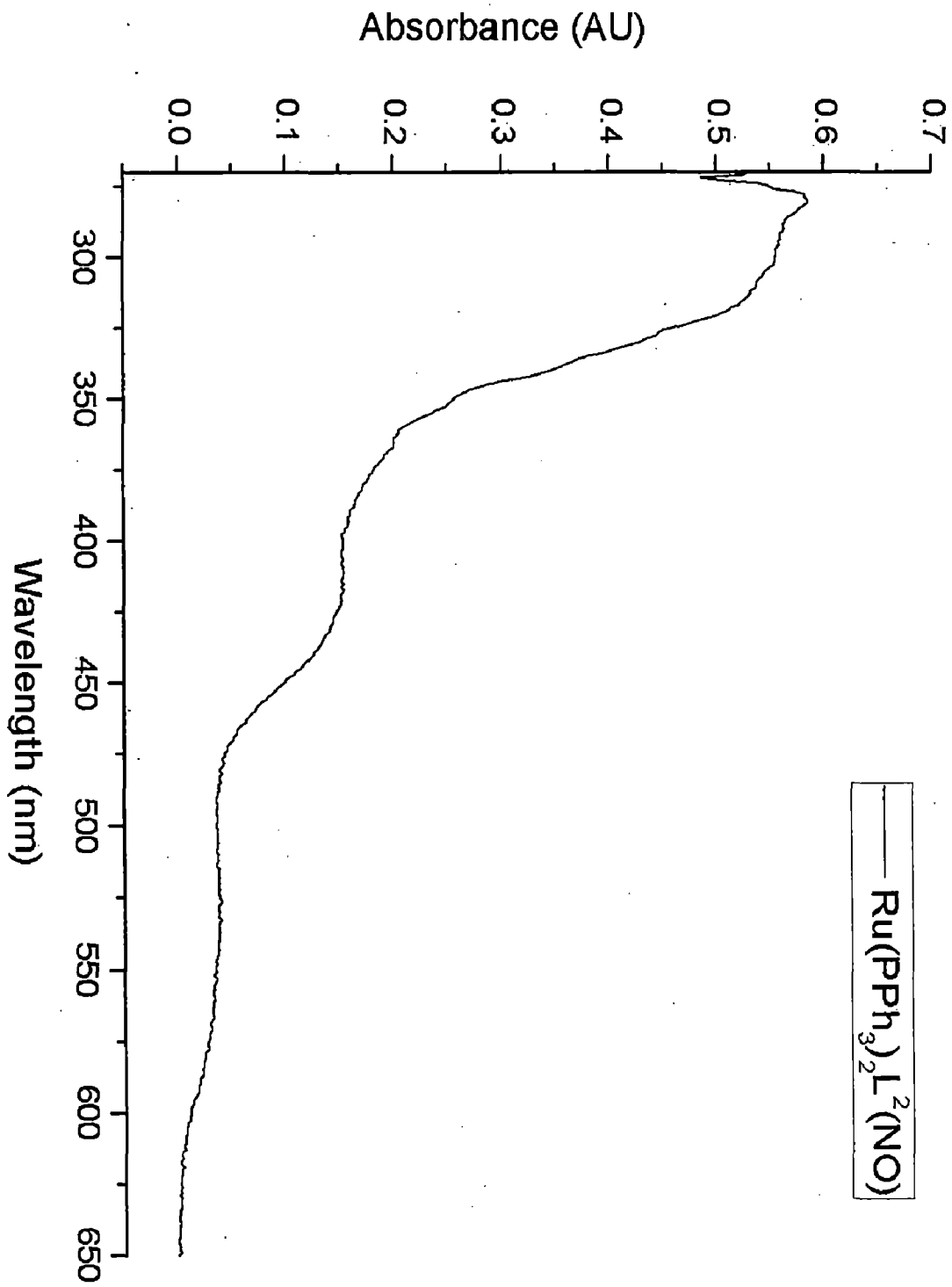

Figure D.5: UV-Vis Spectrum of $Ru(PPh_3)_2L^2(NO)$

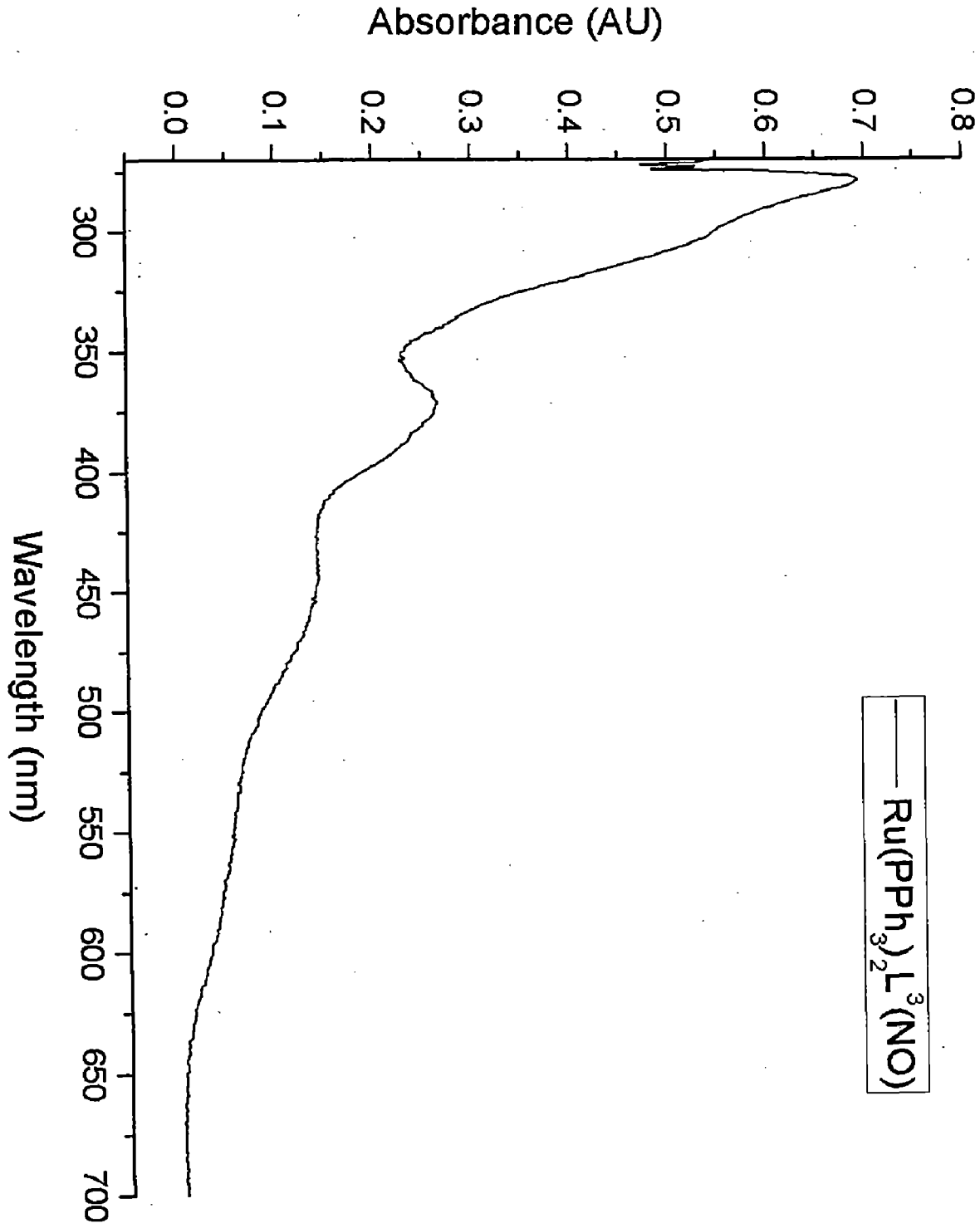

Figure D.6: UV-Vis Spectrum of $Ru(PPh_3)_2L^3(NO)$

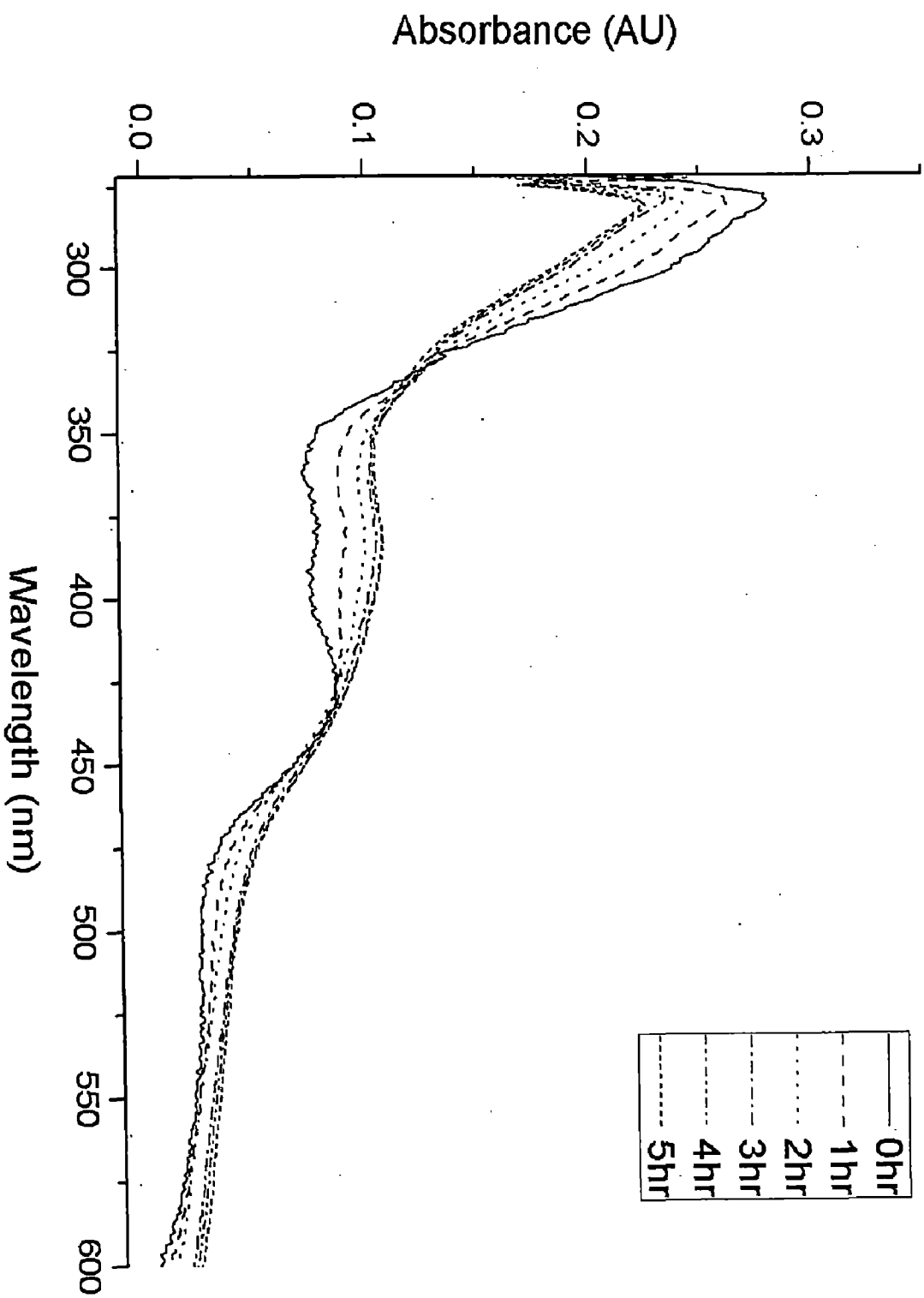

Figure D.7: Photolability of $Ru(PPh_3)_2L^1(NO)$

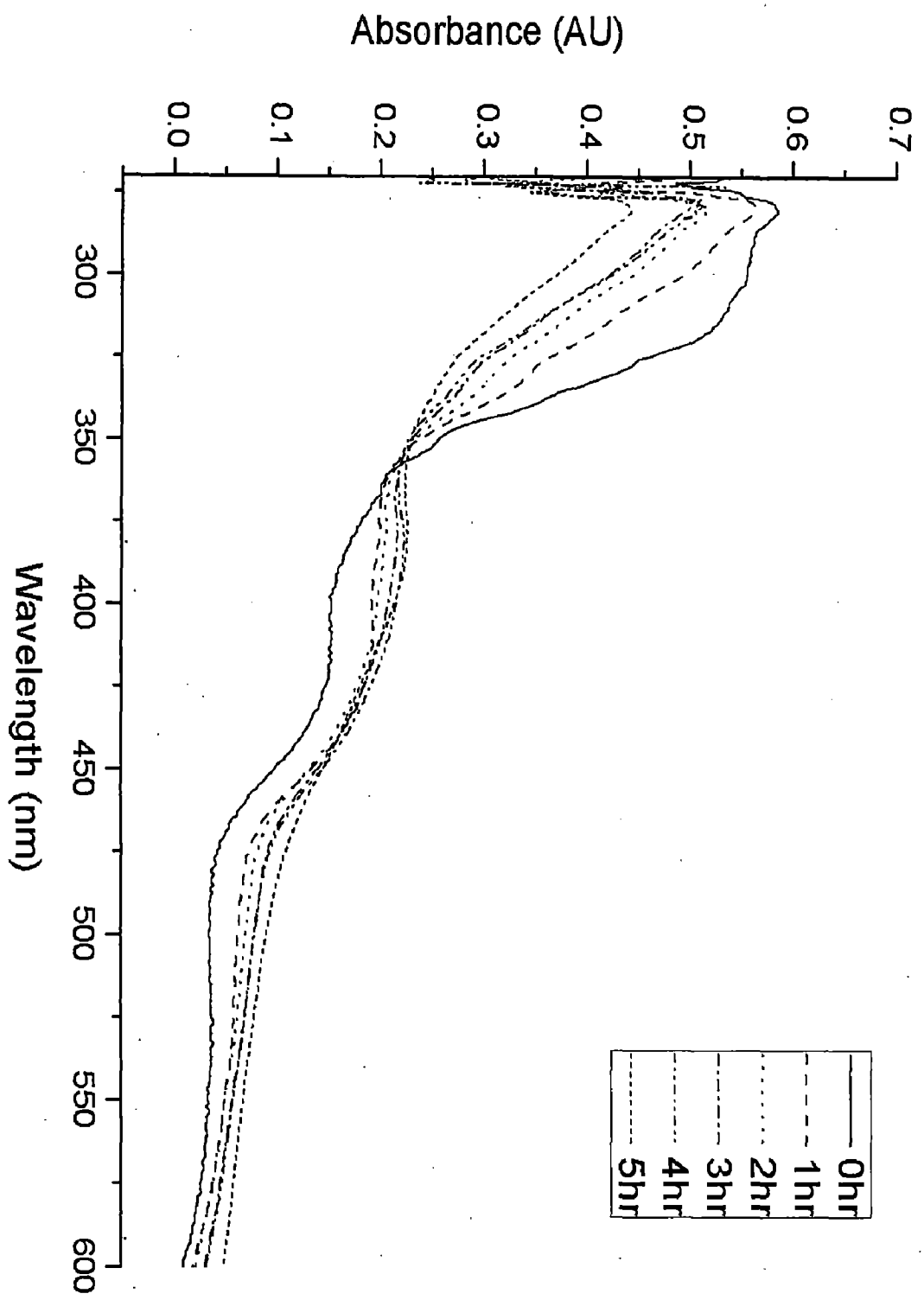

Figure D.8: Photolability of $Ru(PPh_3)_2L^2(NO)$

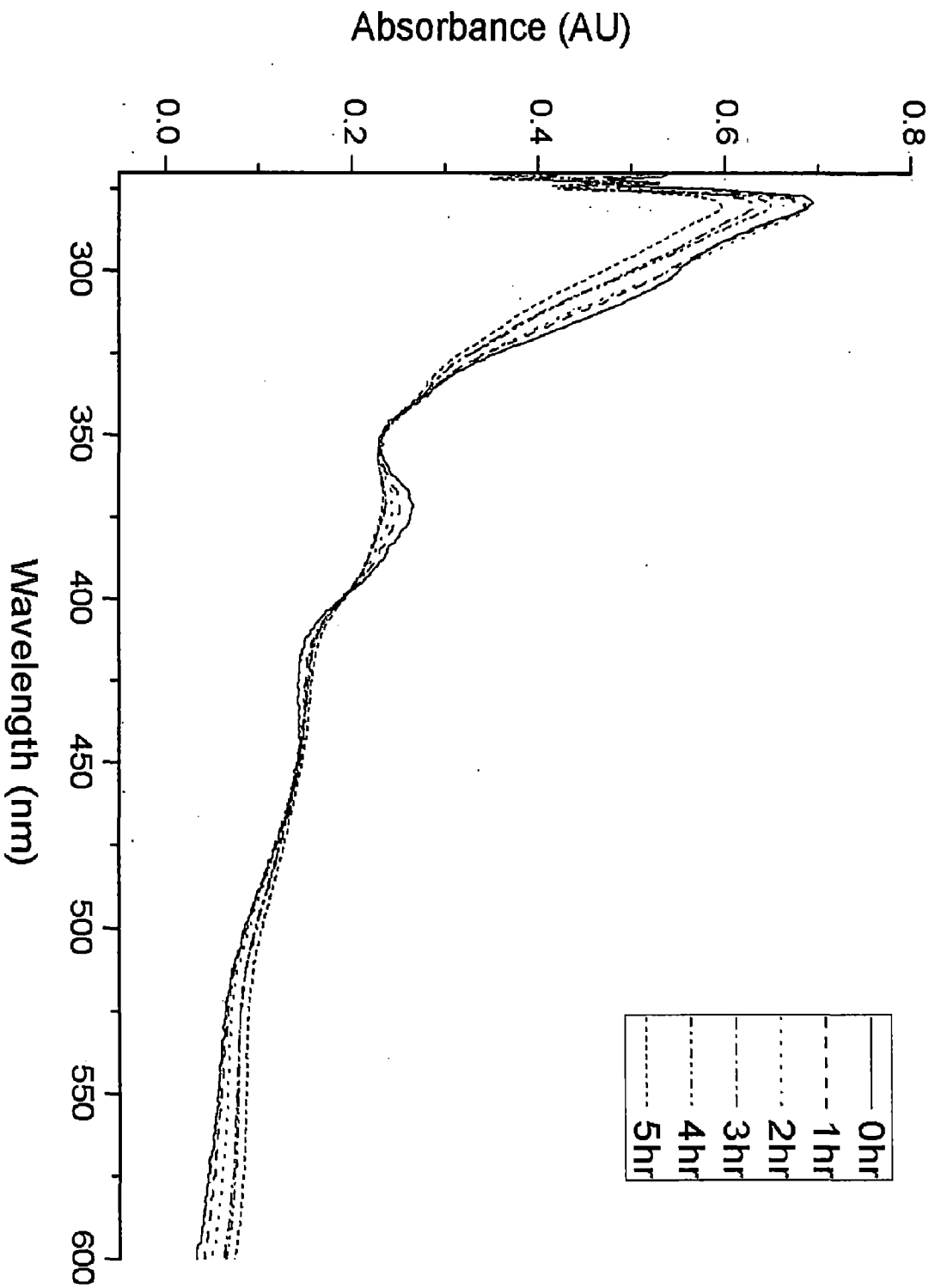

Figure D.9: Photolability of $Ru(PPh_3)_2L^3(NO)$

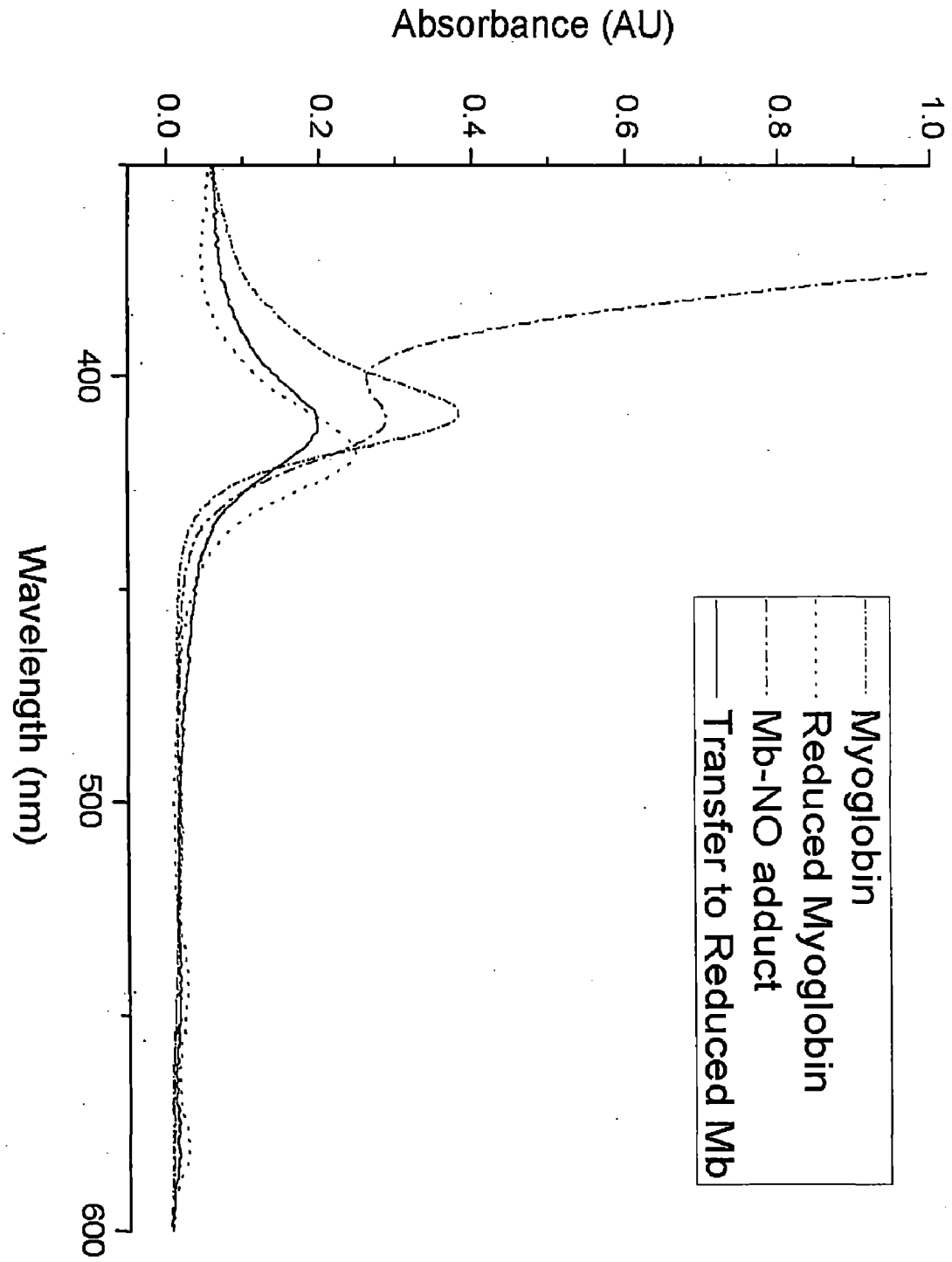

Figure D.10: Transfer of NO from $Ru(PPh_3)_2L^2(NO)$ to Reduced Myoglobin

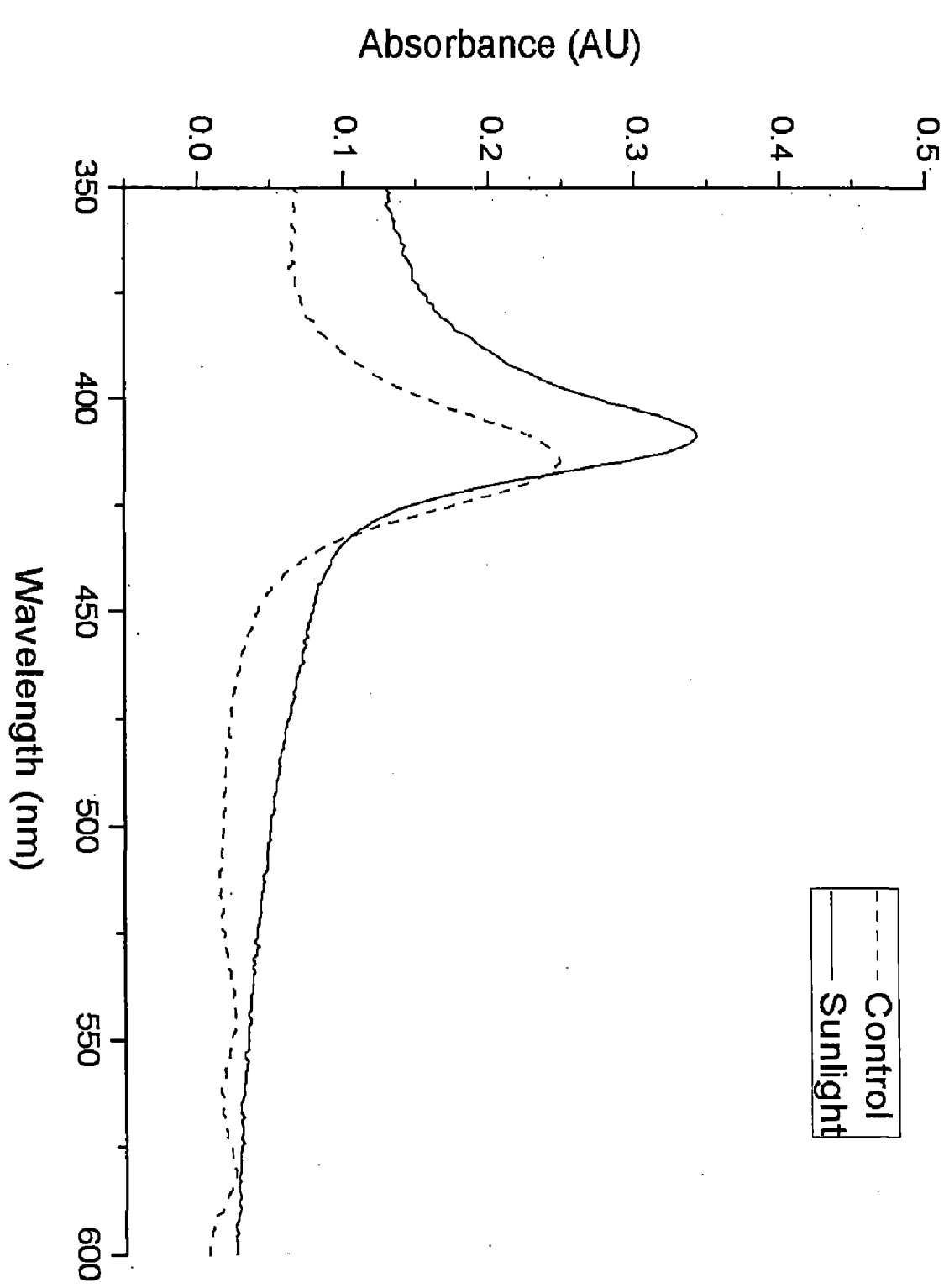

Figure D.11: Transfer of NO from $Ru(PPh_3)_2L^1(NO)$ to Reduced Myoglobin

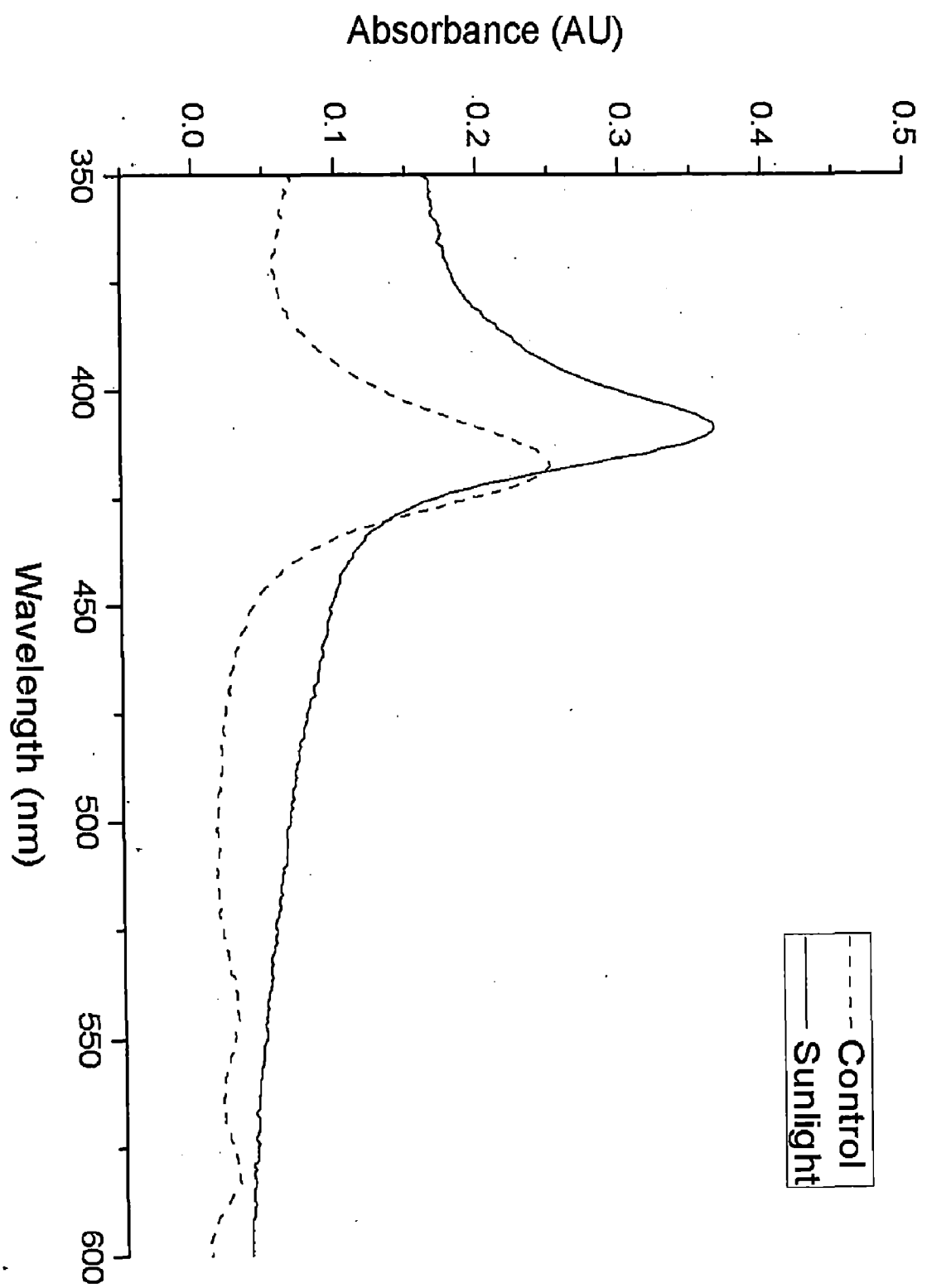

Figure D.12: Transfer of NO from $Ru(PPh_3)_2L^2(NO)$ to Reduced Myoglobin

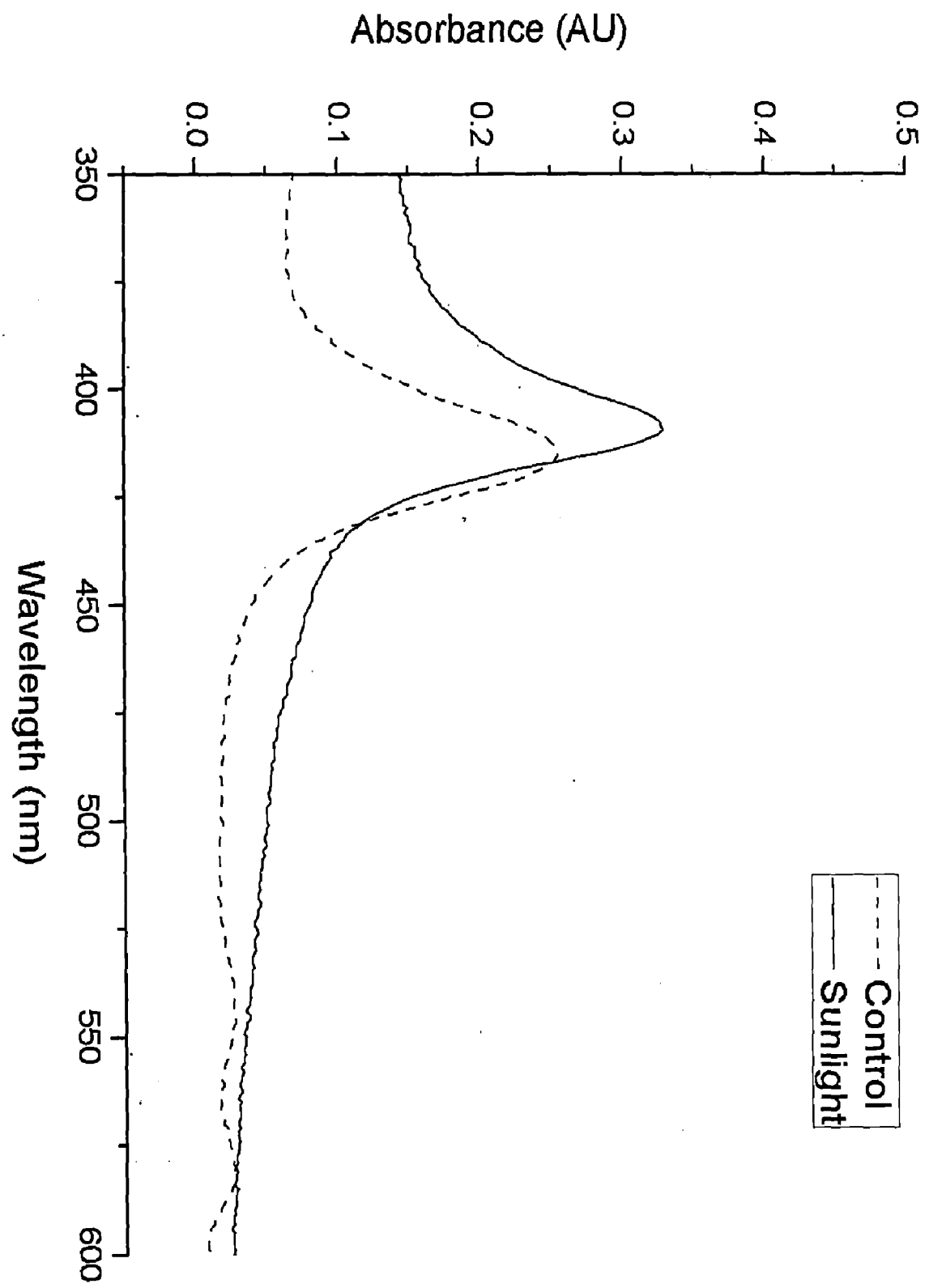

Figure D.13: Transfer of NO from $Ru(PPh_3)_2L^3(NO)$ to Reduced Myoglobin